



University of Kentucky
UKnowledge

Theses and Dissertations--Molecular and
Cellular Biochemistry

Molecular and Cellular Biochemistry

2014

NEUROFILIN IN THE VASCULAR SYSTEM: MECHANISTIC BASIS OF ANGIOGENESIS

Hou-Fu Guo

University of Kentucky, hguo3@g.uky.edu

[Right click to open a feedback form in a new tab to let us know how this document benefits you.](#)

Recommended Citation

Guo, Hou-Fu, "NEUROFILIN IN THE VASCULAR SYSTEM: MECHANISTIC BASIS OF ANGIOGENESIS" (2014). *Theses and Dissertations--Molecular and Cellular Biochemistry*. 16.
https://uknowledge.uky.edu/biochem_etds/16

This Doctoral Dissertation is brought to you for free and open access by the Molecular and Cellular Biochemistry at UKnowledge. It has been accepted for inclusion in Theses and Dissertations--Molecular and Cellular Biochemistry by an authorized administrator of UKnowledge. For more information, please contact UKnowledge@lsv.uky.edu.

STUDENT AGREEMENT:

I represent that my thesis or dissertation and abstract are my original work. Proper attribution has been given to all outside sources. I understand that I am solely responsible for obtaining any needed copyright permissions. I have obtained needed written permission statement(s) from the owner(s) of each third-party copyrighted matter to be included in my work, allowing electronic distribution (if such use is not permitted by the fair use doctrine) which will be submitted to UKnowledge as Additional File.

I hereby grant to The University of Kentucky and its agents the irrevocable, non-exclusive, and royalty-free license to archive and make accessible my work in whole or in part in all forms of media, now or hereafter known. I agree that the document mentioned above may be made available immediately for worldwide access unless an embargo applies.

I retain all other ownership rights to the copyright of my work. I also retain the right to use in future works (such as articles or books) all or part of my work. I understand that I am free to register the copyright to my work.

REVIEW, APPROVAL AND ACCEPTANCE

The document mentioned above has been reviewed and accepted by the student's advisor, on behalf of the advisory committee, and by the Director of Graduate Studies (DGS), on behalf of the program; we verify that this is the final, approved version of the student's thesis including all changes required by the advisory committee. The undersigned agree to abide by the statements above.

Hou-Fu Guo, Student

Dr. Craig Vander Kooi, Major Professor

Dr. Michael Mendenhall, Director of Graduate Studies

NEUROPILIN IN THE VASCULAR SYSTEM: MECHANISTIC BASIS OF
ANGIOGENESIS

DISSERTATION

A dissertation submitted in partial fulfillment of the
requirements for the degree of Doctor of Philosophy in the
College of Medicine at the University of Kentucky

BY

Hou-Fu Guo

Lexington, Kentucky

Co-Directors: Dr. Craig Vander Kooi

Associate Professor of Molecular and Cellular Biochemistry
and Dr. David Rodgers

Associate Professor of Molecular and Cellular Biochemistry
Lexington, Kentucky

2014

Copyright © Hou-Fu Guo 2014

ABSTRACT OF DISSERTATION

NEUROFILIN IN THE VASCULAR SYSTEM: MECHANISTIC BASIS OF ANGIOGENESIS

The vascular system is critical for maintaining homeostasis in all vertebrates. The development and function of this essential network is tightly regulated by diffusible cytokines. Interestingly, two families of Nrp-1 ligands, Vascular Endothelial Growth Factor A (VEGF-A) and Semaphorin3F (Sema3F), physically compete for binding to the Nrp-1 b1 domain, and have opposite roles in regulating angiogenesis. Indeed, VEGF-A is a potent pro-angiogenic cytokine while Sema3F is an angiogenesis inhibitor. Although the interaction between VEGF and Nrp-1 is well characterized, little is known about the physical basis of Sema3F binding to Nrp-1. By utilizing chemically synthesized peptides and plate-based binding assays, we showed that Sema3F C-terminal ligand binding motif (C-furSema) binding to Nrp1 requires engagement of two distinct binding sites on the Nrp-1: a C-terminal arginine binding motif and a helical binding motif. Covalent tethering of these two motifs leads to synergistic binding to Nrp-1. In addition, the helical motif was shown to be conserved in all Sema3 family members, suggesting this tethering mode is widely utilized. By using the natural variants of Sema3A, we further demonstrated that the distance between this helical region and the C-terminal arginine determines binding affinity. Finally, we showed that C-furSema potently inhibits VEGF-A signaling in human umbilical vein endothelial cells (HUVECs). These data provide a basis for the rational design of novel high affinity Nrp-1 inhibitor.

VEGF functions via two essential cell surface receptor families: VEGF receptor (VEGFR) and Neuropilin (Nrp). Although Nrp1 is a mandatory co-receptor for VEGF-A-mediated angiogenesis, little is known about the specific role of Nrp-1 and the physical basis of its function. By utilizing biochemical and biophysical tools, we demonstrated that Nrp-1 b1b2 domain directly interacts with the VEGFR-2 membrane proximal domain 7. This suggested that Nrp-1 promotes full VEGFR-2 activation by direct coupling to the active form of VEGFR-2 domain 7. Indeed, we further demonstrated that disrupting the interaction between Nrp-1 b1b2 domain and VEGFR-2 domain 7 decreases VEGFR-2 activation upon VEGF-A stimulation. This defines the molecular mechanism of Nrp-1 in VEGFR-2 activation. This also provides a novel mechanism to inhibit VEGFR-2 signaling.

KEYWORDS: VEGF, receptor coupling, endothelial cells, semaphorin, X-ray crystallography

Hou-Fu Guo

Student Signature

June 10, 2014

Date

NEUROPILIN IN THE VASCULAR SYSTEM: MECHANISTIC BASIS OF
ANGIOGENESIS

By
Hou-Fu Guo

Craig Vander Kooi

Co-Director of Dissertation

David Rodgers

Co-Director of Dissertation

Michael Mendenhall

Director of Graduate Studies

June 10, 2014

Date

FOR MY LOVELY KIDS, MANDY WU GUO AND ERIC WU GUO
MY DEAR WIFE, WENHUI WU
MY PARENTS, FENGZHEN HE AND JIWEI GUO
AND MY SISTER, PENGCHAO GUO

ACKNOWLEDGMENTS

This work would not be possible without the invaluable support, advice and help from many friends, colleagues and supervisors. First, I want to thank my mentor, Dr. Craig Vander Kooi. I greatly appreciated the opportunity he offered me to work in his lab. During the last five years, I have benefited tremendously by having him as my Ph D advisor. He has shown me how to think scientifically, how to identify an isolated scientific question, develop a hypothesis, solve the question using my own reasoning and critical thinking, and then critique our own reasoning and improve the ability to solve the scientific question. The problem solving ability I have developed with his help will benefit me lifetime. I also feel lucky to have the helpful and constructive comments and suggestions from my committee members, Dr. David Rodgers, Dr. Sidney Whiteheart, and Dr. Anne-Frances Miller and outside examiner, Dr. Wei Yinan.

I want to thank my collaborators both at the University of Kentucky and oversea. I think I am extremely fortunate to have Dr. Matthew Gentry and Dr. Sidney Whiteheart in our Biochemistry Department as my collaborators. I feel grateful to you for your trust with your projects, and very much enjoy the exciting science that we have been collaborating on. I have learnt a lot about glucan phosphatases and hemostasis, and have also expanded my skill set by learning many assays for studying these enzymes and platelet function. Special thanks are given to Dr. David Meekins and Dr. Shaojing Ye for teaching me so much

and working with me side by side on these projects. I will definitely miss these days that we worked together. Finally, I want to thank Dr. Andrew Morris from University of Kentucky and Dr. Jianghua Yan from Xiamen University for providing generous help with one of my projects.

Working in the Vander Kooi lab is really a fascinating experience. This is because all of the Vander Kooi lab members, Matthew Parker, Xiaobo Li, Ping Xu, Andrew Linkugel, Tingting Wu, Daemon Revelette, Bithika Dhar, Chris Gerwe, Lauren Saley, are always delightful and only too willing to offer help and talk science. Thanks to you all for providing me this friendly, warm, inspiring and exiting work environment in this lab. I also really appreciate Ping Xu, Xiaobo Li, Matthew Parker, and Andrew Linkugel for their help on my projects.

Additionally, I want to thank our department DGS, Dr. Kevin Sarge and Michael Mendenhall for their numerous academic suggestions throughout my stay in Biochemistry. I also very much enjoy the friendship with Martin Chow, Liuqing Yang, Jinchao Zhang, Peng Jiang, Shanshan Pei, Qian Chen, Min Chen, Ye Li, Lingfeng Tang, Wen Wen, Ting Zhang, Daipayan Banerjee (Deep), Swagata Ghosh and many others. I really appreciate their support and help during my Ph D work. Special thanks are given to Jinchao Zhang for his help on preparing liposomes. I also want to thank the departmental staff for their daily help.

I thank Drs Matthew Gentry and David Rodgers, and David Meekins for helpful discussions about the manuscript “Mechanistic Basis for the Potent Anti-angiogenic Activity of Semaphorin 3F”. I thank Samuel Zeeman and members of the Gentry and Vander Kooi labs for fruitful discussions as well as Dr. Carol Beach and Dr. Martin Chow for technical assistance on the manuscript “Structure of the Arabidopsis Glucan Phosphatase LIKE SEX FOUR2 Reveals a Unique Mechanism for Starch Dephosphorylation”.

Finally but not at least, I greatly appreciate my wife Dr. Wenhui Wu, as always, for the incredible help she has provided both at school and at home. She helped me go through so many of my manuscripts, proposals, talks and posters. Her suggestions on science, statistics and graphics made a big difference. I want to thank my daughter Mandy Guo and my son Eric Guo for giving me so much fun. Moreover, I also want to thank my parents, Fengzhen He and Jiwei Guo, and my sister, Pengchao Guo for their consistent support from oversea.

TABLE OF CONTENTS

Acknowledgments.....	iii
List of Tables.....	viii
List of Figures.....	ix
Chapter One - Vascular Development, Function and Maintenance.....	1
General introduction.....	1
Vasculogenesis, angiogenesis and VEGF.....	2
The receptors of VEGF: VEGF receptor and Neuropilin.....	2
Nrp independent signaling capacity.....	3
The other Nrp ligand family: Class 3 semaphorins.....	4
VEGF and Sema3 competition and Nrp inhibitor design.....	5
Summary.....	6
Chapter Two - Mechanistic basis for the potent anti-angiogenic activity of semaphorin 3F.....	10
Introduction.....	10
Methods.....	11
Results.....	14
Discussion.....	17
Chapter Three - Semaphorin 3F anti-angiogenic activity regulation.....	26
Introduction.....	26
Methods.....	27
Results.....	29
Discussion.....	31
Chapter Four - The physical mechanism of Neuropilin function in VEGF signaling.....	39
Introduction.....	39

Methods.....	40
Results.....	44
Discussion.....	47
Chapter Five - Conclusions, significance and future directions.....	58
General conclusions and significance.....	58
Nrp and VEGFR coupling <i>in cis</i> and <i>trans</i> VEGFR activation.....	58
The basis of Nrp in angiogenesis.....	59
Nrp increases the affinity of VEGF to VEGFR-2.....	59
Nrp increases the efficiency of signal transmission.....	60
VEGFR-2 trafficking.....	61
Nrp coupling to other receptors.....	61
VEGF and Sema3 C-terminus competes for binding to Nrp.....	62
Explore the non-canonical roles of Nrp in other cell types.....	62
The biological significance of Nrp promiscuous ligand binding.....	64
References.....	67
Vita.....	80

LIST OF TABLES

Table 3.1, Data collection and refinement statistics.....	33
Table 4.1, VEGFR-2 D7 data collection and refinement statistics.....	50
Table 4.2, VEGFR-2 D7 and Nrp1 b1b2 domain data collection and refinement statistics.....	51

LIST OF FIGURES

Figure 1.1, Cross-talk between Nrp ligands allows coordinated regulation of vascular and neuronal tissues.....	8
Figure 1.2, Nrp function is essential for VEGF mediated angiogenesis and Semaphorin 3 dependent axon guidance.....	9
Figure 2.1, C-furSema potently inhibits VEGF-A mediated VEGFR2 activation in situ.....	20
Figure 2.1, C-furSema potently inhibits VEGF-A mediated VEGFR2 activation in situ.....	20
Figure 2.2, Effect of the intermolecular disulfide on C-furSema potency.....	21
Figure 2.3, C-furSema C-terminal arginine contributes to high affinity binding to Nrp.....	22
Figure 2.4, The N-terminal helical motif is a structured region that contributes to potency.....	23
Figure 2.5, The helical motif determines potent competitive Nrp1 binding.....	24
Figure 2.6, Semaphorin 3 family members engage Nrp1 utilizing two distinct regions in their C-terminal domain, a C-terminal arginine and upstream helical region.....	25
Figure 3.1, The Nrp1-Semaphorin 3F recombinant protein shows interesting tetrahedron like shape with each tip of the 4 Nrp1 b1 domains (purple) pointing out.....	34
Figure 3.2, Semaphorin 3F helical motif from the C-terminal basic domain extends out of the Nrp1 b1 domain.....	35
Figure 3.3, Semaphorin 3F helical motif from the C-terminal basic domain is mainly stabilized by an intermolecular disulfide bond, and to a less extent by further molecular interactions	36
Figure 3.4, C-furSema serves as a pan-Nrp inhibitor.....	37
Figure 3.5, Differential furin processing of Semaphorin 3A.....	38
Figure 4.1, Structure of the VEGFR-2 D7 dimer.....	52
Figure 4.2, Physical coupling between Nrp and VEGFR-2 D7.....	53
Figure 4.3, Crystal structure of VEGFR-2 D7 (cyan) and Nrp1 b1b2 domain (green).....	54

Figure 4.4, Critical residues in VEGFR-2 D7 for Nrp1 b1b2 domain interaction are well conserved across species (shown in A), and are further confirmed to decrease VEGFR-2 D7 and Nrp1 b1b2 domain interaction with mutagenesis (Shown in B).....55

Figure 4.5, VEGFR-2 D7 and mutants have similar CD spectrum, *suggesting that mutations are not* deleterious to protein structure.....56

Figure 4.6, Blocking VEGFR-2 D7 and Nrp1 b1b2 domain interaction inhibits VEGF signaling.....57

Figure 5.1, Blocking VEGFR-2 D7 and Nrp1 b1b2 domain interaction inhibits VEGF signaling.....66

CHAPTER ONE

Vascular Development, Function and Maintenance

General Introduction

The closed circulatory system is a highly specialized organ system in vertebrates that transports oxygen and nutrients to the parts of the bodies where they are consumed, and helps to get rid of the waste products produced, such as carbon dioxide. This efficient pressurized vascular system greatly accelerates the metabolism of animals and provides a platform to support the functionalities of energy demanding tissues/organs, such as muscle, heart, and the central nervous system. In addition, the circulatory system also regulates immune function, body temperature and pH.

Since the circulatory system plays critical roles, most cells in an organism are located within 50–100 μm of a capillary. Interestingly, the vasculature is not a static structure, but undergoes constant remodeling not only during development, but also in adulthood under physiological and pathological conditions, such as wound healing, cancer and wet macular degeneration. Because it has essential roles in human physiology and pathology, the vascular system has already been studied in early human history. Indeed, the first written record of the vasculature can be dated to 3,500 years ago in an Egyptian book named Ebers Papyrus ⁽¹⁾. However, the physiological and molecular details underlying the vascular system has only been described until the last century. Based on decades of research, we now have produced a model of the process of circulatory system development and homeostasis.

Vasculogenesis, angiogenesis and VEGF

The development of the vascular system is an early step in organogenesis, which starts from the aggregation of angioblasts, vascular precursor cells, into a primitive vascular plexus, a process that is called vasculogenesis. This is followed by a complicated remodeling process named angiogenesis, during which blood vessels split and sprout to form a functional circulatory system. Vasculogenesis is absolutely essential during development for the formation of

central vessels but has also been shown to take place in adults. Angiogenesis is not only important during development, but also plays a critical role in the maintenance of vasculature and wound healing.

Intensive research has been done to study how angiogenesis is regulated on a molecular level. Groundbreaking work was performed by Michaelson in 1948 ⁽²⁾. Based on his own research on retinal angiogenesis during development, he argued that an unknown factor, named tissue factor X, forms a concentration gradient in the area in need of blood vessels, and new blood vessels are formed toward the initiating tissue. At the same time, it was reported that tumor cells are able to attract blood vessels suggesting that they secrete a tissue factor X. Indeed, in 1971, Folkman demonstrated that a protein fraction around 40 kDa isolated from tumor cell lysate is able to activate angiogenesis, which was then named tumor angiogenesis factor based on its function ⁽³⁾. Later on, in 1989, Ferrara independently identified a cytokine from tumor cells and sequenced its DNA ⁽⁴⁾. Since this factor is able to stimulate endothelial cell proliferation, it was named Vascular Endothelial Growth Factor (VEGF), again based on its function. Interestingly, it was finally established that VEGF plays a critical role in angiogenesis in all these settings.

Vasculogenesis and angiogenesis are driven by hypoxia. When tissues face the challenge of hypoxia, the degradation of a widely expressed oxygen sensor hypoxia-inducible factor (HIF) is inhibited ^(5, 6). The accumulation of HIF transcriptional complex turns on the expression of a variety of hypoxia response genes, such as VEGF ⁽⁷⁾. The formation of VEGF gradient in tissues regulates vasculogenesis and angiogenesis (Figure 1.1). The critical roles of VEGF in vasculogenesis and angiogenesis during early development have been demonstrated using transgenic mice ^(8, 9). The knockout of a single VEGF allele results in embryonic lethality due to cardiovascular defects. Interestingly, VEGF was the first haplo-insufficient gene identified. In addition to the first member of the VEGF ligand family, now known as VEGF-A, vertebrates also possess four other VEGF family members, VEGF-B,-C,-D, and placental growth factor (PlGF) ⁽¹⁰⁾. The different family members appear to have both unique and partially overlapping functions. It is thought that angiogenesis is primarily regulated by VEGF-A, -B, and PlGF, whereas lymphangiogenesis is regulated by VEGF-C and -D ⁽¹¹⁾.

The receptors of VEGF: VEGF receptor and Neuropilin

VEGF family cytokines function by binding to VEGF receptor (VEGFR) tyrosine kinase and Neuropilin (Nrp) family members (Figure 1.2). In the human genome, there are three VEGFRs, named VEGFR-1,-2,-3, and two Nrp family members, which are Nrp 1 and 2. All 3 VEGFRs have 7 extracellular immunoglobulin-like (Ig) domains, a transmembrane domain and an intracellular portion containing a split kinase domain ⁽¹²⁾. Nrp family members are 130 KDa type I transmembrane proteins with a short intracellular domain and five extracellular domains including: two complement binding CUB domains (a1 and a2), two coagulation factor domains (b1 and b2), and a Meprin/A5-protein/PTPmu (MAM) domain (c) ^(13, 14).

VEGFR-2 and Nrp-1 are considered the major receptors for VEGF-A mediated angiogenesis. Indeed, VEGFR-2 and Nrp-1 knockout mice have similar vascular defects and embryonic lethality phenotype ^(15, 16). It is generally believed that VEGF-A signaling is delivered into the cell via VEGFR initiated tyrosine kinase cascade ⁽¹⁷⁾. Nrp enhances VEGF stimulated VEGFR-2 downstream tyrosine kinase signaling cascade and increases chemotactic activity when expressed together with VEGFR-2 in endothelial cells ^(18, 19). However, the specific role of Nrp and mechanism of Nrp function in this pathway are still not understood, although models have been proposed.

Nrp independent signaling capacity

It has been recently proposed that the vascular development defects seen in Nrp knockout are due to Nrp mediated independent signaling cascade, which works in parallel with VEGFR-2 signaling in angiogenesis ⁽²⁰⁾. Interestingly, several studies indicate that Nrp-1 intracellular domain and synectin play a role in cell migration independent of VEGFR-2 ⁽²¹⁻²³⁾, which agrees with this model. However, accumulating data from other groups do not support it. It has been reported that Porcine Aortic Endothelial (PAE) cells overexpressing Nrp itself do not respond to VEGF suggesting Nrp does not have independent signaling capacity ⁽¹⁸⁾. However, this negative result could be due to the possibility that PAE may not express the necessary downstream signaling molecules needed for Nrp-mediated signaling.

Strikingly enough, it has been shown that the defective angiogenesis phenotype observed in Nrp null mouse embryos could largely be complemented by intraperitoneal injecting pregnant mice with Nrp ectodomain Fc fusion protein during early development, although this injection is not sufficient to rescue the embryonic lethality ⁽²⁴⁾. Interestingly, it has been further demonstrated that transgenic mice with Nrp-1 lack of the intracellular domain are viable without the

vessel loss phenotype observed in Nrp-1 null mouse embryos, demonstrating that the membrane-anchored extracellular domain is largely able to compensate Nrp-1 loss ⁽²⁵⁾. However, it was later determined that these mice have impaired arteriogenesis ⁽²⁶⁾. As a result, it suggests that angiogenesis could largely proceed without the need of the Nrp intracellular domain mediated signaling, and Nrp intracellular domain is important for arteriogenesis but the mechanism is not very clear and still needs to be determined.

The other Nrp ligand family: Class 3 semaphorins

Class III Semaphorins (Sema3) are a family of seven secreted cytokines that play critical roles in Nrp/plexin mediated axon guidance during neural development ⁽²⁷⁾ (Figure 1.1 and Figure 1.2). Indeed, axon guidance cues mediated by Sema3 family members are essential during development for correct neuronal patterning in dorsal root ganglia, facial, vagal, olfactory-sensory, cortical, hippocampal, and cerebellar nerves, along with others ⁽²⁸⁾. Previous studies have shown that both Nrp and Plexin are required for correct neuronal patterning during early development ⁽²⁹⁻³²⁾. Sema3 regulates axonal patterning by binding to plexin family members and inhibiting axonal repulsive signal ⁽²⁹⁻³²⁾. Interestingly, Nrp has also been shown to be able to reverse Sema3-mediated axonal repulsion to attraction in certain cases ^(33, 34).

All Sema3 members have the same overall domain architecture: a 500 amino acid Sema domain, a PSI domain, an Ig-like C2-type (immunoglobulin-like) domain, and a short C-terminal basic domain. A disulfide bond in a helical motif located in the c-terminal basic domain of Sema3 links two Sema3s into a dimer, and dimeric nature of Sema3 is essential for engaging two receptor molecules for signaling. The N-terminal a1 domain of Nrp-1 and Nrp-2 selectively binds the Sema domain of different Sema3 family members, which determines the specificity of ligand and receptor pairing ⁽³⁵⁻³⁷⁾. Notably, Sema3A specifically signals via Nrp-1 ^(13, 14) and Sema3F via Nrp-2 ⁽³⁸⁾. The Nrp b1 domain allows high-affinity non-selective binding to the Sema3 C-terminal domain ⁽³⁸⁻⁴⁰⁾. Following Sema3 binding by Nrp, Plexin family signaling receptors (PlexinA1-4) are then engaged and activated to directly guide axonal growth ^(30, 41). Nrp functions by coupling specific high-affinity Sema3 binding to Plexin-dependent regulation of cytoskeleton dynamics in the axonal growth cone ⁽³⁰⁾.

Accumulating studies suggest that Sema3 is also an endogenous anti-angiogenic factor with unique roles under physiological and pathological conditions. For example, Sema3F forms a barrier that maintains the outer retina avascularity,

and Sema3E provides a guidance cue for retinal vascular pathfinding ^(42, 43). This Sema3 mediated anti-angiogenic activity was shown to result from PlexinD1 signaling and downstream small GTPase RhoJ activation in endothelial cells. However, direct competition between the C-termini of Sema3 and VEGF-A for binding to Nrp b1 domain has been shown to be another mechanism for the anti-angiogenic activity of Sema3 ⁽⁴⁰⁾, emphasizing the importance of understanding the mechanism of Nrp ligand binding.

VEGF and Sema3 competition and Nrp inhibitor design

Indeed, intensive studies have been focused on illustrating the mechanisms of VEGF and Sema3 ligand and Nrp receptor interactions. It has been shown that VEGF-A binds to the first coagulation factor (b1) domain of Nrp, and mutation in this binding site generates a dominant negative angiogenesis inhibitor ^(44, 45). The C-terminal basic rich region of Sema3 mediates the high affinity Nrp interaction by binding to its coagulation factor domain ⁽⁴⁴⁾, however, there had been a long debate about whether they bind to the same site competitively or distinct sites independently.

Previous work in our laboratory provides evidence for the competitive nature of the interactions between these two ligands to Nrp. We have first demonstrated that all VEGF family members possess a C-terminal arginine, which is both necessary and sufficient for binding to Nrp-1 b1 domain. We have further shown that additional C-terminal residues of VEGF from both exon 7 and 8 contributes to Nrp-1 b1 domain binding ⁽⁴⁶⁾. Interestingly, none of the 7 Sema3 family members has a C-terminal arginine. We have showed that the C-terminus of Sema3 is proteolytically processed by furin, which is required for producing a C-terminal arginine to compete with the C-terminal arginine of VEGF for binding to the Nrp coagulation factor domain ^(40, 47).

VEGF mediated angiogenesis is not only important during development and wound healing, it is also critical for tumor progression. As a result, intensive effort has been made for Nrp peptide inhibitor development and tumor targeting. For example, a phage display study identified a C-terminal arginine based peptide RPARPAR with a $K_d=1.7 \pm 0.4\mu M$ ⁽⁴⁸⁾. Others used microfluidic systems and discovered two additional peptides with comparable binding affinity to Nrp (GGKRPAR and RIGRPLR) ⁽⁴⁹⁾. Moreover, cyclic tumor-homing peptide LyP-1 CGNKRTRGC was shown to be able to penetrate tumor tissue ⁽⁵⁰⁾. Interestingly, this peptide was further shown to be processed by tumor tissue to release the C-

terminal arginine for Nrp binding, suggesting a similar C-terminal arginine based mechanism ⁽⁵¹⁾.

Ligand-derived inhibitory peptide design has been employed as another promising approach for targeting Nrp. EG3287, derived from the C-terminal amino acid 138 to 165 of VEGF-A, was shown to inhibit VEGF-A binding to Nrp-1 with an $IC_{50}=2\mu M$ ^(52, 53). A larger peptide derived from the C-terminal amino acid 111 to 165 of VEGF-A has been shown to inhibit VEGF-A binding to Nrp-1 with an IC_{50} about 300nM ⁽⁵⁴⁾. Finally, work from our lab identifies a peptide from the C-terminus of Sema3F, which potently inhibits VEGF-A binding to Nrp-1 with an $IC_{50}=45nM$, but the mechanism of this potent inhibition was unknown ⁽⁴⁰⁾.

Moreover, a C-glycosyl scaffold functionalized with side chains of amino acids mimicking ATWLPPR peptide yields an inhibitor with the $IC_{50}=92\mu M$ against VEGF-A binding to Nrp-1 ⁽⁵⁵⁾. Interestingly, $D(LPR)$ synthesized with D-amino acids is shown to be resistant to protease degradation but retain similar inhibition potency compared to its L-amino acid counterpart ⁽⁵⁶⁾, which represents an interesting approach for optimizing peptide based Nrp-1 inhibitors. Finally, a small molecule Nrp inhibitor EG00229 has been shown to inhibit tumor cell survival and migration especially when given in combination with chemotherapeutic reagents ⁽⁵⁷⁾.

To further improve the Nrp inhibition efficiency, some of the peptide inhibitors have been coupled with cytotoxic reagents. For example, Kawakami et al fused Sema3A-derived peptide with lytic-type peptide to enhance its biological effect ⁽⁵⁸⁾, while others conjugated ATWLPPR peptide with photosensitizer ^(59, 60). The Arap and Pasqualini groups have also demonstrated that Nrp-targeting peptide and pro-apoptotic peptide conjugate (CGFYWLRSC-GG-D(KLAKLAK)2) inhibits leukemias and lymphomas *in vitro* ⁽⁶¹⁾. Since it has been shown that these peptide conjugates are degraded rapidly after *in vivo* injection ^(59, 62), further effort was made to delay degradation. For instance, a pseudopeptide conjugate has been shown to be able to improve the *in vivo* stability dramatically ⁽⁶³⁾, however, the inhibitory effect of this conjugate on tumor progression remains to be determined.

Summary

The cardiovascular system is critical for the daily life of all vertebrates. VEGF and its receptors, VEGFRs and Nrps, play an essential role in regulating the formation and homeostasis of this organ system starting from early development throughout the entire adulthood. In this dissertation, the author mainly focused on

one of VEGF membrane receptors Nrp-1 and utilized a variety of cell biology, biochemical and biophysical techniques to determine the mechanism of ligand receptor interaction and receptor activation, which are two critical steps required to sense and integrate extracellular ligand signals and transmit them into the target cells.

Note: Part of this chapter has been published and is reproduced here for completeness of the dissertation ⁽⁶⁴⁾.

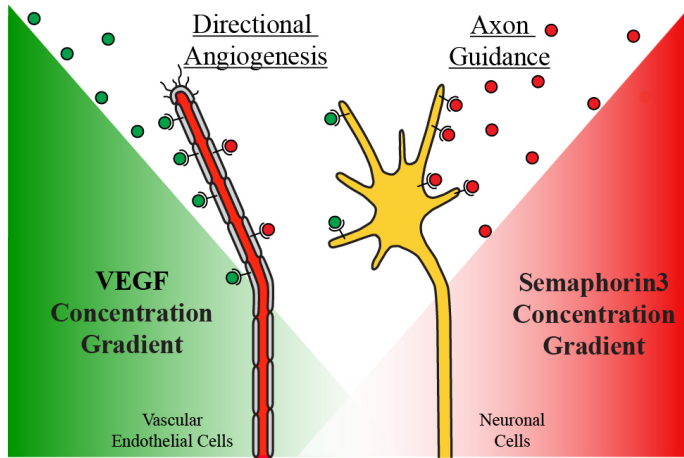


Figure 1.1: Cross-talk between Nrp ligands allows coordinated regulation of vascular and neuronal tissues. Both endothelial cells and neurons express Nrp which can respond to either VEGF or Sema3 family guidance cues. Regulation of competitive Nrp binding between different ligands allows for an additional level of dominant control of Nrp function.

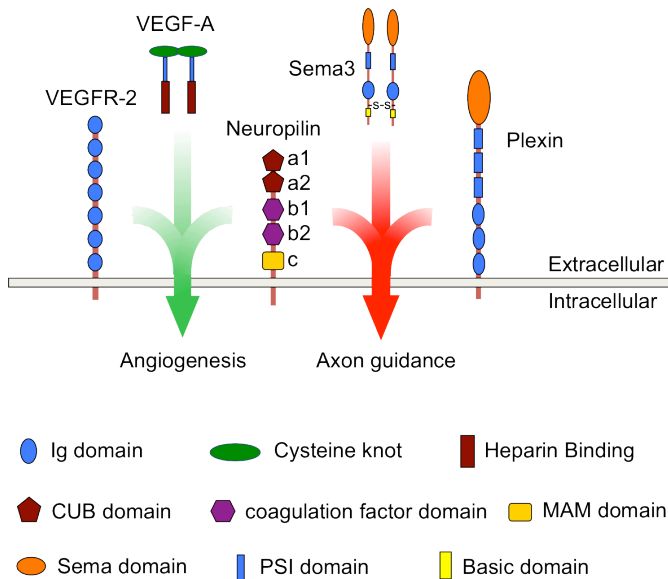


Figure 1.2: Nrp function is essential for VEGF mediated angiogenesis and Sema3 dependent axon guidance. Cooperative binding of VEGF by VEGFR and Nrp activates the angiogenic cascade necessary for developmental and homeostatic angiogenesis and also pathological signaling associated with tumorigenesis and other types of aberrant signaling. Engagement and activation of Nrp and Plexin family receptors is required for axon guidance signaling.

CHAPTER TWO

Mechanistic basis for the potent anti-angiogenic activity of semaphorin 3F

Introduction

Neuropilins (Nrps) are an essential cell surface receptor family⁽⁶⁴⁾. They function with Vascular Endothelial Growth Factor Receptors (VEGFRs) in VEGF-dependent angiogenesis and with Plexin receptors in Semaphorin 3-dependent axon guidance⁽⁶⁵⁻⁶⁹⁾. In addition to their function in neurons, a critical role for specific Semaphorin 3 family members in physiological and pathological regulation of the cardiovascular system has been increasingly recognized⁽⁷⁰⁻⁷²⁾. For example, Semaphorin 3F is critical for maintaining an avascular outer retina, while Semaphorin 3A and Semaphorin 3E have important roles in vascular patterning^(42, 43, 72, 73). In contrast, mutation and down-regulation of Semaphorin 3 family members is also observed in many types of solid tumors and has been directly correlated with tumor angiogenesis and cancer progression^(70, 74, 75). Indeed, restoring the expression of Semaphorin 3B and Semaphorin 3F in tumors inhibits tumor cell proliferation *in vitro* and further cancer progression *in vivo*⁽⁷⁶⁻⁷⁹⁾.

Nrp serves a central role in integrating the opposing signals of VEGF and Semaphorin 3 in both physiological and pathological contexts through competitive ligand binding. The Nrp-1 b1 coagulation factor domain has a conserved C-terminal arginine binding pocket that is critical for competitive VEGF and Semaphorin 3 binding^(40, 47). Alternative splicing of VEGF-A regulates Nrp-1 binding⁽⁸⁰⁾, with the exon eight encoded C-terminal arginine residue being necessary for binding Nrp-1-b1⁽⁴⁶⁾. In contrast, furin proteolysis of Semaphorin 3 is critical for regulating its ability to bind Nrp and function. Furin processing can either inactivate or activate Semaphorin 3 by processing at sites in the central or C-terminal domains, respectively. Processing in the central region of Semaphorin 3 has been primarily reported to inactivate Semaphorin 3 activity by cleaving the protein into two fragments, although the fragments may still possess activity⁽⁸¹⁻⁸³⁾. Furin processing within the Semaphorin 3 C-terminal domain is critical to activate the Semaphorin 3 pro-protein by producing a C-terminal arginine, allowing competitive engagement of Nrp-1-b1^(40, 84).

Multiple C-terminal arginine containing peptides and peptido-mimetics have been produced as competitive antagonists of VEGF-A/Nrp-1 binding^(48, 85, 86). While functioning as inhibitors *in vitro* and *in situ*, these peptides and peptidomimetics

suffers from limited potency ($IC_{50} \approx 10-50 \mu M$). In contrast, endogenous Sema3F functions as a potent inhibitor of VEGF-A binding to Nrp-1⁽⁴⁰⁾. However, the molecular mechanism of high-affinity Sema3F binding to Nrp-1 has not been elucidated, leaving open the question of how Sema3F potentially competes for Nrp-1 binding.

In the present study, we demonstrate the mechanistic basis for the potency of the furin-processed C-terminal domain of Sema3F (C-furSema) (Figure 2.1A) *in vitro* and *in situ*. We find that C-furSema exhibits unique hetero-bivalent engagement and that this bivalent binding is essential for high affinity Nrp-1 binding.

Methods

C-furSema and Variant Production

Homodimeric C-furSema (GLIHQYCQGYWRHVPPSPREAPGAPRSPEPDQK KPRNRR), truncations, and point mutants were synthesized using solid phase synthesis, oxidized to produce the natural intermolecular disulfide, and purified with reversed phase high-performance liquid chromatography (HPLC) using 4.6mm*250mm, SinoChrom ODS-BP column to >95% purity (Neo-Peptide, Cambridge, MA). The monomeric C-furSema^{Mon} (GLIHQYSQGYWRHVPPSPREAPGAPRSPEPDQKKPRNRR) was produced in the same manner without oxidization. C-furSema^{Het} was produced by combining separately synthesized reduced C-furSema and C-furSema^{Helix} (GLIHQYCQGYWRH), oxidized in the presence of the excess C-furSema^{Helix}, and purified with reversed phase HPLC using 4.6mm*250mm, SinoChrom ODS-BP column to >95% purity (LifeTein, South Plainfield, NJ). All C-furSema variants were well behaved in solution and soluble to >1 mM. A dimeric construct of C-furSema^{Helix} alone showed limited solubility, with a maximal solubility in Phosphate Buffered Saline (PBS) of 20 μM , and no ability to inhibit VEGF-A binding up to the limit of solubility.

Protein and peptide concentrations were determined using OD₂₈₀ measured on a Nanodrop 1000 (Thermo Fisher Scientific, Wilmington, DE).

In situ inhibition assays

Porcine aortic endothelial (PAE) cells stably overexpressing VEGFR-2 and Nrp-1 were utilized to measure the ability of C-furSema to block VEGF-A activation of VEGFR-2⁽⁸⁷⁾. PAE cells were grown in F12 medium (Invitrogen, Grand Island,

NY) supplemented with 10% Fetal Bovine Serum (FBS) (Invitrogen, Grand Island, NY) and 1% Pen/Strep in 6-well cell culture plates to 70% confluence. Cells were then serum starved for 16 hours in Endothelial Cell Basal Growth Medium-2 (EBM-2) (Lonza, Walkersville, MD). C-furSema samples were resuspended in EBM-2, added at a final concentration of 10 mM, and incubated for 90 minutes at 37°C. Cells were then stimulated with 100 ng/ml VEGF-A (R&D Systems, Minneapolis, MN) for 3 minutes. After 3 minutes, media was removed and cells solubilized in RIPA buffer supplemented with phosphatase and protease inhibitor (Roche, Germany). Total VEGFR-2 and VEGFR-2 phosphorylation was determined by western blotting using 55B11 and 19A10 antibodies (Cell Signaling, Danvers, MA), respectively, at a 1:1000 dilution followed by goat anti-rabbit HorseRadish Peroxidase (HRP) conjugated secondary antibody at 1:20000 dilution (sc-2301, Santa Cruz). The SuperSignal West Femto chemiluminescence (ECL) detection system (Thermo Fisher Scientific, Rockford, IL) was used for detection of immunoreactivity on X-ray films (HyBlot CL; Denville Scientific, Inc. Metuchen, NJ). Experiments were performed in triplicate and results reported as the mean \pm 1 standard deviation.

For determination of *in situ* potency, a VEGFR-2 cellular phosphorylation sandwich Enzyme-Linked ImmunoSorbent Assay (ELISA) was utilized (ProQinase, Germany). Primary Human Umbilical Vein Endothelial Cells (HUVECs) were plated in Endothelial Cell Growth Medium (ECGM) supplemented with 10% FBS (PromoCell, Germany), serum starved for 16 hours, incubated with varying concentration of C-furSema for 90 minutes, and then activated with VEGF-A at 100ng/ml for 3 minutes. The level of VEGFR-2 phosphorylation was determined via sandwich ELISA using a VEGFR-2 capture antibody and anti-phosphotyrosine detection antibody (PromoCell, Germany). Raw data were converted into percent phosphorylation relative to high and low controls. Cells treated with VEGF-A alone were defined as high control (100%), and those treated with 1 μ M sunitinib, a well characterized VEGFR-2 kinase inhibitor with an IC_{50} =10nM, were defined as low control (0%). Inhibition curves were fit using a standard four-parameter sigmoidal curve to yield the IC_{50} . Experiments were performed in duplicate and results reported as the mean \pm 1 standard deviation.

Protein expression and purification

Proteins were expressed and purified using established protocols ⁽⁴⁰⁾. Briefly, Nrp-1-b1b2 (residue 274 to 586) was expressed in *E. coli* and purified using nickel affinity chromatography (IMAC) followed by heparin affinity

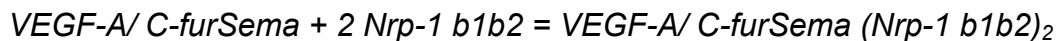
chromatography. Alkaline Phosphatase (AP) fused VEGF-A was produced from Chinese Hamster Ovary (CHO) cells.

In vitro inhibition assays

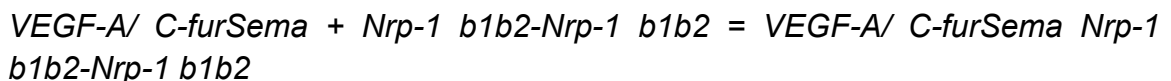
Plate-based inhibition assays were performed as previously reported⁽⁴⁰⁾. Briefly, AP-VEGF-A (410 μ M *para*-nitrophenol phosphate (p-NPP) hydrolyzed/min/ μ L) was combined with Sema3F-derived peptides in binding buffer (20 mM Tris, pH 7.5/50 mM NaCl), incubated with Nrp-1 affinity plates for 1 hour at 25°C, washed three times with PBS-T (0.01M Phosphate buffered saline, 0.1% Tween 20, pH 7.4), incubated with PBS-T for 5 minutes, aspirated, and developed by addition of 100 μ L of 1X alkaline phosphatase pNPP substrate⁽⁸⁸⁾ followed by quenching with 100 μ L of 0.5N NaOH. AP activity was quantitatively measured at 405nm using a SpectraMax M5 instrument (Molecular Devices, Sunnyvale, CA). Binding curves were fit using a standard four-parameter sigmoidal curve to yield the IC₅₀. Inhibitory potency is expressed per-subunit for peptides to allow direct comparison between dimeric and monomeric peptides. Experiments were performed in triplicate and results reported as the mean \pm 1 standard deviation. An unpaired t-test was used to compare IC₅₀ values.

Thermodynamic Calculations

Since VEGF-A and C-furSema are dimeric ligands, the interaction between Nrp-1 b1b2 and VEGF-A/ C-furSema follows the following equation.



Since VEGF-A and Sema3 receptor Nrp-1 b1b2 is immobilized onto the plate, the equation can be simplified into the following form.



In this equation, we assume that two copies of Nrp-1 b1b2 (Nrp-1 b1b2-Nrp-1 b1b2) are engaged by ligands simultaneously. Since the dissociation constant K_d of VEGF-A Nrp-1 b1b2 complex in our plate based binding assay is 3 nM (Matthew Parker personal communication), IC₅₀ values of C-furSema, truncations, and point mutants were then converted into inhibitor dissociation constant K_i using Cheng-Prusoff equation.

$$K_i = IC_{50}/(1+[Ligand]/K_d)$$

Where [ligand] is the concentration of AP-VEGF-A used in the plate based inhibition assay, which is 2.83 nM.

The inhibitor and Nrp-1 interaction free energy ΔG was then calculated from inhibitor dissociation constant K_i using the following equation.

$$\Delta G = -RT \ln K_i$$

Where R = gas constant and T = absolute temperature.

Circular Dichroism (CD)

C-furSema and C-furSema^{Mon} were dissolved in 0.01M sodium phosphate 50mM NaCl, pH=6.5 at a concentration of 0.5mg/ml. CD spectra were measured using a J-810 spectropolarimeter (Jasco, Easton, MD) with a 1 mm path length quartz cuvette. All measurements were performed at 25°C and three scans averaged for each spectrum. A blank spectrum was collected in the same manner and used for background subtraction. The fraction of secondary structure was determined by K2D3 using the wavelength range from 200nm to 240nm ⁽⁸⁹⁾.

Results

C-furSema is a potent inhibitor in situ

To determine the potency of C-furSema function in cellular context, we examined its ability to inhibit VEGF-A mediated activation of VEGFR-2. Nrp-1 and VEGFR-2 were stably expressed in PAE cells ⁽⁸⁷⁾, and the ability of C-furSema to inhibit VEGF-A dependent phosphorylation of VEGFR-2 Y1175 was assessed. C-furSema markedly inhibited VEGF-A dependent VEGFR-2 activation (Figure 2.1B). To confirm this finding in a distinct cell type, and determine the potency and extent of this inhibition in primary endothelial cells, we measured the dose-dependent inhibitory effect of C-furSema on the activation of VEGFR-2 in HUVEC cells using a quantitative sandwich ELISA. Strikingly, C-furSema showed potent inhibition of VEGFR-2 activation with an $IC_{50}=34 \pm 15$ nM (Figure 2.1C), consistent with its potency *in vitro* ⁽⁴⁰⁾, and more than two orders of magnitude greater than short peptide inhibitors of Nrp-1 ^(57, 85, 86, 90). Additionally, complete inhibition of VEGFR-2 activation was observed in HUVEC cells, in contrast to other Nrp inhibitors that are able to only partially inhibit VEGFR-2 activation even at maximal dose ⁽⁸⁶⁾. Thus, C-furSema is a potent inhibitor of Nrp-1-dependent activation of endothelial cells *in situ*.

Mechanism of C-furSema potency

C-furSema, which corresponds to the full C-terminal basic domain of Sema3F, is larger and more complex than peptide and peptido-mimetic inhibitors that have been developed to target Nrp-1. Given the dimeric nature of C-furSema, due to its conserved inter-molecular disulfide bond, we predicted that the potency of C-furSema might be attributable to avidity effects arising from dual engagement of Nrp-1. Indeed, previous studies have demonstrated that oligomeric peptide inhibitors of Nrp have enhanced potency ⁽⁸⁶⁾.

To test this, we produced a monomeric form of C-furSema by mutating the single conserved cysteine residue responsible for dimerization to serine (C-furSema^{Mon}). The ability of C-furSema and C-furSema^{Mon} to competitively block VEGF-A binding to Nrp-1 was compared (Figure 2.2). A significant decrease in potency was observed for the monomer (black line, IC₅₀ = 1.3 ± 0.7 μM) compared to the dimer (grey line, IC₅₀ = 24 ± 1 nM). The monomer has a 9.7 ± 2.7 KJ mol⁻¹ decrease in binding free energy compared to dimer. While these data indicate a direct correlation of oligomerization and potency, it is notable that the monomeric species of C-furSema is still an order of magnitude more potent than previously published inhibitors ^(57, 85, 86, 90), suggesting that additional mechanisms may contribute to C-furSema potency.

A C-terminal arginine has been shown to be critical for Nrp ligand binding ⁽⁴⁷⁾. In the Sema3 family, furin processing liberates a C-terminal arginine and is required for Nrp binding ^(40, 84). In Nrp-1 ligands, residues near the C-terminal arginine have been shown to contribute to potency and selectivity ⁽⁴⁶⁾. Thus, we hypothesized that residues directly upstream of the C-terminus might be responsible for enhanced potency.

To test the role of the C-terminal residues, we performed alanine scanning mutagenesis of the seven C-terminal residues of C-furSema (Figure 2.3A & B). As expected, mutation of the C-terminal arginine of C-furSema to alanine, R779A, dramatically decreased its inhibition potency by greater than two orders-of-magnitude (IC₅₀ = 4.5 ± 0.2 mM). Surprisingly, no other mutation decreased C-furSema potency. In fact, the R778A was slightly more potent, consistent with a recent report of a role for the C-1 position in tuning potency ⁽⁹¹⁾. These data confirm the importance of a C-terminal arginine in Sema3 binding to Nrp-1, but indicate that the residues directly upstream minimally contribute to potent competitive binding to Nrp-1. Therefore, the enhanced potency of C-furSema

relative to other peptide inhibitors cannot be explained by additional interactions within the region directly proximal to the C-terminal arginine.

Contribution of the N-terminal helical region

In addition to the C-terminus, the N-terminal sequence of C-furSema is conserved across species. Furthermore, secondary structure predictions indicate α -helical propensity for the eleven amino acids centered around the cysteine (Figure 2.4A). Notably, this is the only predicted structured region in the otherwise extended C-terminal basic domain of Sema3. Based on this, we hypothesized that the N-terminus may be involved in binding to Nrp-1. To test this, we produced a protein with half of the predicted helix deleted but which retained the conserved cysteine residue necessary and sufficient for dimerization (DN-C-furSema). Based on a simple avidity model, DN-C-furSema should have unaltered inhibitory potency. Strikingly, DN-C-furSema was approximately five-fold less potent than C-furSema ($IC_{50} = 111 \pm 21$ nM and 25 ± 3 nM, respectively) (Figure 2.4B). This means that DN-C-furSema has 3.6 ± 0.6 KJ mol⁻¹ decrease in binding free energy compared to C-furSema. These data suggest that the N-terminal region of C-furSema, centered around the conserved cysteine, contributes to potent competitive inhibition of VEGF-A binding to Nrp-1. However, this could be due to either direct binding of the N-terminal region to Nrp-1 or indirect effects of orienting the two C-terminal arginines for optimal Nrp binding.

The conserved cysteine of C-furSema is required both for oligomerization and potent competitive Nrp-1 binding. Interestingly, the cysteine is centered within the predicted N-terminal helix. This led us to examine the possibility of an additional role for the intermolecular disulfide in maintaining the structure of the N-terminal region. Thus, we compared the secondary structure of C-furSema and C-furSema^{Mon} using CD. The overall spectra are consistent with the predicted secondary structure of C-furSema, an overall coil with a smaller helical component. The difference spectrum clearly shows a loss of helical character in C-furSema^{Mon} (Figure 2.4C). Fitting the individual spectra reveals an approximately 30% loss in helicity in C-furSema^{Mon}, with 16% overall helical composition for C-furSema compared to 11% for C-furSema^{Mon}. These data indicate that the conserved cysteine that forms the key intermolecular disulfide in Sema3F is not only important for determining the oligomeric state of C-furSema but also in stabilizing the N-terminal helical region of C-furSema required for potent engagement of Nrp-1.

We interpret these data to indicate that the disulfide stabilized N-terminal helix directly contributes to Nrp-1 binding. However, it remains possible that this region indirectly affects potency by imposing conformational constraints that orient the C-furSema dimer. To distinguish between these possibilities, we designed a heterodimer composed of one subunit of C-furSema and one subunit containing only the thirteen N-terminal helical residues (C-furSema^{Het}) (Figure 2.5A). This construct contains the full N-terminal helix but only a single C-terminal arginine. This unique disulfide linked heterodimer was produced and purified to >95% purity (Figure 2.5B). Strikingly, C-furSema^{Het} was as potent as C-furSema at inhibiting VEGF-A-dependent activation of endothelial cells (Figure 2.5C) and VEGF-A binding to Nrp-1 (Figure 2.5D, $IC_{50} = 35 \pm 3$ nM and 24 ± 1 nM, respectively). This is in stark contrast to C-furSema^{Mon}, with an $IC_{50} = 1.3 \pm 0.7$ mM (Figure 2.5D). These data emphasize the importance of the N-terminal helical region and demonstrate that C-furSema potency is determined by a hetero-bivalent mechanism combining a C-terminal arginine and structured N-terminal helical region.

Discussion

Together, these data demonstrate that Sema3 family members engage Nrp-1 utilizing two distinct regions in their C-terminal domain, a C-terminal arginine and upstream helical region (Figure 2.6). This engagement results in potent competitive binding to Nrp-1 that antagonizes VEGF binding and cellular activation. Importantly, the decreased potency observed between dimeric and monomeric forms of C-furSema is primarily due not to the presence of two C-terminal arginine motifs, but instead the presence of the stable helical motif, as demonstrated by the potency of C-furSema^{Het}. These data indicate that the potent competitive binding of C-furSema to Nrp-1 is determined by a unique hetero-bivalent mechanism requiring only one C-terminal arginine and the novel upstream helical region.

Previously, it has been shown that the exon seven encoded residues of VEGF-A engage the L1 loop of the Nrp-1 b1 domain, enhancing binding and controlling Nrp-1 receptor selectivity⁽⁴⁶⁾. In contrast, the L1 loop of Nrp-1/2 does not play a role in selective Sema3 binding⁽⁹²⁾. Our current data demonstrate that Sema3s utilize its upstream helical motif to enable potent hetero-bivalent engagement of Nrp. The physical location of the Sema3 helical binding site on Nrp-1 is an important future direction for both mechanistic insights into Sema3 function and inhibitor design.

Since Nrp has critical roles in pathological angiogenesis and aberrant axon guidance, significant effort has been devoted to producing Nrp inhibitors. Peptide and small molecule inhibitors have been produced against the C-terminal arginine binding pocket, but generally possess modest (μM) potency ^(57, 86, 90, 93). We demonstrate that by coupling inhibitor oligomerization with covalent tethering of the helical and C-terminal arginine binding motif, a two order-of-magnitude gain in inhibitory potency can be achieved. The identification of two distinct Nrp-1 binding sites that, when tethered together, produce a potent inhibitor presents exciting possibilities for fragment-based design strategies combining existing inhibitors of the C-terminal arginine binding pocket with novel helical motif binding site inhibitors.

The physiological role of furin processing in the regulation of Sema3 signaling, as opposed to inhibition of VEGF binding, remains to be determined. While inhibition only requires avid binding to a single Nrp receptor, Sema3 signaling minimally requires engagement of two receptor molecules and assembly of the signaling complex. Our data indicate that, at a minimum, furin processing is required to activate Sema3 for Nrp b1-domain binding by liberation of a C-terminal arginine. Importantly, C-furSema^{Het} maintains potent engagement of Nrp, suggesting that furin processing of a single subunit of the Sema3 dimer may be sufficient for potent activation. Alternatively, furin processing may effect Sema3 engagement of the Nrp b1 domain quantitatively such that the different forms have progressively increasing signal potency from unprocessed to singly processed to dual processed.

Sema3 engagement of Nrp is more complex than VEGF in that two distinct domains are required. Both Sema3 C-terminal domain binding to the Nrp b1 domain and Sema3 Sema domain binding to the Nrp a1 domain are important for Sema3 signaling ^(36, 44). Recent structural work has provided significant insight into the contribution of the Nrp a1 domain in Sema3 binding ⁽⁹⁴⁾ and assembly of the active Sema3/Plexin/Nrp complex ⁽⁹⁵⁾. The specific contribution of a1 and b1 domains in terms of binding potency, specificity, and coupling between the two interacting domains is an active area of research ⁽⁶⁹⁾.

The ability of Sema3 to engage the Nrp b1-domain has clear implications for Sema3 signaling in the nervous system but also in the cardiovascular systems. For example Sema3A, which is critical for nervous system development ⁽²⁷⁾, has been shown to inhibit VEGF-dependent angiogenesis, yet acts as a vascular permeability factor ⁽⁷³⁾. Inhibition of VEGF is consistent with our data demonstrating direct competition for Nrp binding. However, induction of vascular permeability by Sema3 was found to be due to specific Nrp-dependent signaling rather than competitive binding. It is possible that these two functions of Sema3

in the cardiovascular systems are differentially regulated by furin processing. Indeed, furin processing of Sema3 family members may have significant physiological implications for regulated function in both nervous and cardiovascular systems ⁽⁶⁴⁾.

Note: Part of this chapter has been published and is reproduced here for completeness of the dissertation ⁽⁹⁶⁾.

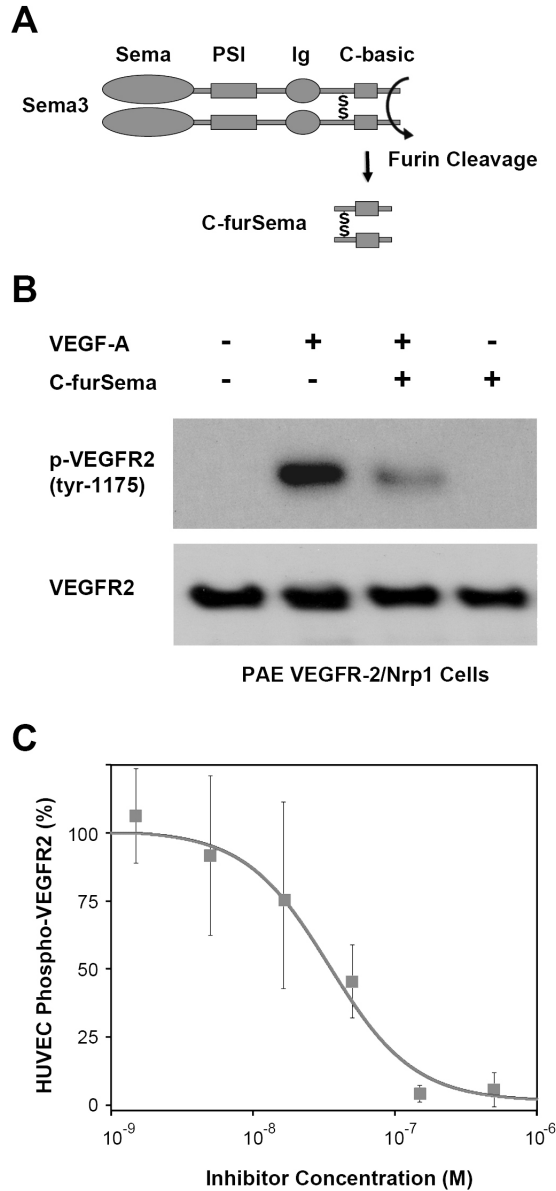


Figure 2.1: *C-furSema* potently inhibits VEGF-A mediated VEGFR-2 activation *in situ*. **A)** A schematic representation of Sema3 highlighting the furin-processed C-terminal domain (*C-furSema*). **B)** Activation of PAE cells stably overexpressing *Nrp-1* and VEGFR-2 by VEGF-A is inhibited by *C-furSema* as demonstrated by a decrease in VEGFR-2 Tyr-1175 auto-phosphorylation. **C)** *C-furSema* is a potent dose-dependent inhibitor of VEGF-A mediated HUVEC activation as demonstrated by sandwich ELISA ($IC_{50} = 34 \pm 15$ nM). Phospho-VEGFR-2 levels were normalized to VEGF-A alone and 1 μ M sunitinib.

A

C-furSema GLIHQY**C**QGYWRHVPPSPREAPGAPRSPEPQDQKKPRNRR
 GLIHQY**C**QGYWRHVPPSPREAPGAPRSPEPQDQKKPRNRR

C-furSema^{Mon} GLIHQY**S**QGYWRHVPPSPREAPGAPRSPEPQDQKKPRNRR

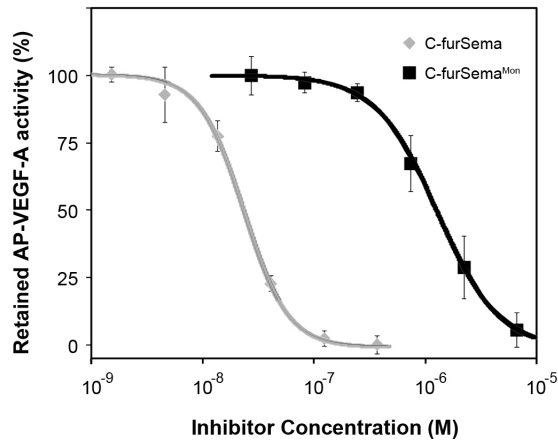
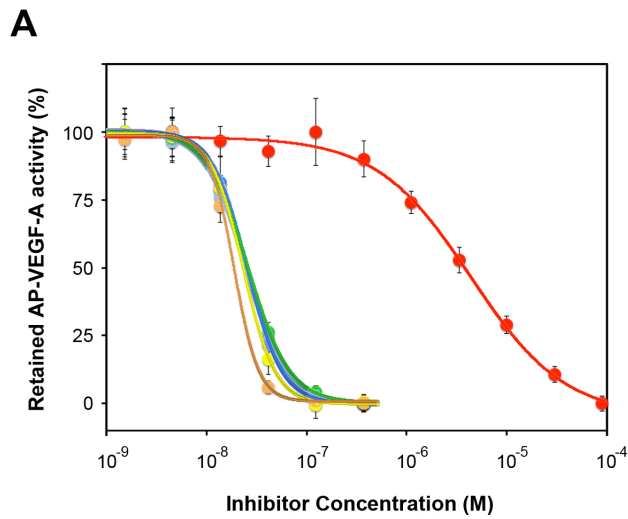
B

Figure 2.2: Effect of the intermolecular disulfide on C-furSema potency. A) Comparison of dimeric C-furSema and C-furSema^{Mon} B) reveals a critical role for the conserved inter-molecular disulfide C-furSema (grey line, $IC_{50} = 24 \pm 1$ nM) and C-furSema^{Mon} (black line, $IC_{50} = 1.3 \pm 0.7$ mM) in inhibiting VEGF-A binding to Nrp-1.



B

Sequence	IC ₅₀
● KKPRNRR (WT)	25 ± 2 nM
● AAPRNRR	23 ± 1 nM
● KKARNRR	25 ± 2 nM
● KKPANRR	25 ± 4 nM
● KKPRARR	23 ± 1 nM
● KKPRNAR	18 ± 1 nM
● KKPRNRA	4500 ± 200 nM

Figure 2.3: C-furSema C-terminal arginine contributes to high affinity binding to Nrp. A) An alanine scan of the C-terminus of C-furSema was performed. The ability of C-furSema and mutants to inhibit AP-VEGF-A binding to Nrp-1 was determined. B) Inhibition curves were utilized to determine peptide potency (IC₅₀), with a significant decrease only observed with the C-terminal arginine mutant.

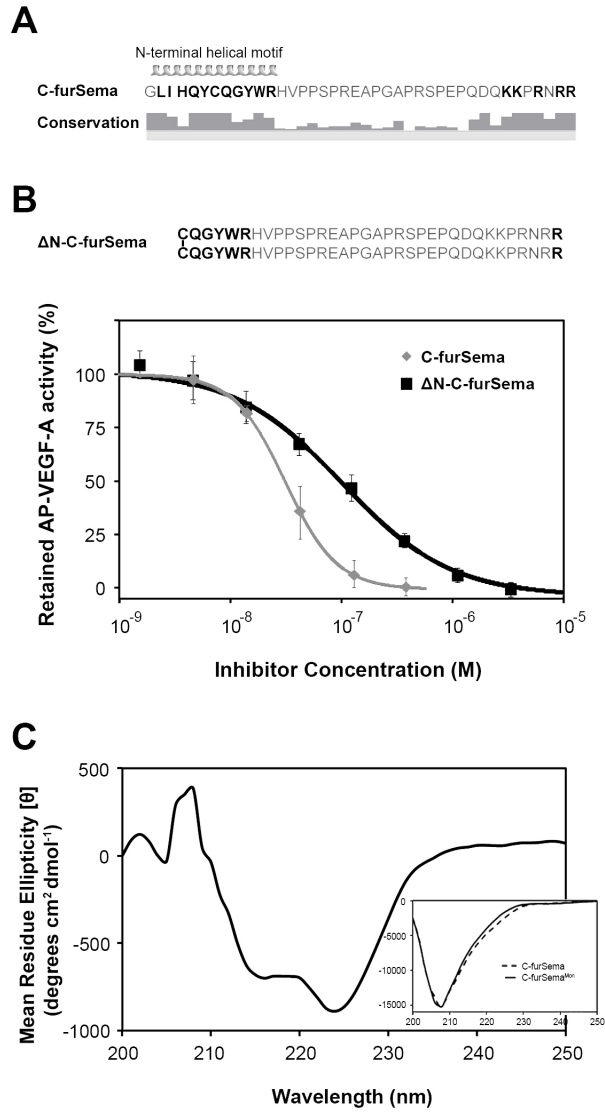


Figure 2.4: The N-terminal helical motif is a structured region that contributes to potency. **A)** Sequence, predicted secondary structure, and conservation of C-furSema (based on an alignment of human, rat, mouse, cow, dog, chicken, and zebrafish orthologs). **B)** DN-C-furSema, a N-terminal helical deletion decreases the potency of C-furSema ($IC_{50} = 111 \pm 21$ nM vs. 25 ± 3 nM, respectively). **C)** Difference CD spectrum of dimeric versus monomeric C-furSema reveals a characteristic loss in α -helical content. (Inset) CD spectra of dimeric C-furSema (dashed line) and C-furSema^{Mon} (solid line).

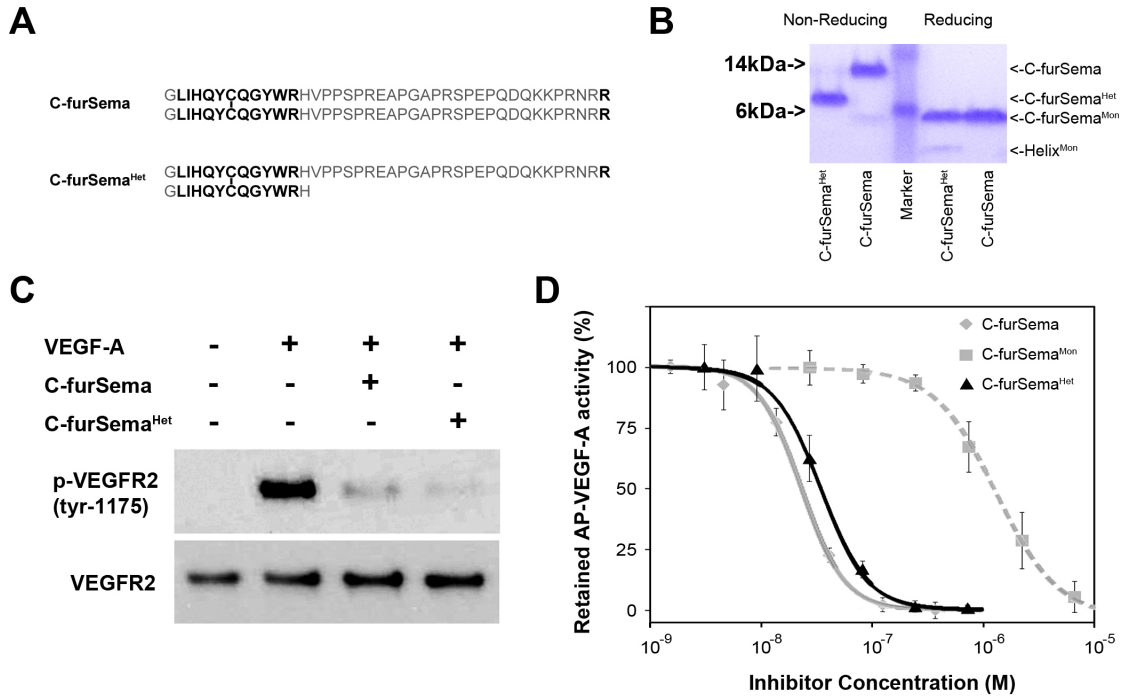


Figure 2.5: The helical motif determines potent competitive Nrp-1 binding. A) To determine the contribution of N-terminal helical region in mediating Nrp inhibition, C-furSema^{Het} was synthesized. B) Comparison of non-reducing versus reducing SDS-PAGE demonstrates the purity and correct intermolecular disulfide bond formation of C-furSema and C-furSema^{Het}. C) C-furSema and C-furSema^{Het} equivalently inhibit VEGF-A dependent activation of PAE cells and D) have nearly equal potencies, $IC_{50} = 24 \pm 1$ nM vs. $IC_{50} = 35 \pm 3$ nM, respectively.

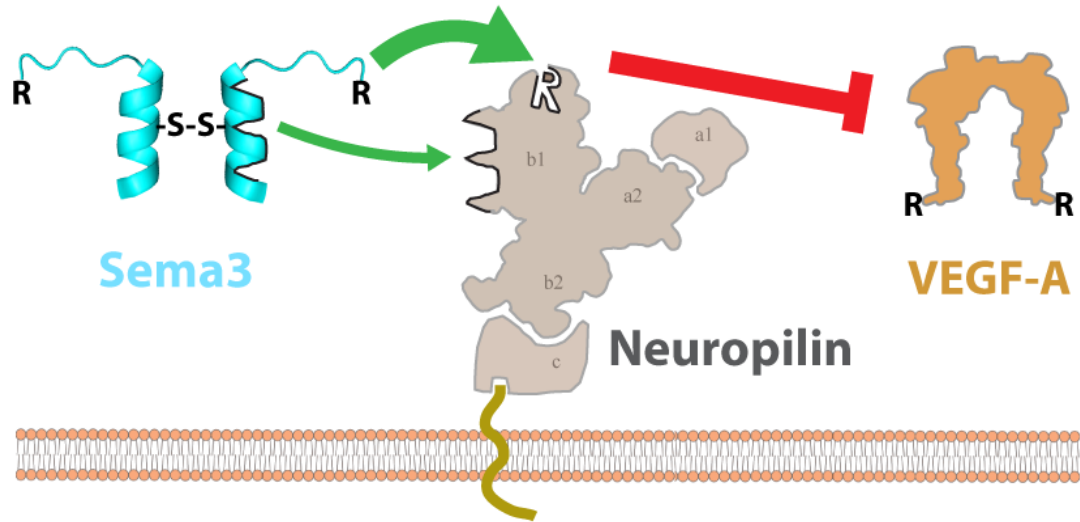


Figure 2.6: Sema3 family members engage Nrp-1 utilizing two distinct regions in their C-terminal domain, a C-terminal arginine and upstream helical region. This divalent synergistic engagement results in potent competitive binding to Nrp-1 that antagonizes VEGF mediated angiogenesis.

CHAPTER THREE

Semaphorin 3F anti-angiogenic activity regulation

Introduction

Sema3 is a family of secreted cytokines with seven family members playing essential roles in Nrp-plexin mediated axon guidance ⁽²⁷⁾. Biochemical and animal studies have shown that both Nrp and Plexin are essential for correct neuronal patterning during early development largely by delivering axonal repulsive signal ⁽²⁹⁻³²⁾. However, interestingly, Nrp expression in certain neurons has also been demonstrated to be able to change their interpretation of Sema3 signal from axonal repulsion to attraction ^(33, 34).

Recent studies have shown that Sema3 also plays anti-angiogenic roles under physiological and pathological conditions. For instance, Sema3F expression in outer retina is critical for maintaining this part of retina avascular, and Sema3E serves as a guidance cue for retina vasculature ^(42, 43). Studies have also shown that Sema3 family members are mutated or down-regulated in many cancers, including lung, ovary, stomach, breast, and prostate cancers ^(70, 74, 75). Restoring the expression of Sema3B and Sema3F has been reported to inhibit cancer progression both in vitro and in vivo ⁽⁷⁶⁾.

All Sema3 family members are disulfide-bonded homo-dimers with 4 domains including, a 500 amino acid Sema domain, a PSI domain, an Ig-like C2-type (immunoglobulin-like) domain, and a short C-terminal basic domain. A single disulfide bond links the molecule into a dimer and is located in the helical motif from the c-terminal basic domain of Sema3, which is critical for Sema3 to interact with two receptor molecules for signaling.

Since Sema3 serves critical roles in Nrp-mediated axon guidance and angiogenesis, intensive effort have been made to define the mechanisms of ligand and receptor interactions. Sema3 functions by binding to Nrp using two different regions, the Sema domain and the C-terminal basic rich region ⁽¹³⁾. The Sema domain of Sema3 family members binds to the CUB domain of Nrp and this interaction determines the specificity of the ligand/receptor pairing ^(36, 44, 94). The C-terminal basic rich region of Sema3 mediates the high affinity Nrp interaction by binding to its coagulation factor domain b1 ⁽⁴⁴⁾. Interestingly, it has been demonstrated VEGF also binds to Nrp b1 domain, just as Sema3, and they compete for Nrp binding ⁽⁴⁰⁾.

Since it has been shown that the anti-angiogenic role of *Sema3* is to physically compete with VEGF for Nrp binding ⁽⁴⁰⁾, the interaction between the *Sema3* C-terminal basic domain and Nrp b1 domain is important for not only engaging Nrp in plexin mediated axonal guidance, but also in *Sema3* mediated anti-angiogenic activities. Structural studies have shown that the Nrp b1 domain has a C-terminal arginine-binding pocket and is able to bind to ligands with a C-terminal arginine ⁽⁴⁷⁾. Indeed, it has been shown that the interaction between VEGF-A and the first coagulation factor (b1) domain of Nrp is largely mediated by VEGF-A C-terminal arginine ^(46, 47). The mechanism is widely used by four other VEGF family members, VEGF-B, -C, -D and PlGF to interact with two Nrp family members, Nrp-1 and Nrp-2. We and other groups have previously shown that the C-terminus of *Sema3* is proteolytically processed by furin, which releases a C-terminal arginine and is required for competing with VEGF-A for binding to the Nrp b1 domain ⁽⁴⁰⁾.

Interestingly, we have also shown that, besides the C-terminal arginine motif, a conserved helical motif in the C-terminal basic domain of *Sema3F* is required for high affinity binding to Nrp b1 domain as shown in chapter 3 and ⁽⁹⁷⁾. Indeed, covalent tethering of this predicted helical binding motif leads to synergistic binding to Nrp, and two orders of magnitude better in binding affinity compared to the other C-terminal arginine based modalities ^(57, 85, 86, 90). Interestingly, the helical motif is conserved in all *Sema3* family members, suggesting this tethering mode is widely utilized in *Sema3* for high affinity Nrp binding.

We have also shown that it is the helical nature of this motif that is critical for Nrp binding ⁽⁹⁷⁾. Indeed, a mutation destabilizing the helical nature of this motif results in near two orders of magnitude loss in binding affinity. In order to determine its helical nature and directly visualize this helix, we have determined the crystal structure of this motif. Our structure showed that indeed this structure is a versatile helix. An intermolecular disulfide bond and further molecular interactions hold two copies of helical motifs into a dimer, which stabilizes the helical structure. Further, It is notable that *Sema3A* possesses three furin processing sites between the helical region and the C-terminal arginine, and different C-terminal furin processed *Sema3A* isoforms show a range of potencies, which correlates with the distance between the helical and C-terminal arginine binding motifs.

Methods

Protein expression and purification

Proteins used in plate binding assay were expressed and purified using the similar method as reported before ⁽⁴⁰⁾. Briefly, rat Nrp-1 coagulation (b1) domain (residue 274 to 429) and human Sema3F helical motif (residue 740 to 752) fusion construct was cloned into pET-28 vector using the Nde1 and EcoR1 sites, expressed in *E. coli*, and purified using IMAC nickel-charged resin. The protein was then left in the presence of thrombin on the nickel resin for 16 hours at 20°C to remove the His tag and facilitate intermolecular disulfide bond formation at the same time. The dimer is then purified by heparin affinity chromatography and eluted at 600 mM NaCl in Tris pH 8.0. Nrp-1-b1b2 (residue 274 to 586) and Nrp-2-b1b2 (residue 276 to 597) was expressed in *E. coli* and purified using nickel affinity chromatography (IMAC) followed by heparin affinity chromatography. Alkaline Phosphatase (AP) fused VEGF-A or VEGF-C was produced from Chinese Hamster Ovary (CHO) cells as discussed in chapter 2.

Crystal Structure Determination and Refinement

Single, high-quality crystals with 2 dimer molecules in the asymmetric unit were obtained via hanging drop vapor diffusion using a Mosquito liquid handling robot (TTPLabtech) using a 200-nL drop with Nrp-1 b1b2-Sema3F helix fusion protein (4.8 mg/mL) in 3 M formate, 100mM HEPES pH 7.5 at 20°C. Diffraction data were collected on the 22-ID beamline of SERCAT at the Advanced Photon Source, Argonne National Laboratory (Table 3.1) at 110K at a wavelength of 1.0 Å. Data were processed using HKL2000 ⁽⁹⁸⁾. The b1 domain of a previously published rat Nrp-1 b1b2 domain was used as a search model for molecular replacement using CCP4i ⁽⁴⁷⁾. The structures were then fully built and refined via iterative model building and refinement using Coot ⁽⁹⁹⁾ and Refmac5 ⁽¹⁰⁰⁾, respectively. Stereochemistry of the model was analyzed using Mol-Probity ⁽¹⁰¹⁾. Molecular graphics were prepared using Pymol ⁽¹⁰²⁾.

C-furSema, Sema3A and Variant Production

C-furSema (GLIHQYCQGYWRHVPPSPREAPGAPRSPEPDQKKPRNRR) and homodimeric peptide derived from a furin processed form of Sema3A C-terminus (LNTMDEFCEQVWKRDRKQRRQRPGHTPGNSNKWKHLQENKKGRNRRTHEFERAPR), and other furin processed shorter isoforms, were synthesized and purified in the same way as discussed in chapter 2 (Neo-Peptide, Cambridge, MA). C-furSema and all Sema3A C-terminus derived peptides were well behaved in solution and soluble to >1 mM.

Protein and peptide concentrations were determined using OD₂₈₀ measured on a Nanodrop 1000 (Thermo Fisher Scientific, Wilmington, DE).

In vitro inhibition assays

Plate-based inhibition assays were performed as discussed in chapter 2 and previously reported ⁽⁴⁰⁾. Briefly, 410 μ M *para*-nitrophenol phosphate (p-NPP) hydrolyzed/min/ μ L of AP-VEGF-A or 5.0 mM *para*-nitrophenol phosphate (p-NPP) hydrolyzed/min/ μ L of AP-VEGF-C was combined with C-furSema or Sema3A-derived peptides in binding buffer (20 mM Tris, pH 7.5/50 mM NaCl), incubated with Nrp-1 or Nrp-2 affinity plates for 1 hour at 25°C. The plates were then washed and developed in the same way as described in chapter 2. Experiments were performed in triplicate and results reported as the mean \pm 1 standard deviation. An unpaired t-test was used to compare IC₅₀ values.

Results

Structure determination and the model

Since the Sema3F helical motif of the c-terminal basic domain has limited solubility, with a maximal solubility in Phosphate Buffered Saline (PBS) of 20 μ M, a construct of this motif fused to the C-terminus of its receptor Nrp-1 b1 domain was designed with a Val-Asp linker between them. The recombinant protein was expressed and purified as stable soluble protein for crystal trials. The diffraction data were collected at 2.6 Å, and the structure was determined by the molecular-replacement method using rat Nrp-1 b1 domain as a searching model ⁽⁴⁷⁾. The Sema3F helical motif was manually built with coot ⁽⁹⁹⁾ and refined using refmac5 ⁽¹⁰⁰⁾ to generate the final model (Table 3.1).

The final refined model has 2 dimer molecules in the asymmetric unit (Figure 3.1). Each monomer molecule has 171 of the 175 residues built into the final refined model. The N-terminal residues (Gly-Ser-His-Met) are part of the thrombin digestion site and restriction enzyme site for cloning, and the electron density for these residues are not clear defined and thus are not included in this model. The rest of the structure including the Sema3F helical motif has well determined electron density and is fully built. This model thus has 684 residues total together with 251 water molecules.

In each of the 4 recombinant protein monomers, the predicted Sema3F helical motif indeed adopts a α -helical secondary structure, which is consistent with

previous circular dichroism results ⁽⁹⁷⁾. Importantly, the Sema3F helical domain extends out from the C-terminus of Nrp-1 b1 domain, and does not make contact with the Nrp-1 b1 domain that it is fused with (Figure 3.2).

A disulfide bond links Sema3F helical monomers together into a dimer, which is known to be critical for Sema3 activity (Figure 3.3A). This helical dimer is further stabilized by other interactions. Interestingly, these two monomers are different in helical content, one of which is highly helical while the other one is only partially helical in nature. The I434 residue from the monomer molecule with high helical content forms a hydrophobic interaction with the ring of Y437 in the other partial helical monomer (Figure 3.3B). The rings from Y441 and W442 residues from the same full helical monomer together with I434 from the other partial helical monomer form a hydrophobic niche for the disulfide bond. These features are consistent in the other molecule in the asymmetric unit.

Within the Sema3F helical motif dimer, two monomer molecules adopt different conformations especially in the residues located to the C-terminus of this motif after the disulfide bond (Figure 3.3A). In one molecule, a continuous helix is present from N-terminus to C-terminus of this motif, with a kink present at the site of disulfide bond. In the other monomer molecule, a similar kink at the site of disulfide bond is also observed, however, the residues located to the C-terminus of this motif after the disulfide bond adopts a loop conformation and folds back to the helical structure. This indicates that this part of the structure is labile and is able to adopt multiple conformations.

C-furSema serves as a pan-Nrp inhibitor

Besides the first member of the VEGF ligand family, VEGF-A, vertebrates also have four other VEGF family members, named VEGF-B,-C,-D, and placental growth factor (PlGF) ⁽¹⁰⁾. The different family members utilize different Nrp family members and play both unique and partially overlapping *in vivo* roles in the vascular system. Angiogenesis is mainly regulated by VEGF-A and Nrp-1 interaction, whereas lymphangiogenesis is largely controlled by VEGF-C and Nrp-2 interaction ⁽¹¹⁾. Since we have demonstrated that a peptide inhibitor C-furSema derived from the C-terminus of Sema3F is able to potently inhibit VEGF-A and Nrp-1 interaction, we sought to determine whether C-furSema inhibits VEGF-C and Nrp-2 interaction as well. To define whether C-furSema works as a pan-Nrp inhibitor, we measured the inhibitory potency of the C-furSema in inhibiting VEGF-C and Nrp-2 interaction. Interestingly, C-furSema inhibits VEGF-A binding to Nrp-1 affinity plate and VEGF-C binding to Nrp-2 affinity plate

equally well (Figure 3.4, $IC_{50} = 20 \pm 2$ nM and 17 ± 1 nM, respectively). These data suggest that Sema3 represents a natural pan-Nrp inhibitor, and is able to inhibit both angiogenesis and lymphangiogenesis.

Insights into distinctly furin processed forms of Sema3A

There are between one and three furin cleavage sites in the C-terminal basic domain of different Sema3 family members, which produce natural variants with different spacing between C-terminal arginine and the dimeric helical region. While Sema3F possesses one furin consensus site, Sema3A possesses three. These three sites in Sema3A are known to be processed and important for function ⁽⁸⁴⁾ (Figure 3.5). To define the role of the multiple furin processing sites in Sema3A, we measured the inhibitory potency of the three processed variants of Sema3A. The furin-processed forms similar in length to C-furSema, Sema3A.2 and Sema3A.3, are similar in potency (Figure 3.5, $IC_{50} = 45 \pm 12$ nM and 27 ± 5 nM, respectively). Intriguingly, the shortest form, Sema3A.1 shows significantly reduced potency ($IC_{50} = 1.1 \pm 0.3$ mM). This form has the same amino acid sequence in both helical and C-terminal motifs, differing only in the spacing of these motifs. These data suggest that furin site selection may represent a natural mechanism to produce Sema3A proteins with differing Nrp binding motif spacing, providing a unique mechanism for fine-tuning Sema3A/Nrp-1 binding.

Discussion

Our previous work demonstrated that a helical motif from the C-terminal basic domain of Sema3F contributes a second binding site for engaging Nrp-1, and it is both necessary and sufficient for enhancing the interaction between Sema3 and Nrp ⁽⁹⁷⁾. It has been suggested that the motif adopts α -helix secondary structure and the helical nature of this motif is critical for Nrp binding. In order to define the helical nature of this motif, we have determined its structure. We have shown that this region adopts an α -helical structure, which is mainly stabilized by an intermolecular disulfide bond, consistent with our previous study. We also define molecular interactions that help stabilize the helical dimer.

Nrp expression is observed in tumor, and its overexpression promotes tumor progression and metastasis *in vivo* for a variety of solid tumors ^(18, 103, 104). Indeed, Nrp-1 has been shown to be important for tumor angiogenesis and progression, while Nrp-2 is shown to promote tumor metastasis by increasing tumor-associated lymphangiogenesis ^(105, 106). As a result, it is urgent to develop pan-

Nrp inhibitor to inhibit both processes for optimal cancer therapy. Interestingly, we have demonstrated that a peptide inhibitor derived from the C-terminus of Sema3F named C-furSema is able to potently inhibit both VEGF-A binding to Nrp-1 and VEGF-C binding to Nrp-2 at similar IC_{50} s. This represents a promising lead compound and may help the future rational design of potent pan-Nrp inhibitor.

Our data demonstrate that the furin cleavage sites in the C-terminal domain of Sema3A are non-equivalent in terms of receptor binding. Thus, C-terminal furin processing functions not only as a binary activation mechanism but can produce activated species with differing physical properties. Recent data indicate that this may have profound physiological implications. Mutations of two different residues in the Sema3A.1 furin site, R730Q and R733H, have recently been shown to cause Kallmann's syndrome, a serious genetic disease resulting from aberrant Sema3A dependent axon guidance ⁽¹⁰⁷⁾. Thus, differential furin processing of the C-terminal domain of Sema3 can have profound functional and physiological effects in human disease. Combined with these mechanistic insights, discovery of these disease associated mutations underline the importance of future studies of the regulation and function of differential furin processing of Sema3 in regulating Nrp engagement in both neuronal and cardiovascular signaling.

Note: Part of this chapter has been published and is reproduced here for completeness of the dissertation ⁽⁹⁶⁾.

Table 3.1. Data collection and refinement statistics

Data collection

Beamline	APS 22-ID
Space group	P4 ₁
Wavelength	1.00000
Unit-cell parameters	88.817, 88.817, 181.575
Unique reflections	38690
Completeness (%)	90.6 (94.2)
Resolution (Å)	2.6 (2.7-2.6)
Rmerge (%)	7.6 (36.3)
Redundancy	2.7 (2.6)
I/σ(I)	10.6 (2.03)

Refinement

Resolution Limits (Å)	20.00-2.61
# reflections/# to compute Rfree	36675/1936
R (Rfree)	19.2 (22.5)
# protein residues	684
# solvent molecules	251

Ramachandran

Most favored	98.2
Allowed	1.8
Disallowed	0

RMS deviation

Bond, Å	0.006
Angle, °	0.970



Figure 3.1: The Nrp-1-Sema3F recombinant protein shows interesting tetrahedron like shape with each tip of the 4 Nrp-1 b1 domains (purple) pointing out. Sema3F helical motifs (green) are buried in the hydrophobic core formed by the bottoms of 4 Nrp b1 domains stacking together.



Figure 3.2: Sema3F helical motif from the C-terminal basic domain extends out of the Nrp-1 b1 domain.

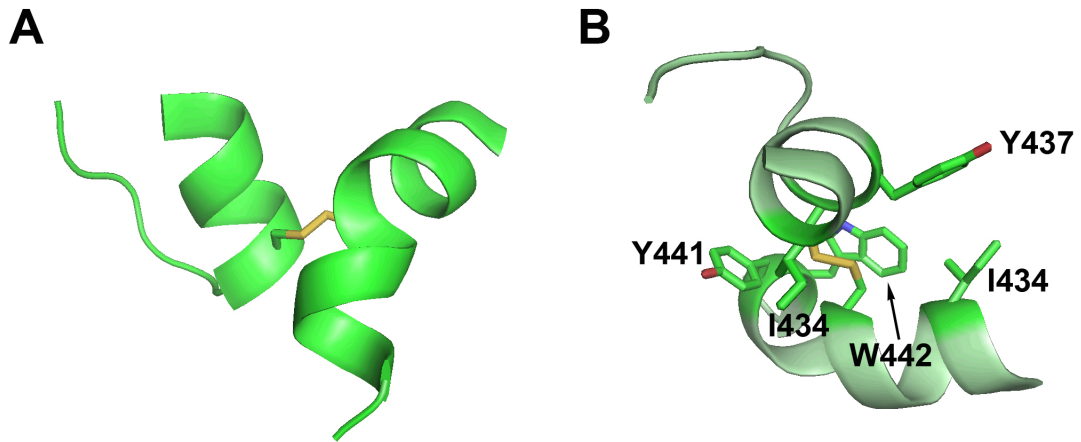


Figure 3.3: Sema3F helical motif from the C-terminal basic domain is mainly stabilized by an intermolecular disulfide bond, and to a less extent by further molecular interactions.

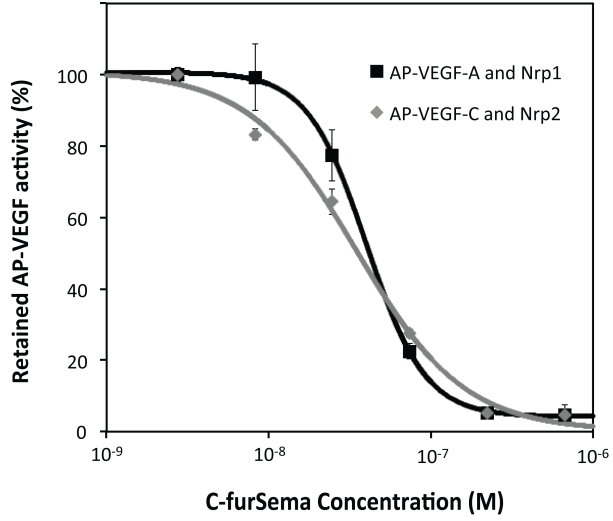



Figure 3.4: C-furSema serves as a pan-Nrp inhibitor. C-furSema inhibits VEGF-A binding to Nrp-1 affinity plate (Black line, $IC_{50} = 20 \pm 2$) and VEGF-C binding to Nrp-2 affinity plate (grey line, $IC_{50} = 17 \pm 1$ nM) at similar IC_{50} s.

Sema3A  **Furin1** **Furin2** **Furin3**
 715 - LNTMDEF**CE**QVWKR - (2) - **KQRR** - (22) - **RNRR** - (5) - **RAPR** - (2)

Isoforms	IC₅₀
Sema3A.1	1100 ± 300 nM
Sema3A.2	45 ± 12 nM
Sema3A.3	27 ± 5 nM

Figure 3.5: Differential furin processing of Sema3A. Sema3A possesses a disulfide bonded dimeric helical motif followed by three furin consensus (RXXR) sites. These three distinct furin processing sites produce C-terminal domains of significantly different length and potencies.

CHAPTER FOUR

The physical mechanism of Neuropilin function in VEGF signaling

Introduction

Vascular endothelial growth factor (VEGF) is a critical cytokine regulating the patterning of vascular structure during development, and homeostasis in adult in many systems and animal models ^(9, 10, 17, 108-110). Interestingly, VEGF was first identified as a tumor vascular permeability factor (VPF) because it is released by tumor cells with the ability to stimulate vascular leakage ^(4, 111, 112). VEGF was then reported to be central to tumor angiogenesis in many types of solid tumors ⁽¹¹³⁻¹¹⁵⁾, which is one of the most critical steps in tumor progression ⁽¹¹⁶⁾. Hyper-activation of VEGF also causes aberrant vascularization in many other disease conditions, such as rheumatoid arthritis, diabetic retinopathy, and age-related macular degeneration (AMD) ^(117, 118).

VEGF functions by binding two families of type I single transmembrane receptors, the receptor tyrosine kinase family members, VEGF receptor 1 (VEGFR1) and VEGFR receptor 2 (VEGFR-2), and Neuropilin family members, Neuropilin 1 (Nrp-1) and 2 (Nrp-2) ^(64, 119-121). VEGFR-2 is considered the main VEGF signaling receptor under physiological and pathological conditions ^(16, 122). VEGFR-2-null mutation leads to the absence of blood vessels and failure of vasculogenesis in mouse embryos ^(16, 122). Nrp-1 works as a mandatory co-receptor. The importance of Nrp-1 in angiogenesis is demonstrated in knockout mice, which show similar embryonic lethal phenotype to VEGFR-2 null mice ^(15, 32).

VEGFR-2 belongs to the class V receptor tyrosine kinase family composing of seven extracellular immunoglobulin-like (Ig) domains, a transmembrane domain and an intracellular portion containing a split kinase domain ⁽¹²³⁾. VEGF ligands exist as disulfide-linked dimers that bind directly to the membrane distal domains (d1-3) of VEGFR receptors and cause receptor dimerization ^(124, 125). However, ligand binding is necessary but not sufficient for receptor activation. Recent evidence showed that dimerization of the membrane proximal seventh Ig domain (VEGFR-2 D7) is critical for the activation of the intracellular kinase domain and subsequent signaling ⁽¹²⁶⁾. Based on these data, it was suggested that ligand binding promotes VEGFR-2 D7 dimerization, which is critical for physically coupling ligand binding to receptor activation.

Nrp is a co-receptor with critical roles in vascular endothelial growth factor receptor 2 (VEGFR-2) mediated angiogenesis ^(13, 14, 64, 120). It has been long accepted that VEGF crosslinks Nrp-1 and VEGFR-2 to form a holo-signaling complex, which leads to full VEGFR-2 activation ⁽¹²⁰⁾. Interestingly, accumulating data suggest that VEGFR-2 and Nrp-1 can directly interact in the absence of ligand ^(127, 128). For example, many groups have shown that this complex is preformed in the absence of ligands in both receptor overexpression cell lines and primary cells ^(19, 128, 129), and this preformed complex is sufficient to enhance VEGFR-2 activation in the presence of VEGF ⁽¹⁹⁾. Further studies suggest that Nrp promotes VEGFR-2 activation via its extracellular domains. Indeed, it has been shown that the Nrp Fc fusion alone is sufficient to activate VEGFR-2 and promote vascular morphogenesis without VEGF added ⁽¹³⁰⁾. It has also been reported that Nrp Fc fusion is able to rescue the vascular bed defects in Nrp null mouse embryos without VEGF, while adding excess VEGF alone cannot, which suggests a unique and distinct requirement of Nrp and VEGFR-2 coupling for full VEGFR-2 activation ⁽²⁴⁾.

Although the importance of Nrp in VEGF signaling pathway is well established, the physical mechanism and specific role of Nrp is not understood. In order to define the role of Nrp in VEGFR activation, we have first determined the crystal structure of VEGFR-2 membrane proximal domain 7 active dimer, and then demonstrated that Nrp is directly physically coupled to VEGFR-2 D7 in the absence of VEGF-A. This interaction between Nrp-1 and VEGFR-2 D7 is further shown to be mediated by Nrp-1 b1b2 domain. To provide physical basis of this interaction, we have then determined the structure of Nrp-1 b1b2 domain and VEGFR-2 D7. Together with the biochemical results, we have demonstrated that VEGFR and Nrp are directly coupled to each other via the interaction between Nrp b1b2 domain and VEGFR-2 D7, and decoupling these two receptors is sufficient to inhibit VEGF signaling. This suggests a new mechanism of Nrp in VEGFR activation.

Methods

Protein production and purification

We have expressed, purified, and crystallized domain 7 from mouse VEGFR-2 (residues 663-755). The protein was expressed as a 6XHis-tagged protein from pET-28 (Novagen) in Rosetta-gami2(DE3) cells. Cells were grown at 37°C in Terrific-Broth media supplemented with 50mg/mL kanamycin. When cells reached OD₆₀₀=1.5, they were placed on ice for fifteen minutes, induced with

1mM isopropyl-D-thiogalactopyranoside (IPTG), and incubated for sixteen hours at 16°C. This protocol yielded approximately 10mg/L of soluble, correctly folded, and disulfide linked protein without the need for refolding. Cells were harvested and lysed using lysozyme and sonication. Protein was purified over His-Select affinity resin (Sigma-Aldrich). The 6XHis-tag was removed by incubation with thrombin (10U/mg protein) overnight at room temperature. Protein was finally purified using size-exclusion chromatography (20mM Tris, pH=7.5, 100mM NaCl) yielding >95% pure protein.

A fusion of rat Nrp-1 b1b2 (residues 274-586) linked to mouse VEGFR-2 D7 (residues 663-755) with an intervening Spe1 restriction site was introduced into the Nde1/EcoR1 sites of pET28b (Novagen). The protein was expressed in a similar way as mouse VEGFR-2 domain 7 construct discussed above as a 6XHis-tagged protein from pET-28 (Novagen) in Shuffle cells. This protocol yielded approximately 3 mg/L of soluble, correctly folded, and disulfide linked protein without the need for refolding. Protein was first purified over His-Select affinity resin (Sigma-Aldrich). The 6XHis-tag was cleaved by incubation with thrombin (10U/mg protein) overnight at room temperature. Protein was finally purified using heparin chromatography to remove the 6XHis-tag.

Alkaline Phosphatase (AP) fused Nrp and VEGFR-2 constructs were produced from Chinese Hamster Ovary (CHO) cells, and purified with heparin chromatography and His-Select affinity resin respectively similarly to previously reported ⁽⁹⁶⁾.

Crystallization

VEGFR-2 D7 protein was diluted 1/10 with MilliQ water and concentrated to 10mg/mL. Hanging-drop vapor diffusion trays were set up using a Mosquito crystallization robot with equal volume protein and reservoir solution. Single high quality crystals were obtained after two weeks at room temperature using a reservoir solution of 0.1M Succinic acid pH 7.0, 15% (w/v) PEG 3350. Crystals with overall dimensions of approximately 200 X 100 X 50 mm were rapidly soaked in reservoir solution supplemented with 15% ethylene glycol and flash frozen in liquid nitrogen.

To crystalize Nrp-1 b1b2 and VEGFR-2 D7 fusion protein, hanging-drop vapor diffusion trays were set up for Nrp-1 b1b2 and VEGFR-2 D7 fusion protein using a Mosquito crystallization robot with volume protein and reservoir solution ratio 3:1. Single high quality crystals were obtained after two months at room temperature using a reservoir solution of 0.1m MES pH6.5, 12% (w/v) PEG 20K.

Crystals with overall dimensions of approximately 100 X 100 X 100 mm were rapidly soaked in mineral oil and flash frozen in liquid nitrogen.

Structure determination

Diffraction data to 1.2 Å resolution for VEGFR-2 D7 and 2.9 Å for Nrp-1 b1b2 and VEGFR-2 D7 fusion protein were collected at the Southeast Regional-Collaborative Access Team (SER-CAT) 22-ID beamline at the Advanced Photon Source (APS) (Table 4.1 and 4.2). Data were indexed, integrated, and scaled using HKL2000⁽⁹⁸⁾. Intensity data were converted to structure factors using Truncate in the CCP4i suite⁽¹³¹⁾. The crystal structure of VEGFR-2 D7 was determined by molecular replacement using PHASER⁽¹³²⁾, with the first Ig-domain of MuSK (PDB 2IEP) as the search model⁽¹³³⁾. This 1.2 Å VEGFR-2 D7 structure and a previously published rat Nrp-1 b1b2 domain structure were used as a molecular replacement search model for Nrp-1 b1b2 domain and VEGFR-2 D7 using CCP4i⁽⁴⁷⁾. Iterative model building and refinement were accomplished using Coot⁽⁹⁹⁾ and Refmac5⁽¹⁰⁰⁾. TLS groups for use in refinement were derived from TLSMD⁽¹³⁴⁾. The final model of the VEGFR-2 D7 dimer included all residues and was fully refined with Rwork/Rfree=18/21 (Table 4.1). The Nrp-1 b1b2 and VEGFR-2 D7 fusion protein was refined with Rwork/Rfree=23/28 (Table 4.2).

Structural analysis

Analysis of the dimer interface was accomplished using PISA⁽¹³⁵⁾, multiple sequence alignment was performed using ClustalW⁽¹³⁶⁾, stereochemistry of the model was analyzed using Mol-Probity⁽¹⁰¹⁾, and molecular graphics were prepared using Pymol⁽¹⁰²⁾.

In vitro binding assays

Plate-based inhibition assays were performed similarly as discussed in chapter 2 and previously reported⁽⁴⁰⁾. Briefly, 41 mM *para*-nitrophenol phosphate (p-NPP) hydrolyzed/min/μL of AP-Nrp constructs were dialyzed into binding buffer (20 mM Tris, pH 7.5/50 mM NaCl), incubated with Nrp-1 affinity plates for 1 hour at 25°C, washed three times with PBS-T (0.01M Phosphate buffered saline, 0.1% Tween 20, pH 7.4), incubated with PBS-T for 3 minutes, aspirated, and developed by addition of 100μL of 1X alkaline phosphatase pNPP substrate⁽⁸⁸⁾ followed by quenching with 100μL of 0.5N NaOH. AP activity was quantitatively measured at

405nm using a SpectraMax M5 instrument (Molecular Devices, Sunnyvale, CA). For Nrp-1 b1b2 and VEGFR-2 D7 binding affinity measurement and VEGFR-2 D7 mutagenesis experiment, AP-VEGFR-2 D7 was added to Nrp-1 b1b2 coated plate. Binding curves were fit using a one-site specific binding mode to determine K_d (Graphpad Prism). Experiments were performed in triplicates and results reported as the mean \pm 1 standard deviation. An unpaired t-test was used to compare results.

In vitro antibody blocking assay

A previously published mouse derived anti-human Nrp-1 monoclonal antibody was further characterized with *in vitro* antibody blocking assays⁽¹³⁷⁾. Briefly, Nrp-1 b1b2 domain affinity plates were pre-incubated with 0.1 μ M of anti-Nrp-1 antibody in binding buffer (20 mM Tris, pH 7.5/50 mM NaCl) for 0.5 hour at 25°C. After incubation, 410 μ M *para*-nitrophenol phosphate (p-NPP) hydrolyzed/min/ μ L of AP-VEGF-A or 41 mM *para*-nitrophenol phosphate (p-NPP) hydrolyzed/min/ μ L of AP-VEGFR-2 D7 was added to the plates and incubated for another 0.5 hour at 25°C. The plates were then washed, developed and read the same way as described above in *In vitro binding assays*. For control plates, 15 μ g/ml of BSA was added for the pre-incubation.

In situ inhibition assays

HUVEC cells were grown with Endothelial Cell Growth Media Kit (Lonza, Walkersville, MD) supplemented with 1% Pen/Strep in 6-well cell culture plates to 70% confluence. Cells were then serum starved for 16 hours in Endothelial Cell Basal Growth Medium-2 (EBM-2) (Lonza, Walkersville, MD). Anti-Nrp-1 monoclonal antibody was first dialyzed into PBS, resuspended in EBM-2, added to HUVEC cells at a final concentration of 10 μ M, and incubated for 90 minutes at 37°C⁽¹³⁷⁾. Cells were then stimulated with 100 ng/ml VEGF-A (R&D Systems, Minneapolis, MN) for 3 minutes. After 3 minutes, media was removed and cells solubilized in RIPA buffer supplemented with phosphatase and protease inhibitor (Roche, Germany). Total VEGFR-2 and VEGFR-2 phosphorylation was determined by western blotting using 55B11 and 19A10 antibodies (Cell Signaling, Danvers, MA), respectively, at a 1:1000 dilution followed by goat anti-rabbit HorseRadish Peroxidase (HRP) conjugated secondary antibody at 1:20000 dilution (sc-2301, Santa Cruz). The SuperSignal West Femto chemiluminescence (ECL) detection system (Thermo Fisher Scientific, Rockford,

IL) was used for detection of immunoreactivity on X-ray films (HyBlot CL; Denville Scientific, Inc. Metuchen, NJ).

Results

The physical basis of VEGFR-2 D7 dimerization and its significance

VEGF signal is delivered into the cell via VEGFR-2 mediated tyrosine kinase cascade under physiological and pathological conditions, and it is suggested that ligand binding induced dimerization of the membrane proximal seventh Ig domain of VEGFR-2 (VEGFR-2 D7) is critical for physically coupling ligand binding to receptor activation ⁽¹²⁶⁾. In order to directly visualize this dimer interface, we have crystalized mouse VEGFR-2 D7. Interestingly, this domain adopts the previously defined active dimer conformation in the crystal structure ⁽¹²⁶⁾, with 518 Å² buried surface per subunit at the interface (Figure 4.1A and 4.1B). Four elements of the structure contribute to the dimerization interface: the loops between sheets A'-B, C'-D, E-F, as well as the single helix, a R724, from the E-F loop, is central to the dimer interface, contributing approximately 36% of the interfacial surface (Figure 4.1C). R724 forms two intermolecular salt bridges with D708 and D728, contributed from the C'-D loop and α , respectively. Additionally, the side-chain NH1 of R724 is oriented to form an intermolecular hydrogen bond with the carbonyl of the other R724 across the dimer. S709, from the C'-D loop, also makes intermolecular contacts, contributing approximately 20% of the dimer interfacial area (Figure 4.1C). The side-chain hydroxyl of S709 is oriented to form an intermolecular hydrogen bond with the side-chain hydroxyl of T681 and the backbone amide of R724. This structure presented here is consistent with the human VEGFR-2 D7 dimer model deduced previously ⁽¹²⁶⁾, but provides a significantly more detailed and accurate picture of the nature of, and residues contributing to, the VEGFR-2 D7 dimer.

While D7 dimerization is thought to be critical for physically coupling ligand binding to VEGFR-2 activation, the dimerization interface must necessarily be limited to avoid ligand independent activation of signaling. Indeed, the VEGFR-2 D7 dimer structure we presented here is consistent with this requirement, with only 518 Å² buried surface per subunit at the interface. Interestingly, this notion is also supported by previous studies. It has been initially shown that D7 dimer formation is beyond detection by analytical ultracentrifugation even at 100 μ M of VEGFR-2 D7 protein, suggesting that the dissociation constant of this interaction is larger than 100 μ M ⁽¹²⁶⁾. A further study has then suggested that the dimerization of domain 4-7 of VEGFR-2 is actually energetically unfavorable ⁽¹³⁸⁾.

As a result, the stable dimerization of membrane proximal domain cannot be easily induced by the ligand-mediated dimerization of D2 and D3, and thus is the limiting step in VEGFR activation. Since Nrp ectodomain has been demonstrated to directly interact with VEGFR-2 and is both necessary and sufficient for VEGFR-2 mediated endothelial cell activation ^(127, 130), we hypothesized that Nrp extracellular domains potentiate VEGFR-2 signaling by promoting dimerization of membrane proximal domain 7 via direct receptor coupling.

Nrp-1 b1b2 domain is directly coupled to VEGFR-2 D7

In order to test this hypothesis, a plate binding assay using purified VEGFR-2 D7 was performed. As shown in Figure 4.2A, Nrp-1 ectodomain clearly binds to VEGFR-2 D7 coated plate. Since the MAM/c domain of Nrp-1 has been suggested to form a dimer, we predicted that Nrp-1 MAM/c domain dimer facilitates the dimerization of VEGFR-2 D7 and thus leads to full VEGFR-2 activation. To test this hypothesis, we have mapped the physical interaction between Nrp-1 extracellular domains and VEGFR-2 D7 using a battery of Nrp-1 extracellular domain truncation constructs. To our surprise, VEGFR-2 D7 directly binds to Nrp-1 b1b2 domain, but not MAM domain. To further determine the binding affinity this interaction, we measured the dose-dependent binding of VEGFR-2 D7 onto Nrp-1 b1b2 domain coated plate and determined the dissociation constant ($K_d=15.3 \pm 1.6 \mu M$) (Figure 4.2B).

In order to define the physical basis of the interaction, we crystallized the fusion protein of VEGFR-2 D7 and Nrp-1 b1b2 domain. High quality crystals of this recombinant protein have been obtained and data collected to 2.92 Å (Table 4.2). The structure has been fully refined with one recombinant protein dimer in the asymmetric unit (Table 4.2). VEGFR-2 D7 makes direct physical contact with Nrp-1 b1b2 domain. The overall structure adapts a butterfly shape with two VEGFR-2 D7 molecules arranged as a parallel dimer (Figure 4.3A) in the center. The VEGFR-2 D7 dimer observed in this structure is consistent with the mouse VEGFR-2 D7 dimer, discussed above, with a 0.7-Å rmsd over 186 residues. The two Nrp-1 b1b2 domains adopt the typical discoidin family β -sandwich fold in a similar confirmation to each other with a 0.8-Å rmsd over 312 residues, and are also arranged as parallel dimer outside and in parallel orientation to VEGFR-2 D7 dimer. As a result, the two VEGF-A binding sites in the tips of Nrp-1 b1 domains are separated by the VEGFR-2 D7 dimer with a distance of about 90 Å. The bottoms of Nrp-1 b2 domain are also apart from each other, and form a cleft for the seven-residue loop located between the end of VEGFR-2 D7 and the predicted beginning of the VEGFR-2 transmembrane helix.

Residues at the VEGFR-2 D7 and Nrp-1 b1b2 domain interface are well resolved and include interactions involving both backbone and side-chains. L732 from F strand of VEGFR-2 D7 establishes hydrophobic interactions with residue L332, M434, V438, and V465 of Nrp-1, which form a hydrophobic patch at the boundary of b1 and b2 domain (Figure 4.3B). Outside this hydrophobic patch, D747 from G strand of VEGFR-2 D7 forms a critical salt bridge with R334 from strand 3 of Nrp-1 b1b2 domain. These interactions contribute near 30% of the heterodimer interfacial area. The heterodimer is further enhanced by a hydrogen bond between K727 from the E-F loop of VEGFR-2 D7 and Q446 from the first strand of Nrp-1 b2 domain. There are also other hydrogen bond interactions involving backbone amine and carbonyl groups. H287 from the N-terminus of Nrp-1 b1 domain makes hydrogen bonding with the backbone carbonyl group of I667 from A strand of VEGFR-2 D7. The backbone NH of I752 from G strand of VEGFR-2 D7 and carbonyl group of S439 from the beginning of Nrp-1 b2 domain also form a hydrogen bond.

Many of the observed residues at the interface are strongly conserved among different isoforms of VEGFRs and Nrps, and cross species. In particular, L732 and L749 from VEGFR-2 D7 are highly conserved among VEGFR-1, 2 and 3, and cross all species (Figure 4.4A). L332, M434, V438, and V465 from Nrp-1 b1b2 domain that form an essential hydrophobic patch at the boundary of Nrp-1 b1 and b2 domain are also highly conserved in Nrp-1 and Nrp-2, and cross species. The observed conservation of the interfacial residues suggests that this hetero-dimerization represents a general mechanism of Nrp for interacting with the membrane proximal domains of VEGFRs in the activated state.

To confirm the contribution of these critical residues to binding, we introduced and analyzed single amino acid mutations in VEGFR-2 D7 (Figure 4.4B). To dissect the contribution of this conserved major hydrophobic interaction between VEGFR and Nrp, we mutated VEGFR-2 L732 and L749 into arginine, both of which poke to the center of a hydrophobic patch on Nrp-1 composed of L332, M434, V438, and V465. Either single amino acid mutation greatly decreases the interaction between VEGFR-2 D7 and Nrp-1 b1b2 domain as demonstrated by plate binding assay. All these mutants were not structurally deleterious as determined by circular dichroism (Figure 4.5).

Blocking Nrp-1 b1b2 domain and VEGFR-2 D7 interaction inhibits signaling

Based on computer modeling, it has been predicted that decoupling VEGFR-2 and Nrp is a more efficient way of inhibiting VEGF signaling compared to

blocking ligand binding ⁽¹³⁹⁾. As a result, we hypothesized that decoupling VEGFR-2 D7 and Nrp-1 b1b2 domain is sufficient to inhibit VEGF signaling. In order to test this hypothesis, we have identified and further characterized an anti-human Nrp-1 b1b2 domain mouse monoclonal antibody ⁽¹³⁷⁾. Since Nrp-1 b1b2 domain has been demonstrated to be able to bind VEGF-A ⁽⁴⁷⁾, we first tested whether this antibody interferes ligand and receptor interaction using Nrp-1 b1b2 domain coated plates. As expected, AP-VEGF-A binds almost equally well to Nrp-1 b1b2 domain coated plates with or without anti-Nrp-1 antibody pre-incubation (Figure 4.6A). This strongly suggests that this anti-Nrp-1 antibody does not block VEGF and Nrp-1 b1b2 domain interaction.

In order to test whether this antibody blocks VEGFR-2 D7 and Nrp-1 b1b2 interaction, AP-VEGFR-2 D7 was utilized as a ligand to interact with Nrp-1 b1b2 domain coated plates. Robust binding was observed when AP-VEGFR-2 D7 was added to Nrp-1 b1b2 domain coated plates (Figure 4.6A). Strikingly, anti-Nrp monoclonal antibody pre-incubation is able to almost fully inhibit this interaction, demonstrating that this antibody specific blocks VEGFR-2 D7 and Nrp-1 b1b2 interaction without affecting the binding of VEGF-A to Nrp-1 (Figure 4.6A). In order to evaluate the effect of decoupling VEGFR-2 D7 and Nrp-1 b1b2 domain on VEGF signaling in situ, we examined the ability of this antibody to inhibit VEGF-A stimulated VEGFR-2 phosphorylation of Y1175 in HUVEC cells (Figure 4.6B). As expected, when the cells were stimulated with VEGF-A, robust VEGFR-2 Y1175 phosphorylation was observed. However, when the cells were pre-incubated with this monoclonal anti-Nrp-1 antibody, potent inhibition of VEGF-A mediated VEGFR-2 activation was observed while the level of total VEGFR-2 and Nrp-2 was not changed. This demonstrated that decoupling these two receptors is indeed sufficient to inhibit VEGF signaling, suggesting a novel strategy for inhibiting VEGF signaling. This monoclonal antibody thus represents a novel class of VEGF inhibitor.

Discussion

Nrp has long been accepted as a mandatory co-receptor for VEGF mediated angiogenesis ^(15, 18). However, little is known about the specific role of Nrp and the physical basis of Nrp function in this pathway. The crystal structure of the Nrp-1 b1b2 domain and VEGFR-2 D7 protein complex presented in this study provides a model of intermolecular contacts required to physically couple ligand binding to full VEGFR activation. Core residues at the Nrp-1 b1b2 domain and VEGFR-2 D7 heterodimer interface are conserved among all Nrp and VEGFR family members, and cross species, suggesting that this interaction is a key

feature of all Nrp and VEGFR family members and is a general mode to couple VEGF ligand binding to receptor activation. Since it has been demonstrated that VEGF-C is able to mediate heterodimerization of VEGFR-2 and VEGFR-3, thereby producing a signaling complex with unique activity ⁽¹⁴⁰⁾, the strong similarity between VEGFR-2 D7 and VEGFR-3 D7 suggests that D7 heterodimerization may be utilized for activation. Additionally, since both Nrp-1 and 2 interact with VEGF-C, a VEGF-C signaling holocomplex composing of VEGF-C, VEGFR-2 and VEGFR-3 heterodimer, Nrp-1 and Nrp-2 heterodimer could form and deliver unique signal.

The VEGFR-2 D7 dimer is parallel in orientation leading to alignment of the C-termini, one essential requirement for a productive signaling dimer. Two Nrp-1 b1b2 domains also adopt a parallel dimer outside of VEGFR-2 D7 dimer with the C-termini Nrp-1 b1b2 domains forming a cleft about 18 Å deep. Since there are seven additional residues located between the end of VEGFR-2 D7 and the predicted beginning of the transmembrane helix and recent reports have demonstrated that the transmembrane domain of VEGFR-2 requires a specific dimeric confirmation to align the intracellular kinase domains, the Nrp-1 b1b2 domain likely functions to orient the VEGFR-2 D7 domain, and may also interact and orient the additional seven residues between the end of VEGFR-2 D7 and the predicted beginning of the transmembrane helix as well. This would help the transmembrane domain of VEGFR-2 adopt a specific confirmation and position the intracellular kinase domains to full activated state. Interestingly, in this VEGFR-2 D7 and Nrp-1 b1b2 receptor complex, two VEGF-A binding sites in Nrp-1 b1 domains are separated by 90 Å. Since the two Nrp-1 binding motifs in VEGF-A165 are located at the C-termini of two flexible heparin-binding domains, they have the potential to extend out and link two Nrp-1s that are up to 120 Å away. As a result, in our model, VEGF-A heparin binding domain could adopt a relative open conformation with two heparin domains extending out to bind Nrp-1 b1 domains. This induces the dimerization of b1b2 domain, and thus orients and stabilizes the active VEGFR-2 D7 dimer.

We have also demonstrated that an antibody blocking Nrp-1 b1b2 domain and VEGFR-2 D7 interaction is sufficient to inhibit VEGF signaling in HUVEC cells *in situ*. Interestingly, we have confirmed that this antibody does not affect the interaction between VEGF and Nrp-1 b1b2 domain. Since it has been predicted that decoupling VEGFR-2 and Nrp is a more efficient way of inhibiting VEGF signaling compared to block ligand binding ⁽¹³⁹⁾, this antibody represents an attractive inhibitory modality for blocking VEGF signaling and belongs to a novel class of VEGF inhibitor. Indeed, this anti-Nrp-1 monoclonal antibody has previously been shown to inhibit proliferation, migration and invasion of glioma

cells both *in vitro* and *in vivo* ⁽¹⁴¹⁾, and more studies are needed to test the effect of this antibody in other cellular and animal models. Using inhibitory modalities decoupling Nrp-1 and VEGFR-2 interaction is an attractive strategy to inhibit VEGFR-2 signaling for many reasons. VEGF level has been reported to increase upon treatment with various VEGF signaling inhibitors ⁽¹⁴²⁻¹⁴⁵⁾, which serves as an unavoidable resistance mechanism for these reagents blocking ligand binding. Since the inhibitory effect of Nrp-1 and VEGFR-2 interaction decoupling reagents does not depend on blocking ligand binding, it was predicted to be less sensitive to VEGF concentration change ⁽¹³⁹⁾. Finally, this novel class of inhibitor may provide unique opportunities to increase VEGF inhibition efficacy by combining with other VEGF signaling inhibitors, which is worth further investigation.

Table 4.1. VEGFR-2 D7 data collection and refinement statistics

Data collection

Beamline	APS 22-ID
Space group	P2 ₁ 2 ₁ 2 ₁
Wavelength	1.00000
Unit-cell parameters	49.634, 69.763, 71.651
Unique reflections	71824
Completeness (%)	91.3 (64.3)
Resolution (Å)	1.2 (1.24-1.20)
Rmerge (%)	9.9 (44.3)
Redundancy	5.1 (3.0)
I/σ(I)	13 (2.4)

Refinement

Resolution Limits (Å)	20.0-1.20
# reflections/# to compute Rfree	68128/3621
R (Rfree)	18.0 (21.0)
# protein residues	192
# solvent molecules	455

Ramachandran

Most favored	94.0
Allowed	6.0
Disallowed	0

RMS deviation

Bond, Å	0.02
Angle, °	1.80

Table 4.2. VEGFR-2 D7 and Nrp-1 b1b2 domain data collection and refinement statistics

Data collection	
Beamline	APS 22-ID
Space group	P4 ₃ 2 ₁ 2
Wavelength	1.00000
Unit-cell parameters	77.320, 77.320, 430.253
Unique reflections	25612
Completeness (%)	90.6 (93.9)
Resolution (Å)	2.92 (3.02-2.92)
Rmerge (%)	16.0 (55.7)
Redundancy	4.1 (3.9)
I/σ(I)	20.3 (9.6)
Refinement	
Resolution Limits (Å)	20.00-2.92
# reflections/# to compute Rfree	25028/1329
R (Rfree)	23.5 (27.6)
# protein residues	819
# solvent molecules	77
Ramachandran	
Most favored	97.0
Allowed	2.9
Disallowed	0.1
RMS deviation	
Bond, Å	0.006
Angle, °	0.88

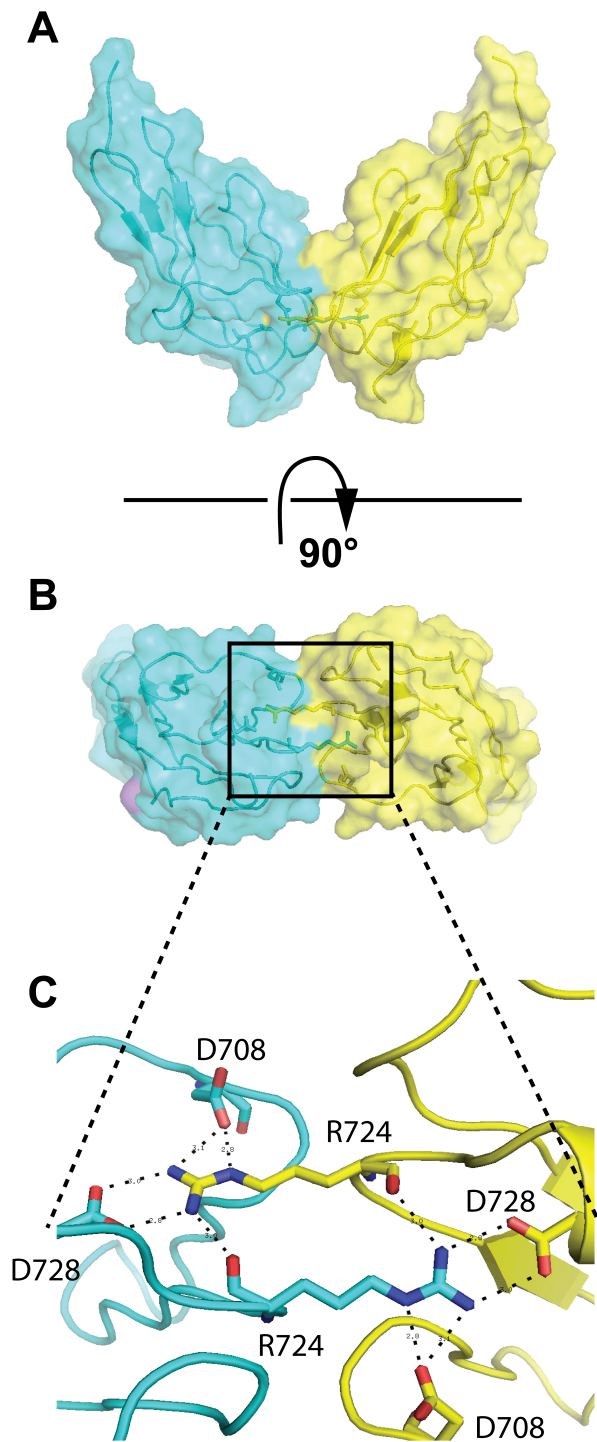


Figure 4.1: Structure of the VEGFR-2 D7 dimer. A) and B) VEGFR-2 D7 crystallizes as a parallel dimer. The two molecules in the dimer are similar, with a backbone r.m.s.d. of 0.6 Å. C) View of the VEGFR-2 D7 dimer interface with residues significantly contributing to the interface.

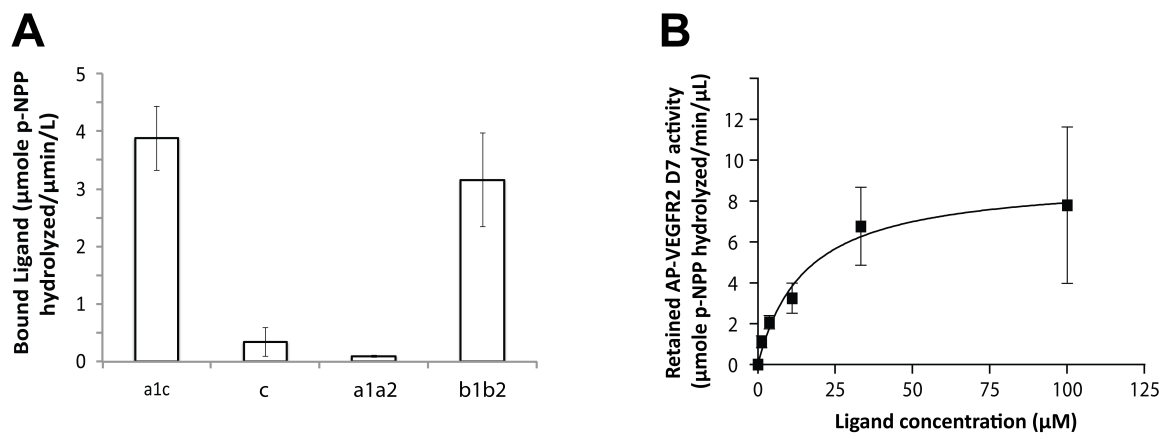


Figure 4.2: Physical coupling between Nrp and VEGFR-2 D7. A) Direct interaction is observed between VEGFR-2 D7 and Nrp-1. This interaction is mapped to Nrp-1 b1b2 domain using a plate based binding assay with purified proteins. B) The binding affinity of this interaction is further determined ($K_d=15.3 \pm 1.6 \mu M$).

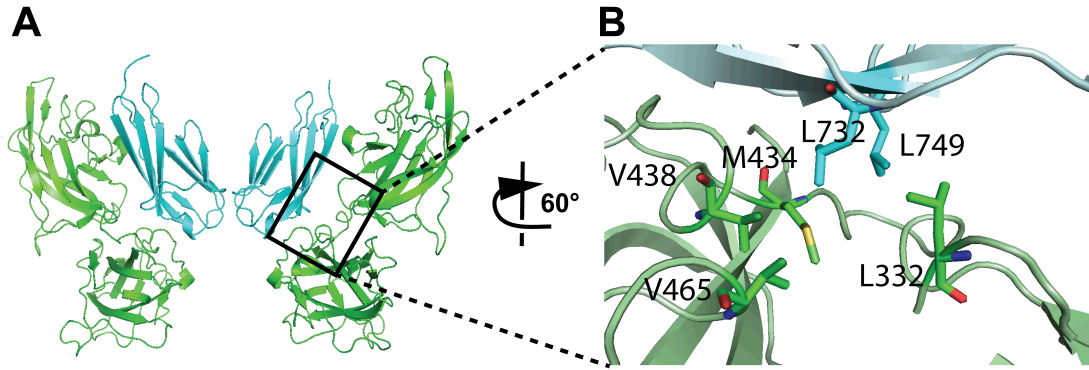


Figure 4.3: Crystal structure of VEGFR-2 D7 (cyan) and Nrp-1 b1b2 domain (green). A) Nrp-1 b1b2 interacts with VEGFR-2 D7 active dimer. B) A detailed view of the interaction interface shows hydrophobic interactions and salt bridge.

A

musculus	730	KEDGG L YTCQACNVLGCA R AET L FIIEG
Sapiens	732	KEDE G L L YTCQACSVLGCA K VE A FFIIEG
lupus	731	KEDE G L L YTCQACSVLGCA K VE A FFIVEG
Taurus	732	KEDE G L L YTCQACSVLGCA K VE A FFIVEG
gallus	723	KEDGG L YTCLACNILGCK K A E A L YFSVEG

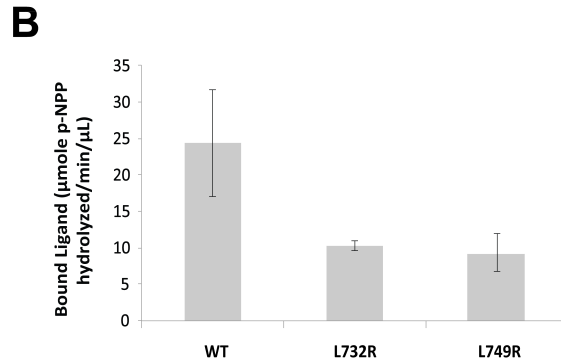


Figure 4.4: Critical residues in VEGFR-2 D7 for Nrp-1 b1b2 domain interaction are well conserved across species (shown in A), and are further confirmed to decrease VEGFR-2 D7 and Nrp-1 b1b2 domain interaction with mutagenesis (Shown in B).

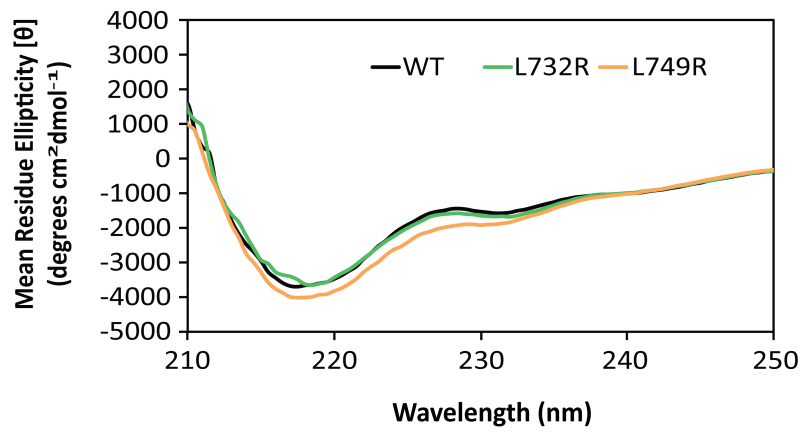


Figure 4.5: VEGFR-2 D7 and mutants have similar CD spectrum, suggesting that mutations are not deleterious to protein structure.

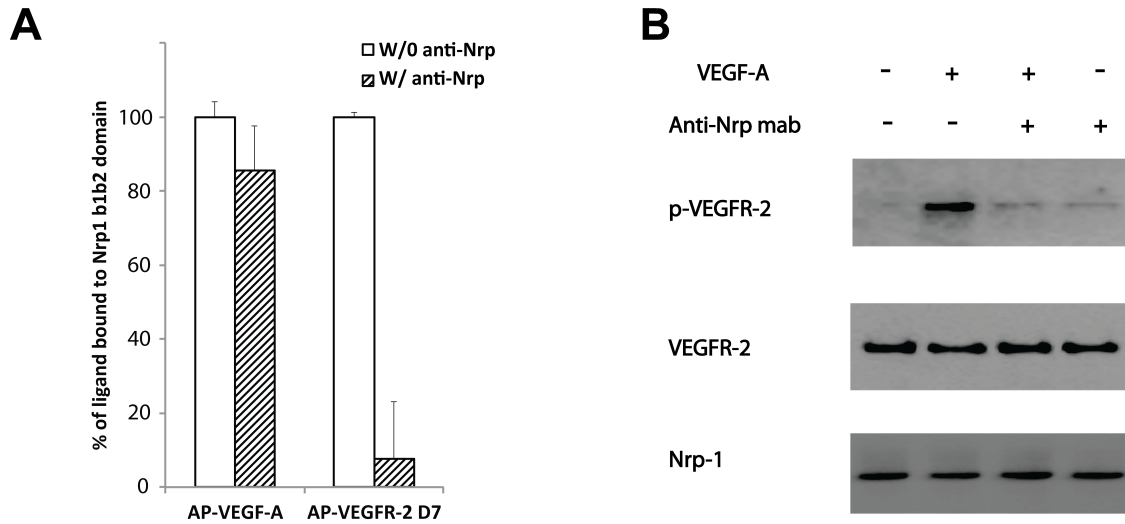


Figure 4.6: Blocking VEGFR-2 D7 and Nrp-1 b1b2 domain interaction inhibits VEGF signaling. A) An anti-Nrp-1 b1b2 domain monoclonal antibody is shown to inhibit the interaction between VEGFR-2 D7 and Nrp-1 b1b2 domain in vitro without affecting the interaction between Nrp and VEGF-A. B) This monoclonal antibody is further shown to inhibit VEGF signaling in situ in human umbilical vein endothelial cells.

CHAPTER FIVE

Conclusions, significance and future directions

General conclusions and significance

In this series of studies I have focused on addressing the basic mechanism of a critical membrane receptor Nrp in vascular development. This was approached by physically dissecting domains and residues involved in the ligand receptor binding and receptor-receptor coupling using X-ray crystallography and other biophysical tools, followed by biochemical and cellular assays to validate the significance of these molecular interactions. I have determined a specific role and mechanism of Nrp in VEGF mediated angiogenesis, defined the ligand-receptor interaction mechanism between Sema3 C-terminus and Nrp. Taken together, these results advance our understanding of VEGF signaling pathway, and identify novel strategies to inhibit Nrp function.

Nrp and VEGFR coupling in cis and trans VEGFR activation

VEGF signals via VEGFR mediated tyrosine kinase cascade under physiological and pathological conditions, and Nrp serves as an essential co-receptor to enhance VEGFR signaling. Although the importance of Nrp in VEGF signaling pathway is well established, the physical mechanism and specific role of Nrp is not understood, which represents one of the critical open questions in Nrp biology. In order to define the role and mechanism of Nrp in VEGFR activation, we have identified and characterized a critical interaction between Nrp b1b2 domain and VEGFR-2 D7, and found that Nrp b1b2 domain functions as a molecular hub to integrate ligand binding and receptor coupling to receptor activation. Together with the cellular assay results, we have demonstrated that the observed direct receptor coupling is essential for correctly orienting the receptor dimer for trans-activation, and disrupting this interaction is sufficient to inhibit VEGF signaling. This work defines a unique physical basis of Nrp in VEGFR activation and disrupting this receptor coupling represents a novel strategy for inhibiting VEGF signaling.

In addition, my results indicate that the Nrp b1b2 domain, rather than the membrane proximal MAM domain, is coupled to VEGFR-2. Since there is a flexible loop between Nrp b1b2 domain and MAM domain, it is possible that Nrp from a non-endothelial cell type may act in trans to enhance VEGFR activation

on endothelial cells and thus stimulate angiogenesis. Indeed, it has been reported that fetal liver CD45⁺ hematopoietic cells derived Nrp-1 enhances VEGFR-2 activation on endothelial cells in the presence of VEGF, and increases endothelial cell proliferation ⁽¹⁴⁶⁾. This trans-interaction has also been shown to be able to rescue vascular loss in the Nrp null P-Sp (paraaortic splanchnopleural mesodermal region) culture and promote angiogenesis *in vivo*. Since many tumor cells overexpress Nrp, tumor derived Nrp has also been suggested to promote endothelial cell survival and proliferation, and increase microvessel density ⁽¹⁰⁴⁾. As a result, the work presented here provides a unique physical basis for Nrp mediated trans-activation as well.

The basis of Nrp in angiogenesis

The importance of Nrp in angiogenesis during development has been well demonstrated utilizing transgenic mice, which leads to embryonic lethality ⁽¹⁵⁾. Further analysis of these mice embryos suggests that Nrp null endothelial cells feature long distance random movement along existing capillaries, but defective directional movement toward VEGF, which results in reduction in vessel branch point and larger vessel diameter phenotype observed in Nrp null embryos ⁽¹⁴⁷⁾. This is probably because Nrp null endothelial cells are unable to respond extracellular matrix bound VEGF next to them. Indeed, it has been well accepted that Nrp increases the directional migration toward VEGF when co-expressed with VEGFR-2 ⁽¹⁸⁾. Interestingly, using conditional knockout with Cre driven by the angiopoietin receptor TIE2, a recent work demonstrated that Nrp-1 was partially deleted only in a population of endothelial cells, while the rest of the population remain various levels of Nrp-1 ⁽¹⁴⁸⁾. By analyzing these mice, they have shown that endothelial cells with higher level of Nrp-1 are more likely to be recruited to the tip of sprouting capillaries, and similar results were observed in Cre transgene driven by the PDGFb, a tip cell marker, suggesting that Nrp-1 does provide an advantage for the cells to respond to VEGF gradient. However, the mechanism of the sensitizing effect of Nrp-1 to VEGF gradient is not clear, although many mechanisms could contribute to it.

Nrp increases the affinity of VEGF to VEGFR-2

The privilege of Nrp-1 expressing cells on VEGF sensing and the potentiation effect of Nrp-1 on VEGF mediated directional migration could simply be due to its ability to increase the binding of VEGF to VEGFR-2. Indeed, this idea is supported by early work, however, this study was semi-quantitative and has not

determined the binding affinities between VEGF and VEGFR expressing cells with and without Nrp ⁽¹⁸⁾. Later follow-up studies did measure their binding affinities but produce contradictory results. Some showed that Nrp does enhance the binding of VEGF to VEGFR-2 ⁽¹⁹⁾, but others failed to observe any obvious changes in the interaction between VEGF and VEGFR-2 in the presence or absence of Nrp although many cell lines were used ⁽¹²⁸⁾. As a result, it is still not clear whether Nrp enhances the interaction between VEGF and VEGFR-2, and whether this mechanism is important for VEGF signaling. More research is definitely needed to figure out the reasons of binding affinity disparities and the contribution of Nrp in increasing the affinity between VEGF and its major signaling receptor VEGFR-2.

Nrp increases the efficiency of signal transmission

The advantage of Nrp-1 expressing cells on VEGF sensing and the potentiation effect of Nrp-1 on VEGF mediated directional migration could also due to its ability to increase the efficiency of signal transmission across the membrane, and thus VEGFR-2 down stream signaling. Indeed, at the molecule level, Nrp greatly potentiates VEGF mediated VEGFR-2 signaling in endothelial cells. In the presence of Nrp, not only the amplitude but also the duration of VEGFR-2 phosphorylation upon VEGF stimulation is enhanced ^(19, 87). This is a general effect and has not been shown to be limited to any specific VEGFR-2 intracellular tyrosine phosphorylation sites. Since VEGFR-2 tyrosine phosphorylation is the signal that the cells detect intracellularly, by increasing the efficiency of signal transmission across the membrane and enhancing the VEGFR-2 phosphorylation, endothelial cells with Nrp are able to detect shallower VEGF gradient that could not be sensed otherwise (Figure 5.1). The structure work described in chapter 4 presents a new working model to explain the mechanism of Nrp in enhancing the efficiency of signal transmission across the cell membrane. Our structures suggest that VEGFR-2 D7 dimerization process is a bottleneck in VEGF signal transmission across the cell membrane and Nrp b1b2 domain facilitates this process by stabilizing VEGFR-2 D7 dimer especially after ligand binding. However, further studies with other cellular and animal models, single molecule techniques, and etc. are still needed to verify the significance of this model in explaining the mechanism of Nrp in VEGF signaling.

VEGFR-2 trafficking

Alternatively, it is also suggested Nrp potentiates VEGFR-2 signaling by modulating VEGFR-2 receptor trafficking ⁽¹⁴⁹⁾. It has been shown that in the presence of Nrp and VEGF, Nrp promotes VEGFR-2 recycling through Rab5, Rab4, and Rab11 recycling pathway, prevents VEGFR-2 degradation, and thus prolongs the signaling time. Moreover, it has then demonstrated that VEGF is required for holding the complex together, since VEGF-A_{166b}, an isoform does not bind Nrp, fails to induce such enhanced signaling effect. The intracellular domain of Nrp-1 was also shown to be necessary for VEGFR-2 receptor trafficking, since the deletion of Nrp intracellular domain abolishes the prolonged VEGFR-2 signaling. These VEGFR-2 trafficking changes introduced by Nrp are interesting and the biological relevance of these changes is still waiting for validation using animal models. Interestingly, another recent study demonstrated that Nrp intracellular domain is able to accelerate the trafficking of endocytosed VEGFR-2 from Rab5+ to EEA1+ endosomes, and thus enhance VEGFR-2 signaling by decreasing PTPN1 (PTP1b)-mediated VEGFR-2 dephosphorylation ⁽²⁶⁾. This enhancing effect of Nrp on VEGFR-2 signaling has then been suggested to play a role in arteriogenesis during vascular development. It will be interesting to study the role of this Nrp mediated trafficking change in other biological settings. In summary, the role of Nrp in modulating VEGFR-2 trafficking is still emerging and it will be interestingly to determine the whole picture of the VEGFR-2 trafficking changes introduced by Nrp.

Nrp coupling to other receptors

Finally, Nrp has been shown to modulate VEGF signaling by coupling to other cell surface receptors, such as integrins. Indeed, Nrp-1 is expressed in pancreatic ductal adenocarcinomas, and has been suggested to associate with β 1 integrin to promote cell invasion ⁽¹⁵⁰⁾. Likewise, Nrp-2 has also been indicated to interact with α 5 integrin and enhance tumor cell extravasation and metastasis ⁽¹⁵¹⁾. However, Nrp and integrin association does not always lead to enhanced cell migration. For instance, α v β 3 integrin and Nrp-1 interaction has been suggested to inhibit angiogenesis probably by sequestering Nrp-1 from the active VEGF/VEGFR-2 signaling complex ⁽¹⁵²⁾. These data have demonstrated that Nrp and integrin receptors function cooperatively to regulate cell migration, and further investigation is definitely needed to determine the importance of these functional interactions in other animal models and the extent of these associations in modulating VEGF gradient sensing in endothelial cell. These data will stimulate more interest in understanding the detailed nature of the physical

coupling between Nrp and integrins in the future. Since the intracellular adaptor protein RGS-GAIP-Interacting Protein C-terminus (GIPC) has been shown to bind to the intracellular domain of both Nrps and integrins ⁽¹⁵³⁻¹⁵⁵⁾, the possibility exists that GIPC plays a role in the functional coupling between Nrp and integrin, which is worth further investigation.

VEGF and Semaphorin 3 C-terminus competes for binding to Nrp

Vascular development is regulated by the balance of pro-angiogenic cytokines exemplified by VEGF-A, and angiogenesis inhibitor, such as Semaphorin 3F ^(77, 78, 156). The anti-angiogenic activity of Semaphorin 3F was shown to result from direct competition between Semaphorin 3F and VEGF-A for binding to their shared C-terminal arginine-binding pocket in the Nrp b1 domain ⁽⁴⁰⁾. Previously, it has been shown that VEGF-A C-terminal residues encoded by the exon seven interacts with the L1 loop of the Nrp-1 b1 domain, enhancing binding and selectivity of this interaction ⁽⁴⁶⁾. Interestingly, the work presented here demonstrated that Semaphorin 3 family members engage Nrp-1 utilizing two distinct regions in their C-terminal domain, a C-terminal arginine and upstream helical region. This synergistic engagement results in potent competitive binding to Nrp-1 that antagonizes VEGF binding and cellular activation. These results define a unique high-affinity hetero-bivalent ligand-receptor interaction mechanism between Semaphorin 3 C-terminus and Nrp, and determine the basis of Semaphorin 3F mediated anti-angiogenic activity, which may help rational Nrp inhibitor design.

In order to define the nature of this motif, we have determined its structure by X-ray crystallography. We have shown that indeed this structure is a parallel helical dimer, which is mainly stabilized by an intermolecular disulfide bond. Since this helical dimer has been suggested to contribute as a second binding site to engage Nrp b1 domain, Semaphorin 3 C-terminal basic domain may bind and bring two Nrp b1 domains to close proximity. It will be interestingly to characterize the detailed b1 domain organization upon Semaphorin 3 binding. This may be distinct from the b1 domain organization during VEGF signaling. Knowing this difference in b1 domain organization may help develop reagents to selectively inhibit or facilitate VEGF or Semaphorin 3 stimulated Nrp signaling.

Explore the non-canonical roles of Nrp in other cell types

Besides Nrp's classical functions in axon guidance and angiogenesis in neurons and endothelial cells, effort has been made to elucidate the non-canonical

signaling and novel roles of Nrp in a variety of tissues. For example, VEGF autocrine signaling pathway has been shown to be important for tumor stem cell maintenance, tumor cell survival and drug resistance in multiple cancer types ⁽¹⁵⁷⁻¹⁶⁰⁾. Recently, it has been reported that hypoxia-induced Sema3A attracts tumor-associated macrophages into tumor hypoxic niche by engaging Nrp-1, plexin and VEGFR1 signaling complex ⁽¹⁶¹⁾. Interestingly, it was originally believed that, out of seven semaphorin families, only class 3 semaphorin members require Nrp as a receptor. However, as an exception to dogma, immune cell expressed Sema4a has also been shown to be able to signal through regulatory T cell (Treg) expressed Nrp, which is required by Treg cells to inhibit anti-tumor immune responses and to cure established inflammatory colitis ⁽¹⁶²⁾.

Nrp-1 ligands VEGF and Sema3 have also been suggested to regulate platelet function. Platelets are small and anucleate blood cells, produced from bone marrow derived precursor cells named megakaryocytes and then released into blood stream. They are critical for maintaining a pressurized vasculature by rapidly responding to vascular damage. At the site of damage, platelets are exposed to agonists at the sub-endothelial layer, which bind to platelet cell surface receptor, and initiate platelet activation and thrombus formation to seal the damage. However, aberrant thrombosis is involved in the pathogenesis of heart attack and stroke. As a result, these cell surface receptors are major drug targets.

Interestingly, it has been reported that VEGF potentiates thrombin-mediated platelet activation by enhancing VEGF receptor signaling ⁽¹⁶³⁾. Sema3, on the other hand, inhibits platelet function by activating the Sema3-plexin pathway ⁽¹⁶⁴⁾. However, a commercially available Sema3A/Fc fusion was used in this study as the ligand. In this fusion protein the C-terminal arginine, critical for high affinity Nrp-1 binding, is embedded as in the precursor form before furin processing. These assays and others have been interpreted based on their effect on other receptors in related pathways, such as VEGFR and plexin. As a result, whether Nrp-1 plays a role in platelet function is unknown. However, this research also raises another interesting question, that is, how is the pacifying effect of Sema3 on platelets removed when platelet activation is necessary ⁽¹⁶⁵⁾. Recently, platelet activation and thrombocytopenia (a potential ramification of platelet activation) was found in an anti-Nrp-1 antibody MNRP-1685A phase 1 and 1b clinical trial, which strongly argues a role of Nrp-1 in platelet activation and function ⁽¹⁶⁶⁾. As a result, dissecting the contribution of Nrp ligands on platelet activation is an interesting topic for future study.

The biological significance of Nrp promiscuous ligand binding

Based on this work and many others, it is well accepted that the Nrp-1 b1 coagulation factor domain has a conserved C-terminal arginine-binding pocket that is the major binding site for interacting with its ligands ^(40, 47). Since many growth factors have a C-terminal arginine, such as VEGF, platelet-derived growth factor (PDGF), basic fibroblast growth factor (bFGF), hepatocyte growth factor (HGF), epidermal growth factor (EGF), and many proteases such as furin and thrombin produce a C-terminal arginine after their enzymatic cleavage, Nrp has the potential to interact with a battery of these cytokines. Indeed, many cytokines, such as VEGF, PDGF, and HGF, have been shown to be Nrp ligands. However, one of the interesting open questions of Nrp biology is what is the physiological relevance of Nrp promiscuous ligand binding.

Interestingly, since Nrp-1 is reported to have sorting ability in endothelial cells ⁽¹⁴⁹⁾ and is able to interact with 9 out of 14 major pro-angiogenic cytokines in platelets ^(64, 167-169), it is possible that Nrp-1 may function as a general sorting receptor ultimately serving to maintain the balance of pro and anti-angiogenic cytokine storage in some cell types, such as platelets. Indeed, many Nrp-1 ligands, such as VEGF and bFGF, are not produced during platelet biogenesis but instead are taken up by circulating platelets presumably by receptor mediated endocytosis, but the receptor that mediates this process is unknown ^(64, 170, 171). As a result, exploring the role of Nrp in regulating platelet cargo loading is an interesting future direction in Nrp field.

It is possible that platelet Nrp may modify angiogenesis by tuning the balance between pro and anti-angiogenic cytokine storage in platelets. Indeed, platelets store a variety of bioactive molecules in their three different granules: α granules, dense granules, and lysosomes, and play an important role in angiogenesis ^(172, 173). Upon activation, many angiogenic cytokines, such as VEGF, platelet-derived growth factor (PDGF), basic fibroblast growth factor (bFGF), epidermal growth factor (EGF), are released from one of the major granules, α granules ⁽¹⁷⁴⁻¹⁸⁰⁾. Release of these cytokines has been shown to be important for wound healing after injury ⁽¹⁸¹⁻¹⁸³⁾. Interestingly, platelet-loaded VEGF has been used to promote angiogenesis after surgeries and to treat stomach ulcers ⁽¹⁸²⁾.

Moreover, previous work has demonstrated that mild activation of platelets enhances granule cargo uptake into platelets, such as fibrinogen and serotonin ^(184, 185). It is thus possible that VEGF triggers mild platelet activation near vascular damage, thereby facilitates Sema3 uptake into platelets. This may serve to sequester excess Sema3, and normalize the angiogenesis cascade. As a result, it is worth the effort to assess the potential enhancing effect of VEGF on

Sema3 uptake. Finally, it has been argued that pro- and anti-angiogenic cytokines are differentially stored in α granules ^(178, 179). Since Nrp-1 mediates endocytosis of Sema3 and VEGF-A differently in endothelial cells ⁽¹⁸⁶⁾, a differential Nrp-1-dependent endocytosis may underlie differential ligand uptake.

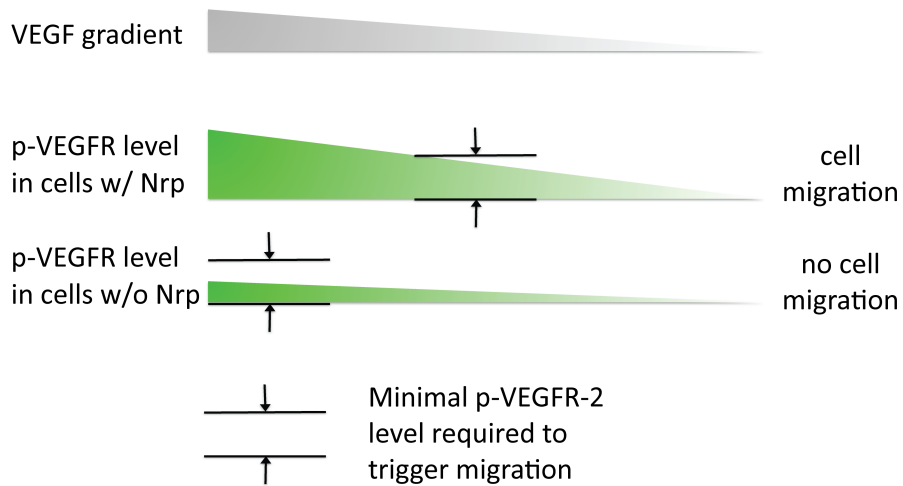


Figure 5.1: Schematic view of how the potentiation effect of Nrp-1 on VEGF signaling increase directional migration. Enhanced VEGFR-2 phosphorylation with the help of Nrp is more likely to reach the threshold for triggering directional cell migration.

REFERENCES

1. Ebbell, B., and Banov, L. (1937) The Papyrus Ebers : the greatest Egyptian medical document.
2. Michaelson, I. C. (1948) The mode of development of the vascular system of the retina with some observations on its significance for certain retinal disorders, *Transactions of the ophthalmological societies of the United Kingdom* 68, 44.
3. Folkman, J., Merler, E., Abernathy, C., and Williams, G. (1971) Isolation of a tumor factor responsible for angiogenesis, *The Journal of experimental medicine* 133, 275-288.
4. Leung, D. W., Cachianes, G., Kuang, W. J., Goeddel, D. V., and Ferrara, N. (1989) Vascular endothelial growth factor is a secreted angiogenic mitogen, *Science* 246, 1306-1309.
5. Ivan, M., Kondo, K., Yang, H., Kim, W., Valiando, J., Ohh, M., Salic, A., Asara, J. M., Lane, W. S., and Kaelin, W. G., Jr. (2001) HIF α targeted for VHL-mediated destruction by proline hydroxylation: implications for O₂ sensing, *Science* 292, 464-468.
6. Jaakkola, P., Mole, D. R., Tian, Y. M., Wilson, M. I., Gielbert, J., Gaskell, S. J., von Kriegsheim, A., Hebestreit, H. F., Mukherji, M., Schofield, C. J., Maxwell, P. H., Pugh, C. W., and Ratcliffe, P. J. (2001) Targeting of HIF- α to the von Hippel-Lindau ubiquitylation complex by O₂-regulated prolyl hydroxylation, *Science* 292, 468-472.
7. Forsythe, J. A., Jiang, B. H., Iyer, N. V., Agani, F., Leung, S. W., Koos, R. D., and Semenza, G. L. (1996) Activation of vascular endothelial growth factor gene transcription by hypoxia-inducible factor 1, *Molecular and cellular biology* 16, 4604-4613.
8. Carmeliet, P., Ferreira, V., Breier, G., Pollefeyt, S., Kieckens, L., Gertsenstein, M., Fahrig, M., Vandenhoek, A., Harpal, K., Eberhardt, C., Declercq, C., Pawling, J., Moons, L., Collen, D., Risau, W., and Nagy, A. (1996) Abnormal blood vessel development and lethality in embryos lacking a single VEGF allele, *Nature* 380, 435-439.
9. Ferrara, N., Carver-Moore, K., Chen, H., Dowd, M., Lu, L., O'Shea, K. S., Powell-Braxton, L., Hillan, K. J., and Moore, M. W. (1996) Heterozygous embryonic lethality induced by targeted inactivation of the VEGF gene, *Nature* 380, 439-442.
10. Ferrara, N., Gerber, H. P., and LeCouter, J. (2003) The biology of VEGF and its receptors, *Nature medicine* 9, 669-676.
11. Mattila, M. M., Ruohola, J. K., Karpanen, T., Jackson, D. G., Alitalo, K., and Harkonen, P. L. (2002) VEGF-C induced lymphangiogenesis is associated with lymph node metastasis in orthotopic MCF-7 tumors, *Int J Cancer* 98, 946-951.
12. Shibuya, M. (1995) Role of VEGF-flt receptor system in normal and tumor angiogenesis, *Adv Cancer Res* 67, 281-316.
13. He, Z., and Tessier-Lavigne, M. (1997) Neuropilin is a receptor for the axonal chemorepellent Semaphorin III, *Cell* 90, 739-751.
14. Kolodkin, A. L., Levengood, D. V., Rowe, E. G., Tai, Y. T., Giger, R. J., and Ginty, D. D. (1997) Neuropilin is a semaphorin III receptor, *Cell* 90, 753-762.
15. Kawasaki, T., Kitsukawa, T., Bekku, Y., Matsuda, Y., Sanbo, M., Yagi, T., and Fujisawa, H. (1999) A requirement for neuropilin-1 in embryonic vessel formation, *Development* 126, 4895-4902.
16. Shalaby, F., Rossant, J., Yamaguchi, T. P., Gertsenstein, M., Wu, X. F., Breitman, M. L., and Schuh, A. C. (1995) Failure of blood-island formation and vasculogenesis in Flk-1-deficient mice, *Nature* 376, 62-66.
17. Olsson, A. K., Dimberg, A., Kreuger, J., and Claesson-Welsh, L. (2006) VEGF receptor signalling - in control of vascular function, *Nature reviews. Molecular cell biology* 7, 359-371.

18. Soker, S., Takashima, S., Miao, H. Q., Neufeld, G., and Klagsbrun, M. (1998) Neuropilin-1 is expressed by endothelial and tumor cells as an isoform-specific receptor for vascular endothelial growth factor, *Cell* 92, 735-745.
19. Shraga-Heled, N., Kessler, O., Prahst, C., Kroll, J., Augustin, H., and Neufeld, G. (2007) Neuropilin-1 and neuropilin-2 enhance VEGF121 stimulated signal transduction by the VEGFR-2 receptor, *FASEB journal : official publication of the Federation of American Societies for Experimental Biology* 21, 915-926.
20. Zachary, I. C., Frankel, P., Evans, I. M., and Pellet-Many, C. (2009) The role of neuropilins in cell signalling, *Biochemical Society transactions* 37, 1171-1178.
21. Wang, L., Zeng, H., Wang, P., Soker, S., and Mukhopadhyay, D. (2003) Neuropilin-1-mediated vascular permeability factor/vascular endothelial growth factor-dependent endothelial cell migration, *The Journal of biological chemistry* 278, 48848-48860.
22. Wang, L., Mukhopadhyay, D., and Xu, X. (2006) C terminus of RGS-GAIP-interacting protein conveys neuropilin-1-mediated signaling during angiogenesis, *FASEB journal : official publication of the Federation of American Societies for Experimental Biology* 20, 1513-1515.
23. Evans, I. M., Yamaji, M., Britton, G., Pellet-Many, C., Lockie, C., Zachary, I. C., and Frankel, P. (2011) Neuropilin-1 signaling through p130Cas tyrosine phosphorylation is essential for growth factor-dependent migration of glioma and endothelial cells, *Molecular and cellular biology* 31, 1174-1185.
24. Yamada, Y., Takakura, N., Yasue, H., Ogawa, H., Fujisawa, H., and Suda, T. (2001) Exogenous clustered neuropilin 1 enhances vasculogenesis and angiogenesis, *Blood* 97, 1671-1678.
25. Fantin, A., Schwarz, Q., Davidson, K., Normando, E. M., Denti, L., and Ruhrberg, C. (2011) The cytoplasmic domain of neuropilin 1 is dispensable for angiogenesis, but promotes the spatial separation of retinal arteries and veins, *Development* 138, 4185-4191.
26. Lanahan, A., Zhang, X., Fantin, A., Zhuang, Z., Rivera-Molina, F., Speichinger, K., Prahst, C., Zhang, J., Wang, Y., Davis, G., Toomre, D., Ruhrberg, C., and Simons, M. (2013) The neuropilin 1 cytoplasmic domain is required for VEGF-A-dependent arteriogenesis, *Developmental cell* 25, 156-168.
27. Pasterkamp, R. J. (2012) Getting neural circuits into shape with semaphorins, *Nature reviews. Neuroscience* 13, 605-618.
28. Koncina, E., Roth, L., Gonthier, B., and Bagnard, D. (2007) Role of semaphorins during axon growth and guidance, *Adv Exp Med Biol* 621, 50-64.
29. Kitsukawa, T., Shimizu, M., Sanbo, M., Hirata, T., Taniguchi, M., Bekku, Y., Yagi, T., and Fujisawa, H. (1997) Neuropilin-semaphorin III/D-mediated chemorepulsive signals play a crucial role in peripheral nerve projection in mice, *Neuron* 19, 995-1005.
30. Takahashi, T., Fournier, A., Nakamura, F., Wang, L. H., Murakami, Y., Kalb, R. G., Fujisawa, H., and Strittmatter, S. M. (1999) Plexin-neuropilin-1 complexes form functional semaphorin-3A receptors, *Cell* 99, 59-69.
31. Cheng, H. J., Bagri, A., Yaron, A., Stein, E., Pleasure, S. J., and Tessier-Lavigne, M. (2001) Plexin-A3 mediates semaphorin signaling and regulates the development of hippocampal axonal projections, *Neuron* 32, 249-263.
32. Gu, C., Rodriguez, E. R., Reimert, D. V., Shu, T., Fritsch, B., Richards, L. J., Kolodkin, A. L., and Ginty, D. D. (2003) Neuropilin-1 conveys semaphorin and VEGF signaling during neural and cardiovascular development, *Dev Cell* 5, 45-57.

33. Wolman, M. A., Liu, Y., Tawarayama, H., Shoji, W., and Halloran, M. C. (2004) Repulsion and attraction of axons by semaphorin3D are mediated by different neuropilins in vivo, *J Neurosci* 24, 8428-8435.
34. Chauvet, S., Cohen, S., Yoshida, Y., Fekrane, L., Livet, J., Gayet, O., Segu, L., Buhot, M. C., Jessell, T. M., Henderson, C. E., and Mann, F. (2007) Gating of Sema3E/PlexinD1 signaling by neuropilin-1 switches axonal repulsion to attraction during brain development, *Neuron* 56, 807-822.
35. Chen, H., He, Z., Bagri, A., and Tessier-Lavigne, M. (1998) Semaphorin-neuropilin interactions underlying sympathetic axon responses to class III semaphorins, *Neuron* 21, 1283-1290.
36. Koppel, A. M., Feiner, L., Kobayashi, H., and Raper, J. A. (1997) A 70 amino acid region within the semaphorin domain activates specific cellular response of semaphorin family members, *Neuron* 19, 531-537.
37. Merte, J., Wang, Q., Vander Kooi, C. W., Sarsfield, S., Leahy, D. J., Kolodkin, A. L., and Ginty, D. D. (2010) A forward genetic screen in mice identifies Sema3A(K108N), which binds to neuropilin-1 but cannot signal, *J Neurosci* 30, 5767-5775.
38. Giger, R. J., Urquhart, E. R., Gillespie, S. K., Levensgood, D. V., Ginty, D. D., and Kolodkin, A. L. (1998) Neuropilin-2 is a receptor for semaphorin IV: insight into the structural basis of receptor function and specificity, *Neuron* 21, 1079-1092.
39. Nakamura, F., Tanaka, M., Takahashi, T., Kalb, R. G., and Strittmatter, S. M. (1998) Neuropilin-1 extracellular domains mediate semaphorin D/III-induced growth cone collapse, *Neuron* 21, 1093-1100.
40. Parker, M. W., Hellman, L. M., Xu, P., Fried, M. G., and Vander Kooi, C. W. (2010) Furin processing of semaphorin 3F determines its anti-angiogenic activity by regulating direct binding and competition for neuropilin, *Biochemistry* 49, 4068-4075.
41. Puschel, A. W. (2002) The function of neuropilin/plexin complexes, *Adv Exp Med Biol* 515, 71-80.
42. Buehler, A., Sitaras, N., Favret, S., Bucher, F., Berger, S., Pielen, A., Joyal, J. S., Juan, A. M., Martin, G., Schlunck, G., Agostini, H. T., Klagsbrun, M., Smith, L. E., Sapieha, P., and Stahl, A. (2013) Semaphorin 3F forms an anti-angiogenic barrier in outer retina, *FEBS letters* 587, 1650-1655.
43. Fukushima, Y., Okada, M., Kataoka, H., Hirashima, M., Yoshida, Y., Mann, F., Gomi, F., Nishida, K., Nishikawa, S., and Uemura, A. (2011) Sema3E-PlexinD1 signaling selectively suppresses disoriented angiogenesis in ischemic retinopathy in mice, *The Journal of clinical investigation* 121, 1974-1985.
44. Gu, C., Limberg, B. J., Whitaker, G. B., Perman, B., Leahy, D. J., Rosenbaum, J. S., Ginty, D. D., and Kolodkin, A. L. (2002) Characterization of neuropilin-1 structural features that confer binding to semaphorin 3A and vascular endothelial growth factor 165, *J Biol Chem* 277, 18069-18076.
45. Herzog, B., Pellet-Many, C., Britton, G., Hartzoulakis, B., and Zachary, I. C. (2011) VEGF binding to NRP1 is essential for VEGF stimulation of endothelial cell migration, complex formation between NRP1 and VEGFR2, and signaling via FAK Tyr407 phosphorylation, *Mol Biol Cell* 22, 2766-2776.
46. Parker, M. W., Xu, P., Li, X., and Vander Kooi, C. W. (2012) Structural basis for the selective vascular endothelial growth factor-A (VEGF-A) binding to neuropilin-1, *J Biol Chem*.

47. Vander Kooi, C. W., Jusino, M. A., Perman, B., Neau, D. B., Bellamy, H. D., and Leahy, D. J. (2007) Structural basis for ligand and heparin binding to neuropilin B domains, *Proc Natl Acad Sci U S A* 104, 6152-6157.
48. Teesalu, T., Sugahara, K. N., Kotamraju, V. R., and Ruoslahti, E. (2009) C-end rule peptides mediate neuropilin-1-dependent cell, vascular, and tissue penetration, *Proceedings of the National Academy of Sciences of the United States of America* 106, 16157-16162.
49. Wang, J., Liu, Y., Teesalu, T., Sugahara, K. N., Kotamraju, V. R., Adams, J. D., Ferguson, B. S., Gong, Q., Oh, S. S., Csordas, A. T., Cho, M., Ruoslahti, E., Xiao, Y., and Soh, H. T. (2011) Selection of phage-displayed peptides on live adherent cells in microfluidic channels, *Proceedings of the National Academy of Sciences of the United States of America* 108, 6909-6914.
50. Laakkonen, P., Porkka, K., Hoffman, J. A., and Ruoslahti, E. (2002) A tumor-homing peptide with a targeting specificity related to lymphatic vessels, *Nature medicine* 8, 751-755.
51. Roth, L., Agemy, L., Kotamraju, V. R., Braun, G., Teesalu, T., Sugahara, K. N., Hamzah, J., and Ruoslahti, E. (2011) Transtumor targeting enabled by a novel neuropilin-binding peptide, *Oncogene*.
52. Jia, H., Cheng, L., Tickner, M., Bagherzadeh, A., Selwood, D., and Zachary, I. (2010) Neuropilin-1 antagonism in human carcinoma cells inhibits migration and enhances chemosensitivity, *British journal of cancer* 102, 541-552.
53. Cheng, L., Jia, H., Lohr, M., Bagherzadeh, A., Holmes, D. I., Selwood, D., and Zachary, I. (2004) Anti-chemorepulsive effects of vascular endothelial growth factor and placental growth factor-2 in dorsal root ganglion neurons are mediated via neuropilin-1 and cyclooxygenase-derived prostanoid production, *The Journal of biological chemistry* 279, 30654-30661.
54. Kong, J. S., Yoo, S. A., Kim, J. W., Yang, S. P., Chae, C. B., Tarallo, V., De Falco, S., Ryu, S. H., Cho, C. S., and Kim, W. U. (2010) Anti-neuropilin-1 peptide inhibition of synoviocyte survival, angiogenesis, and experimental arthritis, *Arthritis and rheumatism* 62, 179-190.
55. Novoa, A., Pellegrini-Moise, N., Bechet, D., Barberi-Heyob, M., and Chapleur, Y. (2010) Sugar-based peptidomimetics as potential inhibitors of the vascular endothelium growth factor binding to neuropilin-1, *Bioorganic & medicinal chemistry* 18, 3285-3298.
56. Giordano, R. J., Cardo-Vila, M., Salameh, A., Anobom, C. D., Zeitlin, B. D., Hawke, D. H., Valente, A. P., Almeida, F. C., Nor, J. E., Sidman, R. L., Pasqualini, R., and Arap, W. (2010) From combinatorial peptide selection to drug prototype (I): targeting the vascular endothelial growth factor receptor pathway, *Proceedings of the National Academy of Sciences of the United States of America* 107, 5112-5117.
57. Jarvis, A., Allerston, C. K., Jia, H., Herzog, B., Garza-Garcia, A., Winfield, N., Ellard, K., Aqil, R., Lynch, R., Chapman, C., Hartzoulakis, B., Nally, J., Stewart, M., Cheng, L., Menon, M., Tickner, M., Djordjevic, S., Driscoll, P. C., Zachary, I., and Selwood, D. L. (2010) Small molecule inhibitors of the neuropilin-1 vascular endothelial growth factor A (VEGF-A) interaction, *J Med Chem* 53, 2215-2226.
58. Ueyama, H., Horibe, T., Nakajima, O., Ohara, K., Kohno, M., and Kawakami, K. (2011) Semaphorin 3A lytic hybrid peptide binding to neuropilin-1 as a novel anti-cancer agent in pancreatic cancer, *Biochemical and biophysical research communications* 414, 60-66.
59. Thomas, N., Tirand, L., Chatelut, E., Plenat, F., Frochot, C., Dodeller, M., Guillemin, F., and Barberi-Heyob, M. (2008) Tissue distribution and pharmacokinetics of an ATWLPPR-conjugated chlorin-type photosensitizer targeting neuropilin-1 in glioma-bearing nude

- mice, *Photochemical & photobiological sciences : Official journal of the European Photochemistry Association and the European Society for Photobiology* 7, 433-441.
60. Thomas, N., Bechet, D., Becuwe, P., Tirand, L., Vanderesse, R., Frochot, C., Guillemin, F., and Barberi-Heyob, M. (2009) Peptide-conjugated chlorin-type photosensitizer binds neuropilin-1 in vitro and in vivo, *Journal of photochemistry and photobiology. B, Biology* 96, 101-108.
 61. Karjalainen, K., Jaalouk, D. E., Bueso-Ramos, C. E., Zurita, A. J., Kuniyasu, A., Eckhardt, B. L., Marini, F. C., Lichtiger, B., O'Brien, S., Kantarjian, H. M., Cortes, J. E., Koivunen, E., Arap, W., and Pasqualini, R. (2011) Targeting neuropilin-1 in human leukemia and lymphoma, *Blood* 117, 920-927.
 62. Tirand, L., Thomas, N., Dodeller, M., Dumas, D., Frochot, C., Maunit, B., Guillemin, F., and Barberi-Heyob, M. (2007) Metabolic profile of a peptide-conjugated chlorin-type photosensitizer targeting neuropilin-1: an in vivo and in vitro study, *Drug Metab Dispos* 35, 806-813.
 63. Thomas, N., Pernot, M., Vanderesse, R., Becuwe, P., Kamarulzaman, E., Da Silva, D., Francois, A., Frochot, C., Guillemin, F., and Barberi-Heyob, M. (2010) Photodynamic therapy targeting neuropilin-1: Interest of pseudopeptides with improved stability properties, *Biochemical pharmacology* 80, 226-235.
 64. Parker, M. W., Guo, H. F., Li, X., Linkugel, A. D., and Vander Kooi, C. W. (2012) Function of members of the neuropilin family as essential pleiotropic cell surface receptors, *Biochemistry* 51, 9437-9446.
 65. Geretti, E., Shimizu, A., and Klagsbrun, M. (2008) Neuropilin structure governs VEGF and semaphorin binding and regulates angiogenesis, *Angiogenesis* 11, 31-39.
 66. Pellet-Many, C., Frankel, P., Jia, H., and Zachary, I. (2008) Neuropilins: structure, function and role in disease, *Biochem J* 411, 211-226.
 67. de Wit, J., and Verhaagen, J. (2003) Role of semaphorins in the adult nervous system, *Progress in neurobiology* 71, 249-267.
 68. Gu, C., and Giraudo, E. (2013) The role of semaphorins and their receptors in vascular development and cancer, *Exp Cell Res* 319, 1306-1316.
 69. Hota, P. K., and Buck, M. (2012) Plexin structures are coming: opportunities for multilevel investigations of semaphorin guidance receptors, their cell signaling mechanisms, and functions, *Cell Mol Life Sci* 69, 3765-3805.
 70. Futamura, M., Kamino, H., Miyamoto, Y., Kitamura, N., Nakamura, Y., Ohnishi, S., Masuda, Y., and Arakawa, H. (2007) Possible role of semaphorin 3F, a candidate tumor suppressor gene at 3p21.3, in p53-regulated tumor angiogenesis suppression, *Cancer Res* 67, 1451-1460.
 71. Gaur, P., Bielenberg, D. R., Samuel, S., Bose, D., Zhou, Y., Gray, M. J., Dallas, N. A., Fan, F., Xia, L., Lu, J., and Ellis, L. M. (2009) Role of class 3 semaphorins and their receptors in tumor growth and angiogenesis, *Clin Cancer Res* 15, 6763-6770.
 72. Joyal, J. S., Sitaras, N., Binet, F., Rivera, J. C., Stahl, A., Zaniolo, K., Shao, Z., Polosa, A., Zhu, T., Hamel, D., Djavari, M., Kunik, D., Honore, J. C., Picard, E., Zabeida, A., Varma, D. R., Hickson, G., Mancini, J., Klagsbrun, M., Costantino, S., Beausejour, C., Lachapelle, P., Smith, L. E., Chemtob, S., and Sapieha, P. (2011) Ischemic neurons prevent vascular regeneration of neural tissue by secreting semaphorin 3A, *Blood* 117, 6024-6035.
 73. Acevedo, L. M., Barillas, S., Weis, S. M., Gothert, J. R., and Cheresh, D. A. (2008) Semaphorin 3A suppresses VEGF-mediated angiogenesis yet acts as a vascular permeability factor, *Blood* 111, 2674-2680.

74. Sekido, Y., Bader, S., Latif, F., Chen, J. Y., Duh, F. M., Wei, M. H., Albanesi, J. P., Lee, C. C., Lerman, M. I., and Minna, J. D. (1996) Human semaphorins A(V) and IV reside in the 3p21.3 small cell lung cancer deletion region and demonstrate distinct expression patterns, *Proc Natl Acad Sci U S A* 93, 4120-4125.
75. Capparuccia, L., and Tamagnone, L. (2009) Semaphorin signaling in cancer cells and in cells of the tumor microenvironment--two sides of a coin, *Journal of cell science* 122, 1723-1736.
76. Potiron, V. A., Roche, J., and Drabkin, H. A. (2009) Semaphorins and their receptors in lung cancer, *Cancer Lett* 273, 1-14.
77. Bielenberg, D. R., Hida, Y., Shimizu, A., Kaipainen, A., Kreuter, M., Kim, C. C., and Klagsbrun, M. (2004) Semaphorin 3F, a chemorepellent for endothelial cells, induces a poorly vascularized, encapsulated, nonmetastatic tumor phenotype, *J Clin Invest* 114, 1260-1271.
78. Kessler, O., Shraga-Heled, N., Lange, T., Gutmann-Raviv, N., Sabo, E., Baruch, L., Machluf, M., and Neufeld, G. (2004) Semaphorin-3F is an inhibitor of tumor angiogenesis, *Cancer Res* 64, 1008-1015.
79. Castro-Rivera, E., Ran, S., Thorpe, P., and Minna, J. D. (2004) Semaphorin 3B (SEMA3B) induces apoptosis in lung and breast cancer, whereas VEGF165 antagonizes this effect, *Proc Natl Acad Sci U S A* 101, 11432-11437.
80. Delcombel, R., Janssen, L., Vassy, R., Gammons, M., Haddad, O., Richard, B., Letourneur, D., Bates, D., Hendricks, C., Waltenberger, J., Starzec, A., Sounni, N. E., Noel, A., Deroanne, C., Lambert, C., and Colige, A. (2013) New prospects in the roles of the C-terminal domains of VEGF-A and their cooperation for ligand binding, cellular signaling and vessels formation, *Angiogenesis* 16, 353-371.
81. Varshavsky, A., Kessler, O., Abramovitch, S., Kigel, B., Zaffryar, S., Akiri, G., and Neufeld, G. (2008) Semaphorin-3B is an angiogenesis inhibitor that is inactivated by furin-like pro-protein convertases, *Cancer Res* 68, 6922-6931.
82. Casazza, A., Kigel, B., Maione, F., Capparuccia, L., Kessler, O., Giraudo, E., Mazzone, M., Neufeld, G., and Tamagnone, L. (2012) Tumour growth inhibition and anti-metastatic activity of a mutated furin-resistant Semaphorin 3E isoform, *EMBO molecular medicine* 4, 234-250.
83. Christensen, C., Ambartsumian, N., Gilestro, G., Thomsen, B., Comoglio, P., Tamagnone, L., Guldborg, P., and Lukanidin, E. (2005) Proteolytic processing converts the repelling signal Sema3E into an inducer of invasive growth and lung metastasis, *Cancer Res* 65, 6167-6177.
84. Adams, R. H., Lohrum, M., Klostermann, A., Betz, H., and Puschel, A. W. (1997) The chemorepulsive activity of secreted semaphorins is regulated by furin-dependent proteolytic processing, *EMBO J* 16, 6077-6086.
85. Starzec, A., Vassy, R., Martin, A., Lecouvey, M., Di Benedetto, M., Crepin, M., and Perret, G. Y. (2006) Antiangiogenic and antitumor activities of peptide inhibiting the vascular endothelial growth factor binding to neuropilin-1, *Life Sci* 79, 2370-2381.
86. von Wronski, M. A., Raju, N., Pillai, R., Bogdan, N. J., Marinelli, E. R., Nanjappan, P., Ramalingam, K., Arunachalam, T., Eaton, S., Linder, K. E., Yan, F., Pochon, S., Tweedle, M. F., and Nunn, A. D. (2006) Tuftsin binds neuropilin-1 through a sequence similar to that encoded by exon 8 of vascular endothelial growth factor, *J Biol Chem* 281, 5702-5710.
87. Becker, P. M., Waltenberger, J., Yachechko, R., Mirzapoiazova, T., Sham, J. S., Lee, C. G., Elias, J. A., and Verin, A. D. (2005) Neuropilin-1 regulates vascular endothelial growth factor-mediated endothelial permeability, *Circ Res* 96, 1257-1265.

88. Jardin, B. A., Zhao, Y., Selvaraj, M., Montes, J., Tran, R., Prakash, S., and Elias, C. B. (2008) Expression of SEAP (secreted alkaline phosphatase) by baculovirus mediated transduction of HEK 293 cells in a hollow fiber bioreactor system, *Journal of biotechnology* 135, 272-280.
89. Louis-Jeune C, Andrade-Navarro MA, and Perez-Iratxeta C. (2012) Prediction of protein secondary structure from circular dichroism using theoretically derived spectra, *Proteins: Structure, Function, and Bioinformatics* 80, 374-381.
90. Jia, H., Bagherzadeh, A., Hartzoulakis, B., Jarvis, A., Lohr, M., Shaikh, S., Aqil, R., Cheng, L., Tickner, M., Esposito, D., Harris, R., Driscoll, P. C., Selwood, D. L., and Zachary, I. C. (2006) Characterization of a bicyclic peptide neuropilin-1 (NP-1) antagonist (EG3287) reveals importance of vascular endothelial growth factor exon 8 for NP-1 binding and role of NP-1 in KDR signaling, *J Biol Chem* 281, 13493-13502.
91. Parker, M. W., Linkugel, A. D., and Vander Kooi, C. W. (2013) Effect of C-terminal sequence on competitive semaphorin binding to neuropilin-1, *Journal of molecular biology* 425, 4405-4414.
92. Parker, M. W., Xu, P., Guo, H. F., and Vander Kooi, C. W. (2012) Mechanism of selective VEGF-A binding by neuropilin-1 reveals a basis for specific ligand inhibition, *PLoS one* 7, e49177.
93. Binetruy-Tournaire, R., Demangel, C., Malavaud, B., Vassy, R., Rouyre, S., Kraemer, M., Plouet, J., Derbin, C., Perret, G., and Mazie, J. C. (2000) Identification of a peptide blocking vascular endothelial growth factor (VEGF)-mediated angiogenesis, *EMBO J* 19, 1525-1533.
94. Appleton, B. A., Wu, P., Maloney, J., Yin, J., Liang, W. C., Stawicki, S., Mortara, K., Bowman, K. K., Elliott, J. M., Desmarais, W., Bazan, J. F., Bagri, A., Tessier-Lavigne, M., Koch, A. W., Wu, Y., Watts, R. J., and Wiesmann, C. (2007) Structural studies of neuropilin/antibody complexes provide insights into semaphorin and VEGF binding, *EMBO J* 26, 4902-4912.
95. Janssen, B. J., Malinauskas, T., Weir, G. A., Cader, M. Z., Siebold, C., and Jones, E. Y. (2012) Neuropilins lock secreted semaphorins onto plexins in a ternary signaling complex, *Nature structural & molecular biology* 19, 1293-1299.
96. Guo, H. F., Li, X., Parker, M. W., Waltenberger, J., Becker, P. M., and Vander Kooi, C. W. (2013) Mechanistic basis for the potent anti-angiogenic activity of semaphorin 3F, *Biochemistry* 52, 7551-7558.
97. Guo, H. F., Li, X., Parker, M. W., Waltenberger, J., Becker, P. M., and Vander Kooi, C. W. (2013) Mechanistic Basis for the Potent Anti-angiogenic Activity of Semaphorin 3F, *Biochemistry*, accepted.
98. Otwinowski, Z., and Minor, W. (1997) Processing of X-ray Diffraction Data Collected in Oscillation Mode, *Methods in Enzymology* 276, 20.
99. Emsley, P., Lohkamp, B., Scott, W. G., and Cowtan, K. (2010) Features and development of Coot, *Acta crystallographica. Section D, Biological crystallography* 66, 486-501.
100. Murshudov, G. N., Vagin, A. A., and Dodson, E. J. (1997) Refinement of macromolecular structures by the maximum-likelihood method, *Acta crystallographica. Section D, Biological crystallography* 53, 240-255.
101. Davis, I. W., Leaver-Fay, A., Chen, V. B., Block, J. N., Kapral, G. J., Wang, X., Murray, L. W., Arendall, W. B., 3rd, Snoeyink, J., Richardson, J. S., and Richardson, D. C. (2007) MolProbity: all-atom contacts and structure validation for proteins and nucleic acids, *Nucleic acids research* 35, W375-383.
102. Schrodinger, LLC. (2010) The PyMOL Molecular Graphics System, Version 1.3r1.

103. Parikh, A. A., Fan, F., Liu, W. B., Ahmad, S. A., Stoeltzing, O., Reinmuth, N., Bielenberg, D., Bucana, C. D., Klagsbrun, M., and Ellis, L. M. (2004) Neuropilin-1 in human colon cancer: expression, regulation, and role in induction of angiogenesis, *Am J Pathol* 164, 2139-2151.
104. Miao, H. Q., Lee, P., Lin, H., Soker, S., and Klagsbrun, M. (2000) Neuropilin-1 expression by tumor cells promotes tumor angiogenesis and progression, *FASEB journal : official publication of the Federation of American Societies for Experimental Biology* 14, 2532-2539.
105. Pan, Q., Chantry, Y., Liang, W. C., Stawicki, S., Mak, J., Rathore, N., Tong, R. K., Kowalski, J., Yee, S. F., Pacheco, G., Ross, S., Cheng, Z., Le Couter, J., Plowman, G., Peale, F., Koch, A. W., Wu, Y., Bagri, A., Tessier-Lavigne, M., and Watts, R. J. (2007) Blocking neuropilin-1 function has an additive effect with anti-VEGF to inhibit tumor growth, *Cancer cell* 11, 53-67.
106. Caunt, M., Mak, J., Liang, W. C., Stawicki, S., Pan, Q., Tong, R. K., Kowalski, J., Ho, C., Reslan, H. B., Ross, J., Berry, L., Kasman, I., Zlot, C., Cheng, Z., Le Couter, J., Filvaroff, E. H., Plowman, G., Peale, F., French, D., Carano, R., Koch, A. W., Wu, Y., Watts, R. J., Tessier-Lavigne, M., and Bagri, A. (2008) Blocking neuropilin-2 function inhibits tumor cell metastasis, *Cancer cell* 13, 331-342.
107. Hanchate, N. K., Giacobini, P., Lhuillier, P., Parkash, J., Espy, C., Fouveaut, C., Leroy, C., Baron, S., Campagne, C., Vanacker, C., Collier, F., Cruaud, C., Meyer, V., Garcia-Pinero, A., Dewailly, D., Cortet-Rudelli, C., Gersak, K., Metz, C., Chabrier, G., Pugeat, M., Young, J., Hardelin, J. P., Prevot, V., and Dode, C. (2012) SEMA3A, a gene involved in axonal pathfinding, is mutated in patients with Kallmann syndrome, *PLoS genetics* 8, e1002896.
108. Asahara, T., Takahashi, T., Masuda, H., Kalka, C., Chen, D., Iwaguro, H., Inai, Y., Silver, M., and Isner, J. M. (1999) VEGF contributes to postnatal neovascularization by mobilizing bone marrow-derived endothelial progenitor cells, *EMBO J* 18, 3964-3972.
109. Lee, S., Chen, T. T., Barber, C. L., Jordan, M. C., Murdock, J., Desai, S., Ferrara, N., Nagy, A., Roos, K. P., and Iruela-Arispe, M. L. (2007) Autocrine VEGF signaling is required for vascular homeostasis, *Cell* 130, 691-703.
110. Carmeliet, P., Ng, Y. S., Nuyens, D., Theilmeier, G., Brusselmans, K., Cornelissen, I., Ehler, E., Kakkar, V. V., Stalmans, I., Mattot, V., Perriard, J. C., Dewerchin, M., Flameng, W., Nagy, A., Lupu, F., Moons, L., Collen, D., D'Amore, P. A., and Shima, D. T. (1999) Impaired myocardial angiogenesis and ischemic cardiomyopathy in mice lacking the vascular endothelial growth factor isoforms VEGF164 and VEGF188, *Nature medicine* 5, 495-502.
111. Senger, D. R., Galli, S. J., Dvorak, A. M., Perruzzi, C. A., Harvey, V. S., and Dvorak, H. F. (1983) Tumor cells secrete a vascular permeability factor that promotes accumulation of ascites fluid, *Science* 219, 983-985.
112. Keck, P. J., Hauser, S. D., Krivi, G., Sanzo, K., Warren, T., Feder, J., and Connolly, D. T. (1989) Vascular permeability factor, an endothelial cell mitogen related to PDGF, *Science* 246, 1309-1312.
113. Ferrara, N., Hillan, K. J., Gerber, H. P., and Novotny, W. (2004) Discovery and development of bevacizumab, an anti-VEGF antibody for treating cancer, *Nat Rev Drug Discov* 3, 391-400.
114. Ellis, L. M., and Hicklin, D. J. (2008) VEGF-targeted therapy: mechanisms of anti-tumour activity, *Nature reviews. Cancer* 8, 579-591.
115. Goel, H. L., and Mercurio, A. M. (2013) VEGF targets the tumour cell, *Nature reviews. Cancer* 13, 871-882.

116. Folkman, J. (1971) Tumor angiogenesis: therapeutic implications, *The New England journal of medicine* 285, 1182-1186.
117. Ferrara, N., and Alitalo, K. (1999) Clinical applications of angiogenic growth factors and their inhibitors, *Nature medicine* 5, 1359-1364.
118. Lim, L. S., Mitchell, P., Seddon, J. M., Holz, F. G., and Wong, T. Y. (2012) Age-related macular degeneration, *Lancet* 379, 1728-1738.
119. Terman, B. I., Dougher-Vermazen, M., Carrion, M. E., Dimitrov, D., Armellino, D. C., Gospodarowicz, D., and Bohlen, P. (1992) Identification of the KDR tyrosine kinase as a receptor for vascular endothelial cell growth factor, *Biochemical and biophysical research communications* 187, 1579-1586.
120. Giraudo, E., Primo, L., Audero, E., Gerber, H. P., Koolwijk, P., Soker, S., Klagsbrun, M., Ferrara, N., and Bussolino, F. (1998) Tumor necrosis factor-alpha regulates expression of vascular endothelial growth factor receptor-2 and of its co-receptor neuropilin-1 in human vascular endothelial cells, *J Biol Chem* 273, 22128-22135.
121. Millauer, B., Wizigmann-Voos, S., Schnurch, H., Martinez, R., Moller, N. P., Risau, W., and Ullrich, A. (1993) High affinity VEGF binding and developmental expression suggest Flk-1 as a major regulator of vasculogenesis and angiogenesis, *Cell* 72, 835-846.
122. Fong, G. H., Rossant, J., Gertsenstein, M., and Breitman, M. L. (1995) Role of the Flt-1 receptor tyrosine kinase in regulating the assembly of vascular endothelium, *Nature* 376, 66-70.
123. Terman, B. I., Carrion, M. E., Kovacs, E., Rasmussen, B. A., Eddy, R. L., and Shows, T. B. (1991) Identification of a new endothelial cell growth factor receptor tyrosine kinase, *Oncogene* 6, 1677-1683.
124. Muller, Y. A., Li, B., Christinger, H. W., Wells, J. A., Cunningham, B. C., and de Vos, A. M. (1997) Vascular endothelial growth factor: crystal structure and functional mapping of the kinase domain receptor binding site, *Proc Natl Acad Sci U S A* 94, 7192-7197.
125. Wiesmann, C., Fuh, G., Christinger, H. W., Eigenbrot, C., Wells, J. A., and de Vos, A. M. (1997) Crystal structure at 1.7 Å resolution of VEGF in complex with domain 2 of the Flt-1 receptor, *Cell* 91, 695-704.
126. Yang, Y., Xie, P., Opatowsky, Y., and Schlessinger, J. (2010) Direct contacts between extracellular membrane-proximal domains are required for VEGF receptor activation and cell signaling, *Proc Natl Acad Sci U S A* 107, 1906-1911.
127. Pan, Q., Chathery, Y., Wu, Y., Rathore, N., Tong, R. K., Peale, F., Bagri, A., Tessier-Lavigne, M., Koch, A. W., and Watts, R. J. (2007) Neuropilin-1 binds to VEGF121 and regulates endothelial cell migration and sprouting, *J Biol Chem* 282, 24049-24056.
128. Whitaker, G. B., Limberg, B. J., and Rosenbaum, J. S. (2001) Vascular endothelial growth factor receptor-2 and neuropilin-1 form a receptor complex that is responsible for the differential signaling potency of VEGF(165) and VEGF(121), *J Biol Chem* 276, 25520-25531.
129. Karpanen, T., Heckman, C. A., Keskkitalo, S., Jeltsch, M., Ollila, H., Neufeld, G., Tamagnone, L., and Alitalo, K. (2006) Functional interaction of VEGF-C and VEGF-D with neuropilin receptors, *FASEB J* 20, 1462-1472.
130. Uniewicz, K. A., Cross, M. J., and Fernig, D. G. (2011) Exogenous recombinant dimeric neuropilin-1 is sufficient to drive angiogenesis, *J Biol Chem* 286, 12-23.
131. (1994) The CCP4 suite: programs for protein crystallography, *Acta crystallographica. Section D, Biological crystallography* 50, 760-763.

132. McCoy, A. J., Grosse-Kunstleve, R. W., Adams, P. D., Winn, M. D., Storoni, L. C., and Read, R. J. (2007) Phaser crystallographic software, *Journal of applied crystallography* 40, 658-674.
133. Stiegler, A. L., Burden, S. J., and Hubbard, S. R. (2006) Crystal structure of the agrin-responsive immunoglobulin-like domains 1 and 2 of the receptor tyrosine kinase MuSK, *Journal of molecular biology* 364, 424-433.
134. Painter, J., and Merritt, E. A. (2006) Optimal description of a protein structure in terms of multiple groups undergoing TLS motion, *Acta crystallographica. Section D, Biological crystallography* 62, 439-450.
135. Krissinel, E., and Henrick, K. (2007) Inference of macromolecular assemblies from crystalline state, *Journal of molecular biology* 372, 774-797.
136. Larkin, M. A., Blackshields, G., Brown, N. P., Chenna, R., McGettigan, P. A., McWilliam, H., Valentin, F., Wallace, I. M., Wilm, A., Lopez, R., Thompson, J. D., Gibson, T. J., and Higgins, D. G. (2007) Clustal W and Clustal X version 2.0, *Bioinformatics* 23, 2947-2948.
137. Li, X., Luo, F., Wang, S., Ni, E., Tang, X., Lv, H., Chen, X., Chen, L., and Yan, J. (2011) Monoclonal antibody against NRP-1 b1b2, *Hybridoma (Larchmt)* 30, 369-373.
138. Brozzo, M. S., Bjelic, S., Kisko, K., Schleier, T., Leppanen, V. M., Alitalo, K., Winkler, F. K., and Ballmer-Hofer, K. (2012) Thermodynamic and structural description of allosterically regulated VEGFR-2 dimerization, *Blood* 119, 1781-1788.
139. Mac Gabhann, F., and Popel, A. S. (2006) Targeting neuropilin-1 to inhibit VEGF signaling in cancer: Comparison of therapeutic approaches, *PLoS computational biology* 2, e180.
140. Dixelius, J., Makinen, T., Wirzenius, M., Karkkainen, M. J., Wernstedt, C., Alitalo, K., and Claesson-Welsh, L. (2003) Ligand-induced vascular endothelial growth factor receptor-3 (VEGFR-3) heterodimerization with VEGFR-2 in primary lymphatic endothelial cells regulates tyrosine phosphorylation sites, *J Biol Chem* 278, 40973-40979.
141. Chen, L., Miao, W., Tang, X., Zhang, H., Wang, S., Luo, F., and Yan, J. (2013) Inhibitory effect of neuropilin-1 monoclonal antibody (NRP-1 MAb) on glioma tumor in mice, *Journal of biomedical nanotechnology* 9, 551-558.
142. Motzer, R. J., Michaelson, M. D., Redman, B. G., Hudes, G. R., Wilding, G., Figlin, R. A., Ginsberg, M. S., Kim, S. T., Baum, C. M., DePrimo, S. E., Li, J. Z., Bello, C. L., Theuer, C. P., George, D. J., and Rini, B. I. (2006) Activity of SU11248, a multitargeted inhibitor of vascular endothelial growth factor receptor and platelet-derived growth factor receptor, in patients with metastatic renal cell carcinoma, *J Clin Oncol* 24, 16-24.
143. Rini, B. I., Michaelson, M. D., Rosenberg, J. E., Bukowski, R. M., Sosman, J. A., Stadler, W. M., Hutson, T. E., Margolin, K., Harmon, C. S., DePrimo, S. E., Kim, S. T., Chen, I., and George, D. J. (2008) Antitumor activity and biomarker analysis of sunitinib in patients with bevacizumab-refractory metastatic renal cell carcinoma, *J Clin Oncol* 26, 3743-3748.
144. Rosen, L. S., Kurzrock, R., Mulay, M., Van Vugt, A., Purdom, M., Ng, C., Silverman, J., Koutsoukos, A., Sun, Y. N., Bass, M. B., Xu, R. Y., Polverino, A., Wiezorek, J. S., Chang, D. D., Benjamin, R., and Herbst, R. S. (2007) Safety, pharmacokinetics, and efficacy of AMG 706, an oral multikinase inhibitor, in patients with advanced solid tumors, *J Clin Oncol* 25, 2369-2376.
145. Willett, C. G., Boucher, Y., Duda, D. G., di Tomaso, E., Munn, L. L., Tong, R. T., Kozin, S. V., Petit, L., Jain, R. K., Chung, D. C., Sahani, D. V., Kalva, S. P., Cohen, K. S., Scadden, D. T., Fischman, A. J., Clark, J. W., Ryan, D. P., Zhu, A. X., Blaszkowsky, L. S., Shellito, P. C., Mino-Kenudson, M., and Lauwers, G. Y. (2005) Surrogate markers for antiangiogenic therapy and dose-limiting toxicities for bevacizumab with radiation and chemotherapy:

- continued experience of a phase I trial in rectal cancer patients, *J Clin Oncol* 23, 8136-8139.
146. Yamada, Y., Oike, Y., Ogawa, H., Ito, Y., Fujisawa, H., Suda, T., and Takakura, N. (2003) Neuropilin-1 on hematopoietic cells as a source of vascular development, *Blood* 101, 1801-1809.
 147. Jones, E. A., Yuan, L., Breant, C., Watts, R. J., and Eichmann, A. (2008) Separating genetic and hemodynamic defects in neuropilin 1 knockout embryos, *Development* 135, 2479-2488.
 148. Fantin, A., Vieira, J. M., Plein, A., Denti, L., Fruttiger, M., Pollard, J. W., and Ruhrberg, C. (2013) NRP1 acts cell autonomously in endothelium to promote tip cell function during sprouting angiogenesis, *Blood* 121, 2352-2362.
 149. Ballmer-Hofer, K., Andersson, A. E., Ratcliffe, L. E., and Berger, P. (2011) Neuropilin-1 promotes VEGFR-2 trafficking through Rab11 vesicles thereby specifying signal output, *Blood* 118, 816-826.
 150. Fukasawa, M., Matsushita, A., and Korc, M. (2007) Neuropilin-1 interacts with integrin beta1 and modulates pancreatic cancer cell growth, survival and invasion, *Cancer biology & therapy* 6, 1173-1180.
 151. Goel, H. L., Pursell, B., Standley, C., Fogarty, K., and Mercurio, A. M. (2012) Neuropilin-2 regulates alpha6beta1 integrin in the formation of focal adhesions and signaling, *Journal of cell science* 125, 497-506.
 152. Robinson, S. D., Reynolds, L. E., Kostourou, V., Reynolds, A. R., da Silva, R. G., Tavora, B., Baker, M., Marshall, J. F., and Hodivala-Dilke, K. M. (2009) Alpha6beta3 integrin limits the contribution of neuropilin-1 to vascular endothelial growth factor-induced angiogenesis, *J Biol Chem* 284, 33966-33981.
 153. Cai, H., and Reed, R. R. (1999) Cloning and characterization of neuropilin-1-interacting protein: a PSD-95/Dlg/ZO-1 domain-containing protein that interacts with the cytoplasmic domain of neuropilin-1, *J Neurosci* 19, 6519-6527.
 154. El Mourabit, H., Poinat, P., Koster, J., Sondermann, H., Wixler, V., Wegener, E., Laplantine, E., Geerts, D., Georges-Labouesse, E., Sonnenberg, A., and Aumailley, M. (2002) The PDZ domain of TIP-2/GIPC interacts with the C-terminus of the integrin alpha5 and alpha6 subunits, *Matrix biology : journal of the International Society for Matrix Biology* 21, 207-214.
 155. Tani, T. T., and Mercurio, A. M. (2001) PDZ interaction sites in integrin alpha subunits. T14853, TIP/GIPC binds to a type I recognition sequence in alpha 6A/alpha 5 and a novel sequence in alpha 6B, *J Biol Chem* 276, 36535-36542.
 156. Miao, H. Q., Soker, S., Feiner, L., Alonso, J. L., Raper, J. A., and Klagsbrun, M. (1999) Neuropilin-1 mediates collapsin-1/semaphorin III inhibition of endothelial cell motility: functional competition of collapsin-1 and vascular endothelial growth factor-165, *The Journal of cell biology* 146, 233-242.
 157. Bachelder, R. E., Crago, A., Chung, J., Wendt, M. A., Shaw, L. M., Robinson, G., and Mercurio, A. M. (2001) Vascular endothelial growth factor is an autocrine survival factor for neuropilin-expressing breast carcinoma cells, *Cancer Res* 61, 5736-5740.
 158. Cao, Y., E, G., Wang, E., Pal, K., Dutta, S. K., Bar-Sagi, D., and Mukhopadhyay, D. (2012) VEGF exerts an angiogenesis-independent function in cancer cells to promote their malignant progression, *Cancer Res* 72, 3912-3918.
 159. Stanton, M. J., Dutta, S., Zhang, H., Polavaram, N. S., Leontovich, A. A., Honscheid, P., Sinicrope, F. A., Tindall, D. J., Muders, M. H., and Datta, K. (2013) Autophagy control by

- the VEGF-C/NRP-2 axis in cancer and its implication for treatment resistance, *Cancer Res* 73, 160-171.
160. Beck, B., Driessens, G., Goossens, S., Youssef, K. K., Kuchnio, A., Caauwe, A., Sotiropoulou, P. A., Loges, S., Lapouge, G., Candi, A., Mascré, G., Drogat, B., Dekoninck, S., Haigh, J. J., Carmeliet, P., and Blanpain, C. (2011) A vascular niche and a VEGF-Nrp1 loop regulate the initiation and stemness of skin tumours, *Nature* 478, 399-403.
 161. Casazza, A., Laoui, D., Wenes, M., Rizzolio, S., Bassani, N., Mambretti, M., Deschoemaeker, S., Van Ginderachter, J. A., Tamagnone, L., and Mazzone, M. (2013) Impeding macrophage entry into hypoxic tumor areas by Sema3A/Nrp1 signaling blockade inhibits angiogenesis and restores antitumor immunity, *Cancer cell* 24, 695-709.
 162. Delgoffe, G. M., Woo, S. R., Turnis, M. E., Gravano, D. M., Guy, C., Overacre, A. E., Bettini, M. L., Vogel, P., Finkelstein, D., Bonnevier, J., Workman, C. J., and Vignali, D. A. (2013) Stability and function of regulatory T cells is maintained by a neuropilin-1-semaphorin-4a axis, *Nature* 501, 252-256.
 163. Selheim, F., Holmsen, H., and Vassbotn, F. S. (2002) Identification of functional VEGF receptors on human platelets, *FEBS Lett* 512, 107-110.
 164. Kashiwagi, H., Shiraga, M., Kato, H., Kamae, T., Yamamoto, N., Tadokoro, S., Kurata, Y., Tomiyama, Y., and Kanakura, Y. (2005) Negative regulation of platelet function by a secreted cell repulsive protein, semaphorin 3A, *Blood* 106, 913-921.
 165. Wannemacher, K. M., Wang, L., Zhu, L., and Brass, L. F. (2011) The role of semaphorins and their receptors in platelets: Lessons learned from neuronal and immune synapses, *Platelets* 22, 461-465.
 166. Darbonne, W. C., Du, X., Dhawan, P., Hartley, D., Tarrant, J., Taylor, H., Cain, G., Shih, L. M., Brachmann, R. K., Phung, Q., Weekes, C. D., LoRusso, P., Patnaik, A., Xiang, H., and Ramakrishnan, V. (2011) Mechanism for platelet reduction in anti-neuropilin-1 (MNRP1685A)-treated phase I patients., *J Clin Oncol* 29, 13598 abstr
 167. Gay, L. J., and Felding-Habermann, B. (2011) Contribution of platelets to tumour metastasis, *Nature reviews. Cancer* 11, 123-134.
 168. Cao, J., Rehemtulla, A., Bahou, W., and Zucker, S. (1996) Membrane type matrix metalloproteinase 1 activates pro-gelatinase A without furin cleavage of the N-terminal domain, *J Biol Chem* 271, 30174-30180.
 169. Laprise, M. H., Grondin, F., Cayer, P., McDonald, P. P., and Dubois, C. M. (2002) Furin gene (fur) regulation in differentiating human megakaryoblastic Dami cells: involvement of the proximal GATA recognition motif in the P1 promoter and impact on the maturation of furin substrates, *Blood* 100, 3578-3587.
 170. Kerr, B. A., Miocinovic, R., Smith, A. K., Klein, E. A., and Byzova, T. V. (2010) Comparison of tumor and microenvironment secretomes in plasma and in platelets during prostate cancer growth in a xenograft model, *Neoplasia* 12, 388-396.
 171. Handagama, P. J., George, J. N., Shuman, M. A., McEver, R. P., and Bainton, D. F. (1987) Incorporation of a circulating protein into megakaryocyte and platelet granules, *Proc Natl Acad Sci U S A* 84, 861-865.
 172. Patzelt, J., and Langer, H. F. (2012) Platelets in angiogenesis, *Current vascular pharmacology* 10, 570-577.
 173. Folkman, J., Szabo, S., Stovroff, M., McNeil, P., Li, W., and Shing, Y. (1991) Duodenal ulcer. Discovery of a new mechanism and development of angiogenic therapy that accelerates healing, *Annals of surgery* 214, 414-425; discussion 426-417.

174. Wartiovaara, U., Salven, P., Mikkola, H., Lassila, R., Kaukonen, J., Joukov, V., Orpana, A., Ristimaki, A., Heikinheimo, M., Joensuu, H., Alitalo, K., and Palotie, A. (1998) Peripheral blood platelets express VEGF-C and VEGF which are released during platelet activation, *Thrombosis and haemostasis* 80, 171-175.
175. Klement, G. L., Yip, T. T., Cassiola, F., Kikuchi, L., Cervi, D., Podust, V., Italiano, J. E., Wheatley, E., Abou-Slaybi, A., Bender, E., Almog, N., Kieran, M. W., and Folkman, J. (2009) Platelets actively sequester angiogenesis regulators, *Blood* 113, 2835-2842.
176. Weltermann, A., Wolzt, M., Petersmann, K., Czerni, C., Graselli, U., Lechner, K., and Kyrle, P. A. (1999) Large amounts of vascular endothelial growth factor at the site of hemostatic plug formation in vivo, *Arteriosclerosis, thrombosis, and vascular biology* 19, 1757-1760.
177. Gunsilius, E., Petzer, A., Stockhammer, G., Nussbaumer, W., Schumacher, P., Clausen, J., and Gastl, G. (2000) Thrombocytes are the major source for soluble vascular endothelial growth factor in peripheral blood, *Oncology* 58, 169-174.
178. Kamykowski, J., Carlton, P., Sehgal, S., and Storrie, B. (2011) Quantitative immunofluorescence mapping reveals little functional coclustering of proteins within platelet alpha-granules, *Blood* 118, 1370-1373.
179. Chatterjee, M., Huang, Z., Zhang, W., Jiang, L., Hultenby, K., Zhu, L., Hu, H., Nilsson, G. P., and Li, N. (2011) Distinct platelet packaging, release, and surface expression of proangiogenic and antiangiogenic factors on different platelet stimuli, *Blood* 117, 3907-3911.
180. Battinelli, E. M., Markens, B. A., and Italiano, J. E., Jr. (2011) Release of angiogenesis regulatory proteins from platelet alpha granules: modulation of physiologic and pathologic angiogenesis, *Blood* 118, 1359-1369.
181. Blair, P., and Flaumenhaft, R. (2009) Platelet alpha-granules: basic biology and clinical correlates, *Blood reviews* 23, 177-189.
182. Anitua, E., Andia, I., Ardanza, B., Nurden, P., and Nurden, A. T. (2004) Autologous platelets as a source of proteins for healing and tissue regeneration, *Thrombosis and haemostasis* 91, 4-15.
183. Pietramaggiori, G., Scherer, S. S., Mathews, J. C., Gennaoui, T., Lancerotto, L., Ragno, G., Valeri, C. R., and Orgill, D. P. (2010) Quiescent platelets stimulate angiogenesis and diabetic wound repair, *The Journal of surgical research* 160, 169-177.
184. Carneiro, A. M., Cook, E. H., Murphy, D. L., and Blakely, R. D. (2008) Interactions between integrin alphaIIb beta3 and the serotonin transporter regulate serotonin transport and platelet aggregation in mice and humans, *J Clin Invest* 118, 1544-1552.
185. Vila, V., Martinez-Sales, V., Reganon, E., and Aznar, J. (1997) The effect of thrombin on the dynamic exchange between intraplatelet and extraplatelet fibrinogen, *British journal of haematology* 99, 548-554.
186. Salikhova, A., Wang, L., Lanahan, A. A., Liu, M., Simons, M., Leenders, W. P., Mukhopadhyay, D., and Horowitz, A. (2008) Vascular endothelial growth factor and semaphorin induce neuropilin-1 endocytosis via separate pathways, *Circ Res* 103, e71-79.

VITA

Author's Name – Hou-Fu Guo

Birthplace – Phoenix City, Liaoning Province, China

Education

2009 fall- 2014 August:

PhD in Biochemistry, University of Kentucky, Lexington, KY, USA

2006 fall- 2009 August:

MS in Biology, University of Kentucky, Lexington, KY, USA

2000 fall-2004 fall:

BS in Biological Sciences, School of Life Sciences, University of Science and Technology of China, Hefei, Anhui, China.

Teaching and Mentoring Experiences

2011 summer:

Mentoring undergraduate Andrew D. Linkugel for Research Experiences for Undergraduates (REU) program of National Science Foundation (NSF)

2009 fall:

Graduate Teaching Assistant in Biochemistry, University of Kentucky, Lexington, KY, USA

2006 fall-2009 spring:

Graduate Teaching Assistant in Biology, University of Kentucky, Lexington, KY, USA

Peer Reviewed Publications

1. **H Guo**, J Yan, P Xu, AD Linkugel, CW Vander Kooi. Structural insights of neuropilin function in vascular endothelial growth factor signaling. *In Preparation* **(This work defines the mechanism of neuropilin function in VEGF signaling.)**

2. TB Dunlap, **H Guo**, E Holbrook, J Rumi-Masante, TE Lester, CW Vander Kooi, TP Creamer. Stoichiometry of the calcineurin regulatory domain-calmodulin complex. *Biochemistry in revision*
3. **H Guo**, CW Vander Kooi. Structure of human semaphorin 3f helical motif from the c-terminal basic domain. *Structural Biology and Crystallization Communications in review*
(This work determines the structure of sema3f receptor binding motif.)
4. DA Meekins, M Raththagala, S Husodo, CJ White, **H Guo**, O Kötting, CW Vander Kooi, MS Gentry. Phosphoglucan-bound structure of starch phosphatase Starch Excess4 reveals the mechanism for C6 specificity. *Proceedings of the National Academy of Sciences*, 2014 1400757111v1-201400757.
5. **H Guo**, P Xu, MW Parker, CW Vander Kooi. Mechanistic basis for the potent anti-angiogenic activity of semaphorin 3f. *Biochemistry*, 2013 Oct; 52(43): 7551–7558
(This work defines the mechanism of sema3f-neuropilin interaction.)
6. DA Meekins*, **H Guo***, S Husodo, BC Paasch, TM Bridges, D Santelia, O Kötting, CW Vander Kooi, MS Gentry. Structure of the arabidopsis glucan phosphatase LIKE SEX FOUR2 reveals a unique mechanism for starch dephosphorylation. *The Plant Cell*, 2013 Jun; 25(6): 2302–2314
(*authors contributed equally. This work determines the mechanism of catalysis for glucan phosphatase LSF2.)
-Highlighted in an “In Brief”: NR Hoffman. *The Plant Cell*, 2013 Jun; 25(6): 1915
7. MW Parker, **H Guo**, X Li, AD Linkugel, CW Vander Kooi. Function of the neuropilin family as essential pleiotropic cell surface receptors. *Biochemistry*, 2012 Nov; 51(47): 9437-9446
8. MW Parker, P Xu, **H Guo**, CW Vander Kooi. Mechanism of selective VEGF-A binding by neuropilin-1 reveals a basis for specific ligand inhibition. *PLoS ONE*, 2012 Nov; 7(11): e49177
9. CW Vander Kooi, AO Taylor, RM Pace, DA Meekins, **H Guo**, Y Kim, MS Gentry. Structural basis for the glucan phosphatase activity of Starch Excess4. *Proceedings of the National Academy of Sciences*, 2010 Jun; 107(35): 15379-15384
-Highlighted on the cover and in a commentary: Tagliabracci and Roach. *Proceedings of the National Academy of Sciences*, 2010 Jun; 107(35): 15312-13.
10. L Wu, AA Sluiter, **H Guo**, RA Balesar, DF Swaab, J Zhou, RW Verwer. Neural stem cells improve neuronal survival in cultured postmortem brain tissue

from aged and Alzheimer patients. *Journal of Cellular and Molecular Medicine*, 2008 Sep; 12(5A): 1611-1621

11. C Wang, J Wang, **H Guo**, R Liu. Involvement of annexin I in the dexamethasone-mediated upregulation of A549 cells phagocytosis of apoptotic eosinophils. *Immunology Letters*, 2007 Aug; 111(2): 103-110

12. H Zhu, **H Guo**, H Hou, Y Liu, S Sheng, J Zhou. Increased expression of the Nogo receptor in the hippocampus and its relation to the neuropathology in Alzheimer's disease. *Human Pathology*, 2007 Mar; 38(3): 426-434

Oral Presentations

1. "Neuropilin in Angiogenesis: ligand binding and receptor activation". Molecular and Cellular Biochemistry Student Seminar. Oct 25, 2012

2. "Neuropilin in angiogenesis". Molecular and Cellular Biochemistry Departmental Retreat, Cumberland Falls State Resort Park. Corbin, KY May 16, 2011

3. "Morphological and molecular studies of retinal degeneration and regeneration in Axolotls". Biology Student Seminar. Dec 3, 2008

4. "Morphological studies of retinal degeneration and regeneration in Axolotls". Biology Student Seminar. Feb 4, 2008

Poster Presentations

1. **H Guo**, P Xu, A Linkugel, CW Vander Kooi. "Structural insights of neuropilin function in vascular endothelial growth factor signaling". 16th Gill Heart Institute Cardiovascular Research Day, Lexington, KY Oct 11, 2013

2. **H Guo**, X Li, P Xu, MW Parker, CW Vander Kooi. "Divalent synergistic binding of semaphorin 3 C-terminal basic domain to neuropilin-1 mediates its anti-angiogenic activity". 246th American Chemical Society National Meeting, Indianapolis, IN Sep 10, 2013

3. **H Guo**, P Xu, A Linkugel, CW Vander Kooi. "Structural basis of neuropilin function in vascular endothelial growth factor receptor activation". Molecular and Cellular Biochemistry Departmental Retreat, General Butler State Resort Park. Carrollton, KY Jun 25, 2013

4. **H Guo**, X Li, P Xu, MW Parker, CW Vander Kooi. "Functional and mechanistic studies of potent peptide inhibitors for VEGF-mediated angiogenesis". The 6th Markey Cancer Center Research Day, Lexington, KY Apr 15, 2013
5. **H Guo**, P Xu, MW Parker, CW Vander Kooi. "Divalent synergistic binding of semaphorin 3f c-terminal basic domain to neuropilin-1 mediates its anti-angiogenesis activity". 15th Gill Heart Institute Cardiovascular Research Day, Lexington, KY Oct 5, 2012
6. **H Guo**, P Xu, MW Parker, CW Vander Kooi. "Structure-activity studies of competitive ligand binding to neuropilin in angiogenesis". 9th annual SER-CAT Symposium, Lexington, KY Mar 16, 2012
7. **H Guo**, P Xu, MW Parker, CW Vander Kooi. "Structure-activity studies of competitive ligand binding to neuropilin in angiogenesis". American Society for Biochemistry and Molecular Biology, Annual Meeting, Washington DC Apr 10, 2011
8. **H Guo**, P Xu, MW Parker, CW Vander Kooi. "Structure/function studies of potent peptide inhibitors of neuropilin-mediated angiogenesis". The 4th Markey Cancer Center Research Day, Lexington, KY Mar 22, 2011
9. **H Guo**, JR Monaghan, RS Voss, EA Debski. "The process of retinal degeneration and repair in the axolotl, *Ambystoma mexicanum*". Society for Neuroscience, Annual Meeting, Washington DC Nov 19, 2008
10. **H Guo**, EA Debski, JR Monaghan, SR Voss. "Molecular studies of retinal regeneration in the axolotl". 14th Annual Kentucky Spinal Cord and Head Injury Research Trust Symposium, Lexington, KY Jun 12, 2008

Main Honors Received

2011-2012: Max Steckler Fellowship.
2010-2011: Kentucky Opportunity Fellowship.
2009-2010: Graduate School Academic Year Fellowship.